

Supporting information

Water-soluble NHC-Cu Catalysts: Applications in Click Chemistry, Bioconjugation and Mechanistic Analysis

Heriberto Díaz Velázquez, Yara Ruiz García, Matthias Vandichel, Annemieke Madder,
Francis Verpoort*

Correspondence to: francis.verpoort@Ugent.be

This PDF file includes:

- Materials and Methods (Syntheses, Bioconjugation experiments, Preparation of the heterogeneous catalyst Bis[1-(4-sodiumsulfonatebutyl)-3-(2,4,6-trimethylphenyl)-4,5-imidazolyl-3-ylidene] copper (I) hexafluorophosphate on Amberlyte® IRA-402 resin beads 7-IRA 402, Computational methods)
- Figs. S1 to S32
- Tables S1 to S8
- Supplementary picture S1
- Supplementary graph S1

Table of Contents:

1. Syntheses

- 1.1. General conditions.
- 1.2. Synthesis of ligands.
 - 1.2.1. 1-(2,4,6-trimethylphenyl)-3-(3-sulfonato-propyl)-imidazolidinium (2).
 - 1.2.2. 1-(2,4,6-trimethylphenyl)-3-(4-sulfonato-butyl)-imidazolidinium (4).
- 1.3. Synthesis of catalysts.
 - 1.3.1. Synthesis of Bis[1-(4-potassiumsulfonatebutyl)-3-(2,4,6-trimethylphenyl)-4,5-dihydroimidazolyl-3-ylidene] copper (I) hexafluorophosphate (6).
 - 1.3.2. Synthesis of Bis[1-(4-potassiumsulfonatebutyl)-3-(2,4,6-trimethylphenyl)-4,5-imidazolyl-3-ylidene] copper (I) hexafluorophosphate (9).
 - 1.3.3. Synthesis of Bis[1-(4-sodiumsulfonatepropyl)-3-(2,4,6-trimethylphenyl)-4,5-dihydroimidazolyl-3-ylidene] copper (I) hexafluorophosphate (7).
 - 1.3.4. Synthesis of Bis[1-(4-sodiumsulfonatepropyl)-3-(2,4,6-trimethylphenyl)-4,5-imidazolyl-3-ylidene] copper (I) hexafluorophosphate (8).
- 1.4. Synthesis of triazoles by CuAAC.
 - 1.4.1. Synthesis of 1-benzyl-4-phenyl-1,2,3-triazole.
 - 1.4.2. Synthesis of 1,4-substituted 1,2,3-triazoles under neat conditions.
 - 1.4.3. Synthesis of 1,4-substituted triazoles under with *in-situ* formed azides.
 - 1.4.4. Synthesis of 1,4,5-substituted triazoles.
 - 1.4.5. Synthesis of 1-substituted triazoles.
 - 1.4.6. Synthesis of 4-substituted-1,2,3-triazoles.
 - 1.4.7. Synthesis of 4-substituted-1,2,3-triazoles.
- 1.5. NMR and MS spectra of ligand precursors and catalysts.
- 1.6. NMR spectra of synthesized triazoles

2. Bioconjugation experiments

- 2.1. General information.
- 2.2. Peptide synthesis.
 - 2.2.1. Immobilization of Fmoc-Pra-OH on 2-chlorotrityl chloride resin.
 - 2.2.2. Fmoc deprotection and coupling of Fmoc-Gly-OH.
 - 2.2.3. Automated synthesis of linear peptide.
- 2.3. Bioconjugation via CuAAC.
 - 2.3.1. Immobilization of Fmoc-Aha-OH on 2-chlorotrityl resin.
 - 2.3.2. Fmoc deprotection and coupling of Fmoc-Gly-OH.
 - 2.3.3. Automated synthesis of linear peptide.
- 2.4. Bioconjugation via CuAAC.

3. Preparation of the heterogeneous catalyst Bis[1-(4-sodiumsulfonatebutyl)-3-(2,4,6-trimethylphenyl)-4,5-imidazolyl-3-ylidene] copper (I) hexafluorophosphate on Amberlyte® IRA-402 resin beads 7-IRA 402.

- 3.1. Procedure for the heterogeneous CuAAC reactions for the three component Click reaction of benzyl azide and phenyl acetylene in water.
- 3.2. Procedure for the heterogeneous CuAAC reactions for the three-component Click reaction of benzyl azide and acetylene gas in water.
- 3.3. Recyclability studies of the heterogeneous catalyst 7-IRA 402.
- 3.4. XRF experiments of water phase of 7-IRA 402.

4. Computational methods.

- 4.1. Description of the catalytic cycle with LCuPF₆ as intermediate.

1. Syntheses

1.1 General conditions.

All reagents were used as purchased, Cu(I) sources were stored under argon in a glove box. Solvents were dried under standard procedures. 1-(2,4,6-trimethylphenyl)-3-(3-sulfonato-propyl)-imidazolium and 1-(2,4,6-trimethylphenyl)-3-(4-sulfonato-butyl)-imidazolium were synthesized according to literature procedures¹. Azides were synthesized according to literature procedures². Bis[1,3-bis(cyclohexyl)imidazol-2-ylidene]copper(I) hexafluorophosphate was synthesized according to the literature procedures³. NMR characterizations were carried out using a Bruker Avance 500 MHz spectrometer, chemical shifts (δ) are reported in parts per million (ppm) referenced to tetramethylsilane (^1H) or the internal (NMR) solvent signals (^{13}C). ESI-MS spectra were recorded on a quadrupole ion trap LC mass spectrometer, equipped with electrospray ionization. For the structure of compound **1**, X-ray intensity data were collected on a Agilent Supernova Dual Source (Cu at zero) diffractometer equipped with an Atlas CCD detector using $\text{CuK}\alpha$ radiation ($\lambda = 1.54178 \text{ \AA}$) and ω scans. The images were interpreted and integrated with the program CrysAlisPro (Agilent Technologies)⁴. Using Olex2⁵, the structure was solved by direct methods using the ShelXS structure solution program⁶ and refined by full-matrix least-squares on F^2 using the ShelXL program package⁶. Non-hydrogen atoms were anisotropically refined and the hydrogen atoms in the riding mode and isotropic temperature factors fixed at 1.2 times $U(\text{eq})$ of the parent atoms (1.5 times for methyl groups and the hydroxyl group).

1.2. Synthesis of ligands

1.2.1. 1-(2,4,6-trimethylphenyl)-3-(3-sulfonato-propyl)-imidazolidinium **1**

To a solution of 1-(2,4,6-trimethylphenyl) imidazolidine (0.5 g, 2.7 mmol) in 7 ml of dry dichloromethane was added 1,3-propanesultone (0.32 g, 2.7 mmol), the solution was refluxed for 12 h. The formed suspension was filtered off, washed with diethyl ether and dried under vacuum to yield a white powder; yield 100%. X ray analysis was obtained by recrystallization from methanol:water. A suitable crystal was selected and mounted on a nylon loop on a diffractometer. The crystal was kept at 150(2) K during data collection.

^1H NMR (ppm, DMSO-d_6): 8.65 (1H, s, N-CH-C), 7.03 (2H, s, Ar), 4.15 (4H, m, N- $\text{CH}_2\text{CH}_2\text{-N}$), 3.70 (2H, t, N- CH_2), 2.54 (2H, t, $\text{CH}_2\text{-SO}_3$), 2.27 (3H, s, Me-Ar), 2.26 (6H, s, Me-Ar), 1.95 (2H, q, $\text{CH}_2\text{-(C)-SO}_3$). ^{13}C NMR (dmsO-d_6): 158.9, 139, 135, 131, 129, 50.26, 48.13, 47.59, 46.57, 22.8, 20.48, 17.14 MS, positive mode: $[\text{M}+\text{H}]^+$ 311.1.

Crystal Data: monoclinic, space group C2/c (no. 15), $a = 20.584(4) \text{ \AA}$, $b = 16.0252(13) \text{ \AA}$, $c = 13.038(2) \text{ \AA}$, $\beta = 128.09(3)^\circ$, $V = 3384.9(16) \text{ \AA}^3$, $Z = 4$, $T = 150(2) \text{ K}$, $\mu(\text{MoK}\alpha) = 0.206 \text{ mm}^{-1}$, $D_{\text{calc}} = 1.254 \text{ g/mm}^3$, 12880 reflections measured ($6.4 \leq 2\theta \leq 50.04$), 2897 unique ($R_{\text{int}} = 0.0450$) which were used in all calculations. The final $R1$ was 0.0739 ($>2\sigma(I)$) and $wR2$ was 0.1576 (all data). CCDC number: 1002517.

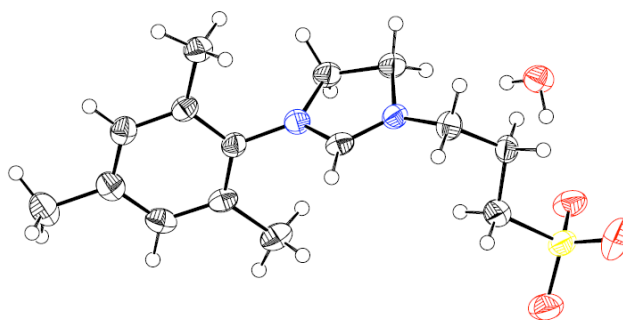


Figure S1: ORTEP plot of 1-(2,4,6-trimethylphenyl)-3-(3-sulfonato-propyl)-imidazolidinium.

1.2.2. 1-(2,4,6-trimethylphenyl)-3-(4-sulfonato-butyl)-imidazolidinium 2

To a solution of 1,4-butanedisulfone (0.37g, 2.7mmol) in 20 mL of dry toluene, was added a solution of 1-(2,4,6-trimethylphenyl)imidazolidine (0.5 g, 2.7 mmol) in 10 mL of toluene, the resultant solution was refluxed for 48 h. The white suspension was filtered off, washed with hexane and ether and dried under vacuum to give a white powder; yield 100%.

^1H NMR (ppm, DMSO- d_6): 8.76 (s, 1H, N-CH-N), 7.03 (s, 2H, Ar), 4.14 (m, 4H, N- $\text{CH}_2\text{CH}_2\text{-N}$), 3.56 (t, 2H, N- CH_2), 2.48 (t, 2H, $\text{CH}_2\text{-SO}_3$) 2.27 (s, 3H, Me-Ar), 2.25 (s, 6H, Me-Ar), 1.78 (t, 2H, NC- CH_2), 1.63 (t, 2H, $\text{CH}_2\text{-CSO}_3$). ^{13}C NMR (ppm, DMSO- d_6): 159.45, 139.87, 136.30, 131.94, 130.02, 74.86, 51.04, 49.01, 47.94, 26.05, 22.42, 21.21, 17.88.

MS, positive mode: $[\text{M}+\text{H}]^+$ 325.1.

1.3. Synthesis of catalysts

1.3.1. Synthesis of Bis[1-(4-potassiumsulfonatebutyl)-3-(2,4,6-trimethylphenyl)-4,5-dihydroimidazolyl-3-ylidene] copper (I) hexafluorophosphate (6)

In an oven-dried vial 324.4 mg of 1-(2,4,6-trimethylphenyl)-3-(4-sulfonato-butyl)-imidazolidinium **4** (1mmol), 186.4 mg of $[\text{Cu}(\text{CH}_3\text{CN})_4]\text{PF}_6$ (0.5mmol) are transferred in 9 ml of dry THF. To the reaction mixture is added 1 ml solution of potassium *t*-butoxide 1M and stirred at room temperature for 16h. Thereafter the reaction mixture was filtrated through a pad of celite and concentrated under reduced pressure. The product was obtained as a clear brown solid upon precipitation with ether. ^1H -NMR (ppm, DMSO- d_6): 6.91 (m, 2H, Ar), 3.78 (m, 2H, N- CH_2), 3.76 (m, 2H, $\text{CH}_2\text{-N}$), 3.53 (t, 2H, N $\text{CH}_2\text{-CH}_3$) SO_3K), 2.50 (t, 2H, N(CH_2) $_3\text{-CH}_2\text{-SO}_3\text{K}$), 2.24 (s, 3H, CH_3 Mes), 2.12 (s, 6H, CH_3 Mes) 1.71 (m, 2H, N $\text{CH}_2\text{-CH}_2\text{-(CH}_2$) $_2\text{SO}_3\text{K}$), 1.61(m, 2H, N(CH_2) $_2\text{-CH}_2\text{-CH}_2\text{SO}_3\text{K}$). ^{13}C -NMR (125 MHz, DMSO- d_6): 199.4, 137.05, 136, 135.5, 129, 51.54, 51.46, 51.02, 48.06, 20.56, 17.66. ^{31}P -NMR (125MHz): -144.18 (m, 1P, PF_6^-).

ESI-MS $[\text{M}-2\text{K}-\text{PF}_6]^+$ 711.1

1.3.2 Synthesis of Bis[1-(4-potassiumsulfonatebutyl)-3-(2,4,6-trimethylphenyl)-4,5-imidazolyl-3-ylidene] copper (I) hexafluorophosphate (8)

324.4 mg of ligand **2** (1 mmol), 186.4 mg of $[\text{Cu}(\text{CH}_3\text{CN})_4]\text{PF}_6$ (0.5 mmol) in 9 ml of dry THF were transferred to an oven-dried vial. To the reaction mixture was added 1 ml solution of potassium *t*-Butoxide 1 M. The reaction mixture is stirred at room temperature for 16h. Thereafter the reaction

mixture was filtrated through a pad of celite and concentrated under reduced pressure. The product (IMDS₂-Cu) was obtained as a clear brown solid upon precipitation with ether.

¹H-NMR (ppm, DMSO-d₆): 7.58 (s, 1H, NCH), 7.35 (s, 1H, CHN), 7.05 (s, 2H, Ar-H), 3.81 (t, 2H, NCH₂), 2.40 (t, 2H, CH₂-SO₃K), 1.92 (s, 3H, CH₃ Mes), 1.83 (s, 6H, CH₃ Mes) 1.63 (m, 2H, NCH₂-CH₂-(CH₂)₂SO₃K), 1.43(m, 2H, N(CH₂)₂-CH₂-CH₂SO₃K). ¹³C-NMR (125 MHz, DMSO-d₆): 176.34, 138.53, 135.44, 134.42, 128.80, 122.39, 122.00, 50.75, 49.94, 31.28, 21.93, 20.60, 17.11.

ESI-MS [M-2K-PF₆]⁺ 707.1

1.3.3 Synthesis of Bis[1-(4-sodiumsulfonatepropyl)-3-(2,4,6-trimethylphenyl)-4,5-dihydroimidazolyl-3-ylidene] copper (I) hexafluorophosphate (5).

Synthesis of this complex was carried out using a similar method as used for the synthesis of complex **6** from ligand **3**. The product was obtained as brown solid.

¹H-NMR (ppm, DMSO-d₆): 6.92 (m, 2H, Ar), 3.34 (m, 2H, N-CH₂), 3.71 (m, 2H, CH₂-N), 3.66 (t, 2H, NCH₂-CH₃)SO₃K), 2.50 (t, 2H, N(CH₂)₃-CH₂-SO₃K), 2.24 (s, 3H, CH₃ Mes), 2.14 (s, 6H, CH₃ Mes) 1.80 (m, 2H, NCH₂-CH₂-CH₂SO₃K). ¹³C-NMR (125 MHz, DMSO-d₆): 201.49, 136.67, 136.73, 135.20, 131.9, 51.30, 67.41, 51.02, 48.06, 16.44. ³¹P-NMR (125MHz): -144.20 (m, 1P, PF₆⁻).

ESI-MS [M-2K-PF₆]⁺ 683.1

1.3.4 Synthesis of Bis[1-(4-sodiumsulfonatepropyl)-3-(2,4,6-trimethylphenyl)-4,5-imidazolyl-3-ylidene] copper (I) hexafluorophosphate (7).

Synthesis of this complex was carried out using a similar method as used for the synthesis of complex **6** from ligand **1**. The product was obtained as dark brown solid.

¹H-NMR (ppm, DMSO-d₆): 7.58 (s, 1H, NCH), 7.33 (s, 1H, CHN), 7.01 (s, 2H, Ar-H), 4.00 (t, 2H, NCH₂), 2.34 (t, 2H, CH₂-SO₃K), 2.28 (s, 3H, CH₃ Mes), 1.77 (s, 6H, CH₃ Mes) 11.76(m, 2H, N(CH₂)₂-CH₂-CH₂SO₃K). ¹³C-NMR (125 MHz, DMSO-d₆): 176.38, 138.51, 135.44, 134.41, 128.79, 122.36, 121.98, 50.73, 49.93, 31.287, 21.93, 17.10.

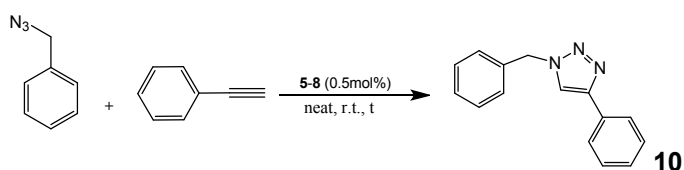
ESI-MS [M-2K-PF₆]⁺ 679.1

1.4 Synthesis of triazoles by CuAAC

1.4.1 Synthesis of 1-benzyl-4-phenyl-1,2,3-triazole.

In a vial fitted with a screw cap, benzyl azide (1 mmol), phenylacetylene (1.05 mmol) and catalyst (0.5 mol%) were loaded. The reaction was allowed to proceed at room temperature and monitored by ¹H NMR analysis of aliquots. After total consumption of benzyl azide, the solid product is collected by filtration and washed with water and pentane. The results are given in Table S1.

Supplementary table S1: %-Yield obtained using **5-8** in neat conditions for click of Benzyl azide and phenylacetylene.



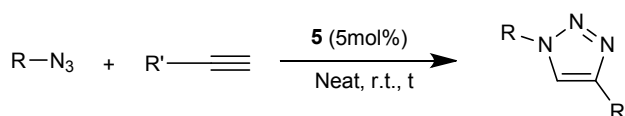
Run	Catalyst ^a	Time (min)	Yield (%) ^b
1	5	8	100
2	6	10	100
3	7	30	99
4	8	35	99

^a Mol% based on copper, ^b Isolated yields are the average of at least two runs.

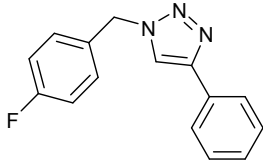
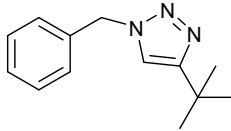
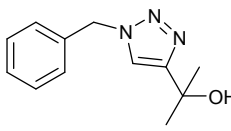
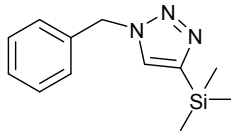
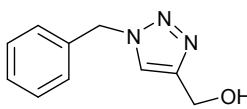
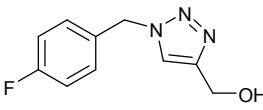
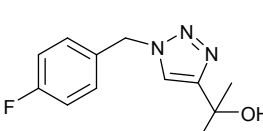
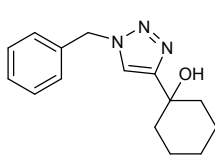
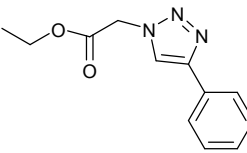
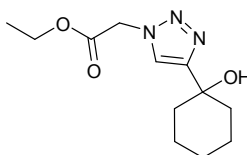
1.4.2. Synthesis of 1,4-substituted 1,2,3-triazoles under neat conditions.

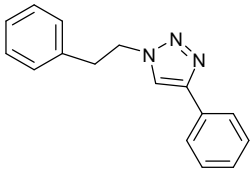
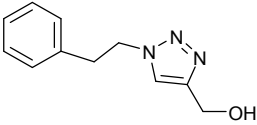
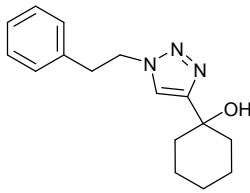
In a vial fitted with a screw cap, an organic azide (1.0 mmol), an alkyne (1.05 mmol) and catalyst Bis[1-(4-sodiumsulfonatebutyl)-3-(2,4,6-trimethylphenyl)-4,5-dihydroimidazolyl-3-ylidene] copper (I) hexafluorophosphate **6** (0.5 mol%, unless specified), are added. In case of molecules bearing two azide groups, a slight excess of terminal alkyne was used (1.1 mmol of alkyne per 0.5 mmol of azide). For molecules holding two terminal alkyne functionalities, 1.05 mmol of alkyne with 2 mmol of azide were used. The reaction was allowed to proceed at room temperature (unless otherwise noted) and monitored by ¹H NMR analysis of aliquots. After total consumption of the azide, the product as collected by filtration and washed with water and pentane. In case of oily products, these were extracted with dichloromethane and washed with aqueous NH₄Cl. Table S2 shows the results for all the triazoles produced. The reported conversions were determined by ¹H NMR and are the average for at least two runs.

Supplementary Table S2: Synthesis of 4-triazoles using **5** in neat conditions.



Run	Triazole Product	Triazole structure	Spectral reference ^a	Time	Yield (%)
1	10		7.70-7.74 (m, 2H, Ar) 7.58 (s, 1H, CH), 7.31-7.36 (m, 4H, Ar), 7.21-7.28 (m, 3H, Ar), 7.19 (s, 1H, Ar), 7.01 (t, 2H, Ar), 5.48 (s, 2H, CH ₂) ⁷	10min	100

2	11		7.71-7.75 (m, 2H, Ar), 7.59 (s, 1H, CH), 7.27-7.36 (m, 4H, Ar), 7.23-7.27 (m, 3H, Ar), 7.19 (s, 1H, Ar), 5.51 (s, 2H, CH ₂). ⁸	30min	100
4	12		7.28-7.31(m, 3H, Ar), 7.18-7.21(m, 1H, Ar), 7.19(s, 1H, Ar), 7.08 (s, 1H, CH), 5.41 (s, 2H, CH ₂), 1.25 (s, 9H, tBu). ¹⁰	1.5h	100
5	13		7.28-7.33(m, 3H, Ar), 7.20-7.23(m, 2H, Ar), 7.19(s, 1H, CH), 5.43 (s, 2H, CH ₂), 1.54 (s, 6H, CH ₃), 2.38 (s, OH). ¹⁰	4h	99
6	14		7.14-7.18(m, 3H, Ar), 7.05-7.02(m, 2H, Ar), 7.21(s, 1H, CH), 5.35 (s, 2H, CH ₂), 0.09(s, 9H, CH ₃) ⁹	30min	88%
7	15		7.34-7.39(m, 3H, Ar), 7.25-7.28(m, 2H, Ar), 7.47(s, 1H, CH), 5.49 (s, 2H, CH ₂), 4.74(s, 2H, CH ₂), 3.61 (s, 1H, OH) ¹¹	2.5h	100
11	16		7.20(t, 2H, Ar), 6.99(t, 2H, Ar), 7.19(s, 1H, CH), 5.42 (s, 2H, CH ₂), 4.78(s, 2H, CH ₂). ¹³	3.5h	99
12	17		7.19-7.22(m, 2H, Ar), 6.99(t, 2H, Ar), 7.20(s, 1H, CH), 5.39 (s, 2H, CH ₂), 1.57(s, 6H, CH ₃), 1.47 (s, OH). ¹⁴	5h	98
13	18		7.34-7.38(m, 3H, Ar), 7.25-7.28(m, 2H, Ar), 7.27(s, 1H, CH), 5.50 (s, 2H, CH ₂), 1.26- 2.07 (m, 10H, Cy), 2.43 (s, 1H, OH). ¹⁵	5min	99
14	19		7.68-7.71(m, 2H, Ar), 7.19-7.31(m, 3H, Ar), 7.76(s, 1H, CH), 5.14 (s, 2H, CH ₂), 4.22 (q, 2H, CH ₂), 1.25 (t, 3H, CH ₃). ¹⁵	30min	100
15	20		7.60 (s, 1H, CH), 5.14 (s, 2H, CH ₂), 4.27 (q, 2H, CH ₂), 1.24-2.06 (m, 10H, Cy), 1.30(t, 3H, CH ₃) ⁴¹	2.5h	99

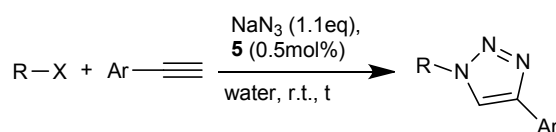
16	21		7.75-7.78 (m, 2H, Ar), 7.12-7.15 (m, 2H Ar), 7.26-7.43 (m, 6H, Ar), 7.46 (s, 1H, CH), 4.63 (t, 2H, CH ₂), 3.25 (t, 2H, CH ₂) ¹⁵	1.5h	99
17	22		7.25-7.33 (m, 2H, Ar), 7.10-7.13 (m, 3H, Ar), 7.28 (s, 2H, CH ₂), 4.74(s, 2H, CH ₂) 4.58 (t, 2H, CH ₂), 3.21 (t, 2H, CH ₂) [®]	1.5h	99
18	23		7.21-7.32 (m, 3H, Ar), 7.07-7.10 (m, 2H, Ar), 7.14 (s, 1H, CH), 4.56 (t, 2H, CH ₂), 3.19 (t, 2H, CH ₂), 1.26-1.98 (m, 5H, Cy), 2.42 (s, 1H, OH). ¹⁶	1.3h	99

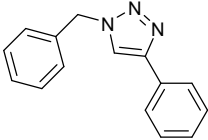
^a ¹H NMR (300Mhz, ppm, CDCl₃, TMS)

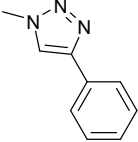
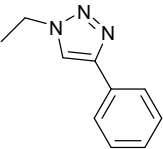
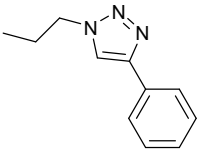
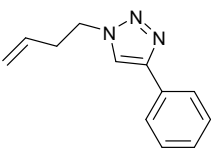
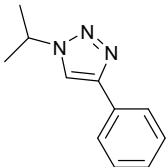
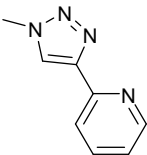
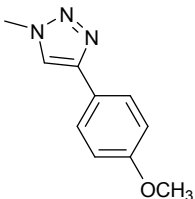
1.4.3. Synthesis of 1,4-substituted triazoles under with *in-situ* formed azides.

In a vial fitted with a screw cap, alkyl halide (1 mmol) and NaN₃ (1.1 mmol) and 1 mL of water (unless otherwise noted) were added. The reaction was allowed to proceed at room temperature (unless otherwise noted) and monitored by ¹H NMR analysis of aliquots. After total consumption of the starting azide, the solid product was collected by filtration and washed with water and pentane. In case of oily products, these were extracted with dichloromethane and washed with aqueous NH₄Cl. Examples of the triazoles synthesized by this procedure are given in table S3 along with the yields and reaction times.

Supplementary table S3: Synthesis of 1,4 substituted triazoles with in-situ azide formation.



Run	Triazole product	Structure of the triazole product	Reaction time (h)	Temperature (°C)	Spectral reference ^e	Yield
1	10 ^a		1.5	R.T.	7.70-7.74 (m, 2H, Ar) 7.58 (s, 1H, CH), 7.31-7.36 (m, 4H, Ar), 7.21-7.28 (m, 3H, Ar), 7.19 (s, 1H, Ar), 7.01 (t, 2H, Ar), 5.48 (s, 2H, CH ₂) ⁷	98

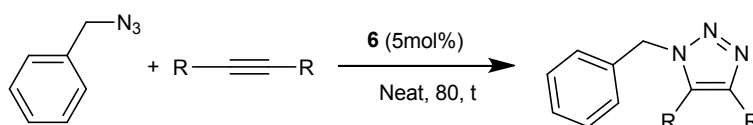
2	24^{b,f}		2.5	R.T.	7.8-7.83 (m, 2H, Ar) 7.33-7.45 (m, 3H, Ar), 7.73 (s, 1H, CH), 4.13 (s, 3H, CH ₃) ¹⁷	95
3	25^a		3	R.T.	7.82 (d, 2H, Ar) 7.42 (t, 2H, Ar), 7.30- 7.34(m, 1H, Ar), 7.76 (s, 1H, CH), 4.43(q, 2H, CH ₂), 1.59 (t, 3H, CH ₃). ¹⁸	90
5	26^a		9	80	7.83 (d, 2H, Ar) 7.42 (t, 2H, Ar), 7.30- 7.35(m, 1H, Ar), 7.74 (s, 1H, CH), 4.36(t, 2H, CH ₂), 1.98 (m, 2H, CH ₂), 0.99(t, 3H, CH ₃). ¹⁸	85
6	27^c		4	R.T.	7.82-7.84 (d, 2H, Ar) 7.42 (t, 2H, Ar), 7.30- 7.35(m, 1H, Ar), 7.74 (s, 1H, CH), 4.47(t, 2H, CH ₂), 5.09(m, 2H, CH ₂), 5.73-5.86(m, 1H, CH), 2.70(q, 2H, CH ₂) ¹⁸	89
7	28^a		12	80	7.8-7.85 (d, 2H, Ar) 7.42 (t, 2H, Ar), 7.30- 7.35(m, 1H, Ar), 7.76 (s, 1H, CH), 4.88(s, 1H, CH), 1.63 (d, 6H, CH ₃). ²¹	75
9	29		8	R.T.	8.58 (s, 1H, Py) 8.16- 8.19 (d, 1H, Py), 7.78(t, 1H, Py), 7.23 (t, 1H, Py), 8.12(s, 1H, CH), 4.17 (s, 3H, CH ₃). ²²	85
10	30		8	R.T.	7.74 (d, 2H, Ar) 6.95 (d, 2H, Ar), 7.65 (s, 1H, CH), 4.12(s, 3H, CH ₃), 3.84 (s, 3H, CH ₃). ²³	91

^a From alkyl (benzyl) bromide, ^b from alkyl iodide, ^c from allyl bromide, solvent: DMSO/water 1:1,^d dibromoethane, solvent DMSO/water 1:1.^e ¹H-NMR (300Mhz, ppm, CDCl₃, TMS). ^f ¹H-NMR (300Mhz, ppm, DMSO-d₆, TMS)

1.4.4. Synthesis of 1,4,5-substituted triazoles.

In a vial fitted with a screw cap, internal alkyne (1.05 mmol) and organic azide (1 mmol) and catalyst (5 mol%) are added. The reaction was allowed to proceed at 80 °C and monitored by ¹H NMR analysis of aliquots. After the reaction time, the solid product was collected by filtration and washed with water and pentane. After the reaction time, the product is purified by column chromatography (ether:hexane 1:1 to ether). The results are given in Table S4.

Supplementary Table S4: Synthesis of 1,4,5 substituted triazoles using catalyst **6** in neat conditions.



Run	Product triazole	Triazole structure	Reaction time (h)	Yield (%)	spectral reference ^a
1	31		24	12	7.46-7.50(m, 2H, Ar), 7.32-7.40 (m, 3H, Ar), 7.14-7.21(m, 7H, Ar), 7.05-7.08 (m, 2H, Ar), 6.93-6.96(m, 2H, Ar), 5.33 (s, 2H, CH ₂) ⁹
2			48	38	7.05-7.08 (m, 2H, Ar), 6.93-6.96(m, 2H, Ar), 5.33 (s, 2H, CH ₂) ⁹
3	32		24	46	7.42-7.27 (m, 3H, Ar), 7.21-7.18 (m, 2H, Ar), 5.48 (s, 2H, CH ₂), 2.65(q, 2H, CH ₂), 2.52(q, 2H, CH ₂), 1.28(t, 3H, CH ₃), 0.96(t, 3H, CH ₃) ⁴⁷
4			48	82	0.96(t, 3H, CH ₃) ⁴⁷

^a ¹H-NMR (300Mhz, ppm, CDCl₃, TMS)

1.4.5. Synthesis of 1-substituted triazoles

Procedure A)

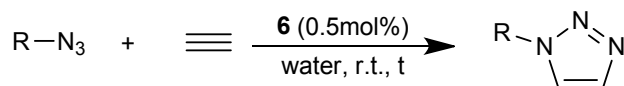
To a vial fitted with screw cap with 1 mmol of azide, 1.5 mmol of CaC₂ and 1 mol% of catalyst relative to the azide is added 1 mL of deoxygenated water. The reaction was stirred at room temperature and monitored by TLC. After the reaction was completed, the mixture was acidified at pH~5 with HCl 0.1N and the organic material was washed with brine and extracted with diethyl ether. Column chromatography may be needed in case the product is not pure enough.

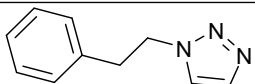
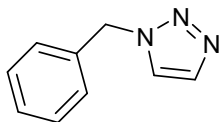
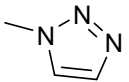
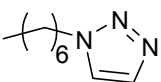
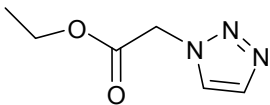
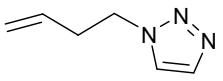
Procedure B)

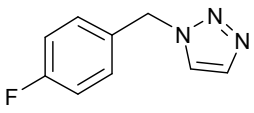
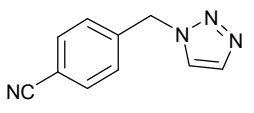
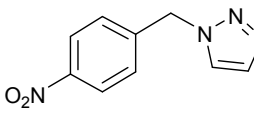
To a vial fitted with screw cap with 1 mmol of azide and 0.5 mol% of catalyst relative to the azide is added 1 mL of deoxygenated water, the vial is purged with acetylene gas and the reaction is stirred under a balloon pressure at room temperature and monitored by TLC. After the reaction was completed, organic material was washed with brine and extracted with diethyl ether. The reaction is also applicable to azides prepared *in-situ* during the catalysis. Table S5 shows the results obtained

with benzyl azide both in pure form and formed *in-situ* in the reaction mixture. Solvents like DMSO, acetonitrile or mixtures of acetonitrile/water and DMSO/water may be used, providing excellent yields.

Supplementary table S5: Synthesis of 1 substituted triazoles using **5** in water.



Run	Triazole product	Triazole structure	Source of alkyne	Solvent	Time (h)	Yield (%)	Spectral reference ^d
1	33		CaC ₂ (1.5eq)	H ₂ O	12	55	7.41 (s, 2H, Ar), 7.04-7.09(m, 3H, Ar), 6.87-6.90(dd, 2H, CH), 4.42 (t,2H, CH ₂), 3.01 (t, 2H, CH ₂) ⁴²
2			CaC ₂ (1.5eq)	H ₂ O:DMSO	12	85	
3			C ₂ H ₂	H ₂ O	12	94	
4			C ₂ H ₂	H ₂ O:DMSO	12	98	
5 ^a			C ₂ H ₂	H ₂ O	18	95	
6	34		C ₂ H ₂	H ₂ O	18	99	7.34-7.40 (m, 3H, Ar), 7.25-7.28 (m, 2H, Ar), 7.72 (s, 1H, CH), 7.48 (s, 1H, CH), 5.57 (s, 2H, CH ₂) ²⁴
7 ^a			C ₂ H ₂	H ₂ O	18	95	
8 ^{ab}	35		C ₂ H ₂	H ₂ O:DMSO	18	75	7.56 (s,1H, CH), 7.73(s, 1H, CH) 4.06 (s, 3H, CH ₃) ⁴³
9	36		C ₂ H ₂	H ₂ O	18	86	7.64 (s, 1H, CH), 7.51 (s,1H, CH), 4.31 (t, 2H, CH ₂), 1.84 (m,2H, CH ₂), 1.18-1.26 (m, 8H,(CH ₂) ₃), 0.8 (m, 3H,CH ₃). ⁴⁴
10 ^{a,b}	37		C ₂ H ₂	H ₂ O:DMSO	18	80	7.61(s, 1H, CH), 7.57(s,1H, CH), 5.06(s, 2H, CH ₂), 4.09(q, 2H, CH ₂), 1.13(t, 3H, CH ₃). ²⁵
11 ^{a,b}	38		C ₂ H ₂	H ₂ O:DMSO	24	75 ^c	7.61(s, 1H, CH), 7.50 (s,1H, CH) 5.62-5.75 (m, 1H, CH, Allyl), 4.98- 5.04 (m, 2H, CH ₂ , Allyl), 4.39 (t, 2H, CH ₂), 2.60 (q,2H, CH ₂) ⁴⁵

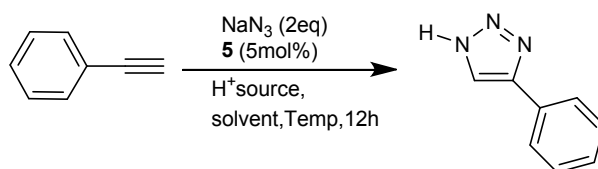
12 ^{a,b}	39		C ₂ H ₂	H ₂ O:DMSO	18	85	7.51 (s, 1H, CH), 7.28 (s, 1H, CH), 7.03-7.08(m, Ar, 2H, 6.85(t, 2H, Ar), 5.33 (s, 2H, CH ₂) ⁴²
13 ^{a,b}	40		C ₂ H ₂	H ₂ O:DMSO	18	88	7.66-7.69(d, 2H, Ar), 7.33-7.36(d, 2H, Ar), 7.78(s, 1H, CH), 7.57(s, 1H, CH), 5.66 (s, 2H, CH ₂) ²⁶
14 ^{a,b,e}	41		C ₂ H ₂	H ₂ O:DMSO	18	95	8.26(d, 2H, Ar), 7.50(d, 2H, Ar), 8.22(s, 1H, CH), 7.81(s, 1H, CH), 5.82(s, 2H, CH ₂) ²⁷

^a From azide formed *in-situ* (benzyl bromide and sodium azide), ^b Solvent mixture H₂O:DMSO 1:1 v/v, ^c Reaction at 75°C. ^d ¹H-NMR (300Mhz, ppm, CDCl₃, TMS). ^e ¹H-NMR (300Mhz, ppm, DMSO-d₆, TMS)

1.4.6. Synthesis of 4-phenyl-1,2,3 triazoles.

To vial fitted with a screw cap was added 1 mmol of the acetylene compound and 2 mmol of NaN₃ in 2mL of solvent, 2mmol of proton source is added to the mixture. The reaction mixture is heated to the given temperature for 12h. Thereafter, water is added to the reaction mixture and extracted with ethyl acetate. If necessary, the product is purified by column chromatography. The results are given in Table S6.

Supplementary table S6: Synthesis of 4-phenyl-1,2,3 triazole with in-situ HN₃ generation applying **5**.



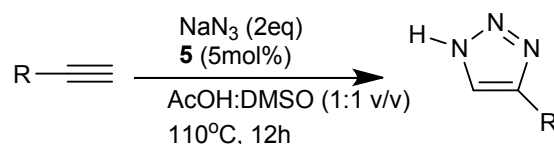
Run	Source of N ₃ ⁻ (2eq)	Source of H ⁺ (2eq)	Solvent	Temp (°C)	Yield (%)
1	NaN ₃	-----	H ₂ O	R.T.	N. R.
2	NaN ₃	-----	H ₂ O	100	N. R.
3	NaN ₃	HCl aq.	H ₂ O	R.T.	N. R.
4	NaN ₃	HCl aq.	H ₂ O	100	N. R.
5	NaN ₃	K ₂ CO ₃	H ₂ O	100	N. R.

6	NaN ₃	NaHCO ₃	H ₂ O	100	N. R.
7	NaN ₃	AcOH	H ₂ O	100	<5
8	NaN ₃	AcOH + DIPEA	H ₂ O	100	<5
9	NaN ₃	AscH	H ₂ O	100	15
10	NaN ₃	AcOH + NaAsc	H ₂ O	100	24
11	NaN ₃	AcOH (ex)+NaAs (1 eq)	AcOH/H ₂ O	100	34
12	TMSN ₃	-----	H ₂ O	100	<5
13	TMSN ₃	AcOH	H ₂ O	100	<15
14	NaN ₃	AcOH(ex.)	DMSO	110	96
15	NaN ₃	AcOH (2 eq)	DMSO	110	95
16	TMSN ₃	----	DMSO/H ₂ O 9:1	110	65
17	TMSN ₃	-----	DMSO/MeOH 9:1	110	94

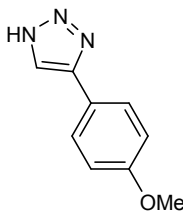
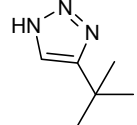
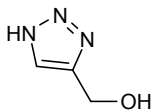
1.4.7. Synthesis of 4-substituted-1,2,3 triazoles.

To vial fitted with a screw cap was added 1 mmol of the acetylene compound and 2 mmol of NaN₃ in a mixture of AcOH: DMSO (1:1, dry). The reaction mixture is heated to 110°C for 12h. Thereafter, water is added to the reaction mixture and extracted with ethyl acetate. If necessary, the product is purified by column chromatography. The results are given in Table S7.

Supplementary table S7: Synthesis of 4-substituted-1,2,3 triazoles with *in-situ* HN₃ generation applying **5**.



Run	Triazole Product	Triazole Structure	Yield (%)	Spectral reference ^a
1	42		96	7.99(s, 1H, CH), 7.81-7.84(m, 2H, Ar), 7.36-7.48(m, 3H, Ar), 7.81(s, 1H, CH), 5.82(s, 2H, CH ₂) ²⁸

2	43^b		92	8.15(s, 1H, CH), 7.79(d, 2H, Ar), 7.02(d, 3H, Ar), 3.79(s, 3H, CH ₃) ²⁸
3	44		60	7.42 (s, 2H, CH), 1.29 (9H, t-Bu) ⁴⁶
4	45		55	7.71(s, 1H, CH), 5.30(s, 2H, CH ₂), 2.12(s, 1H, OH) ²⁹

^a ¹H NMR (300Mhz, ppm, CDCl₃, TMS). ^b ¹H-NMR (300Mhz, ppm, DMSO-d₆, TMS)

1.5. NMR spectra of selected compounds

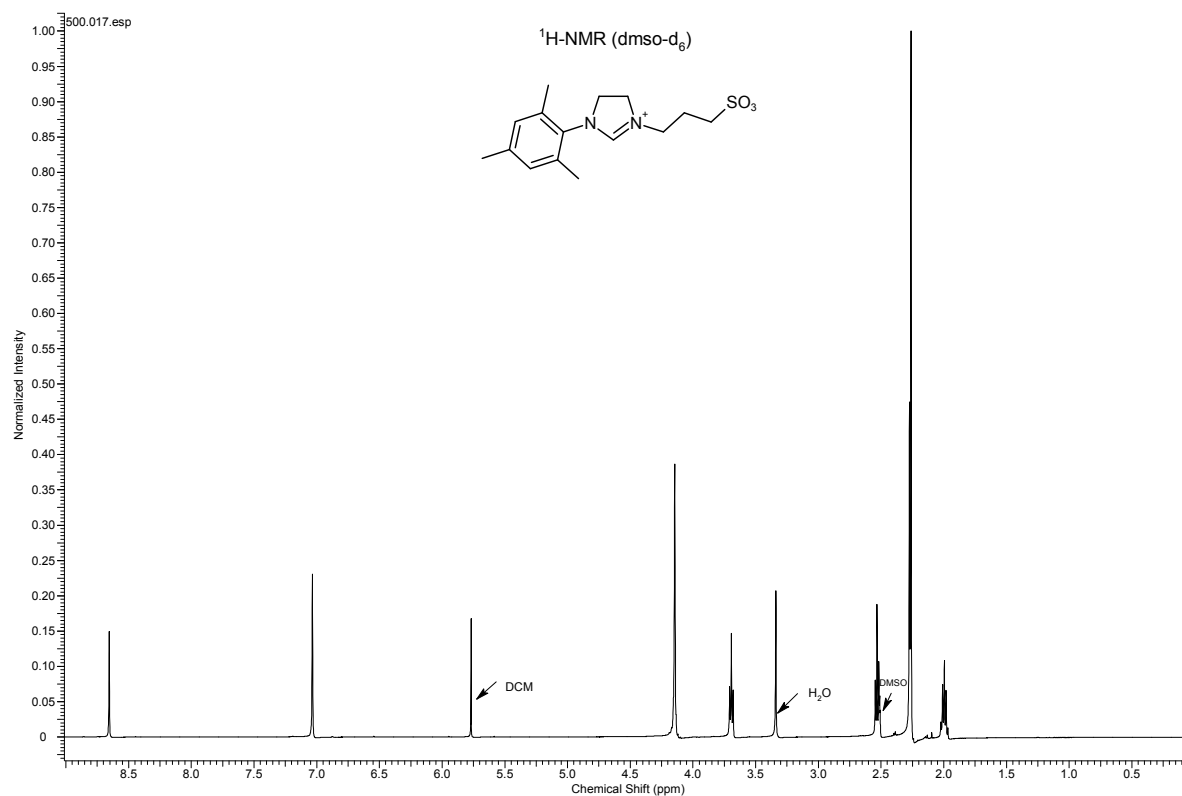


Figure S2: ¹H-NMR spectrum of **3**.

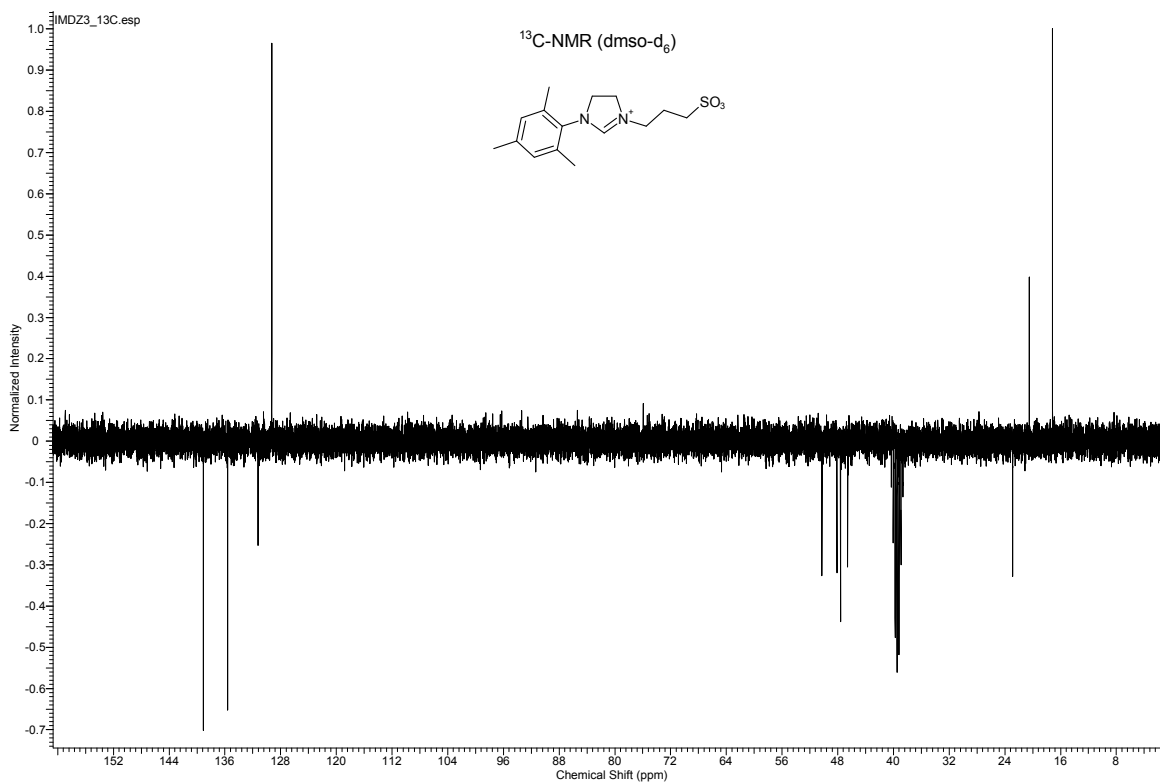


Figure S3: ¹³C-NMR spectrum of **3**.

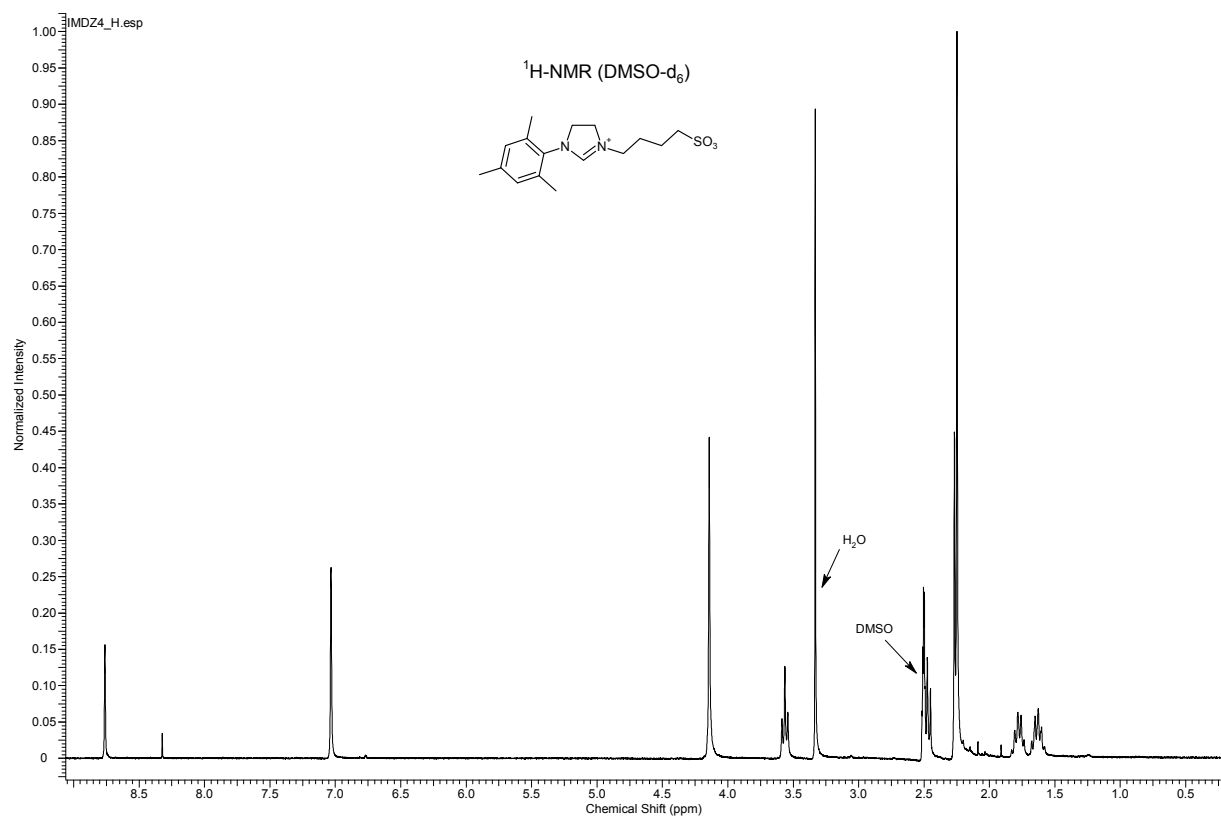


Figure S4: ¹H-NMR spectrum of **4**.

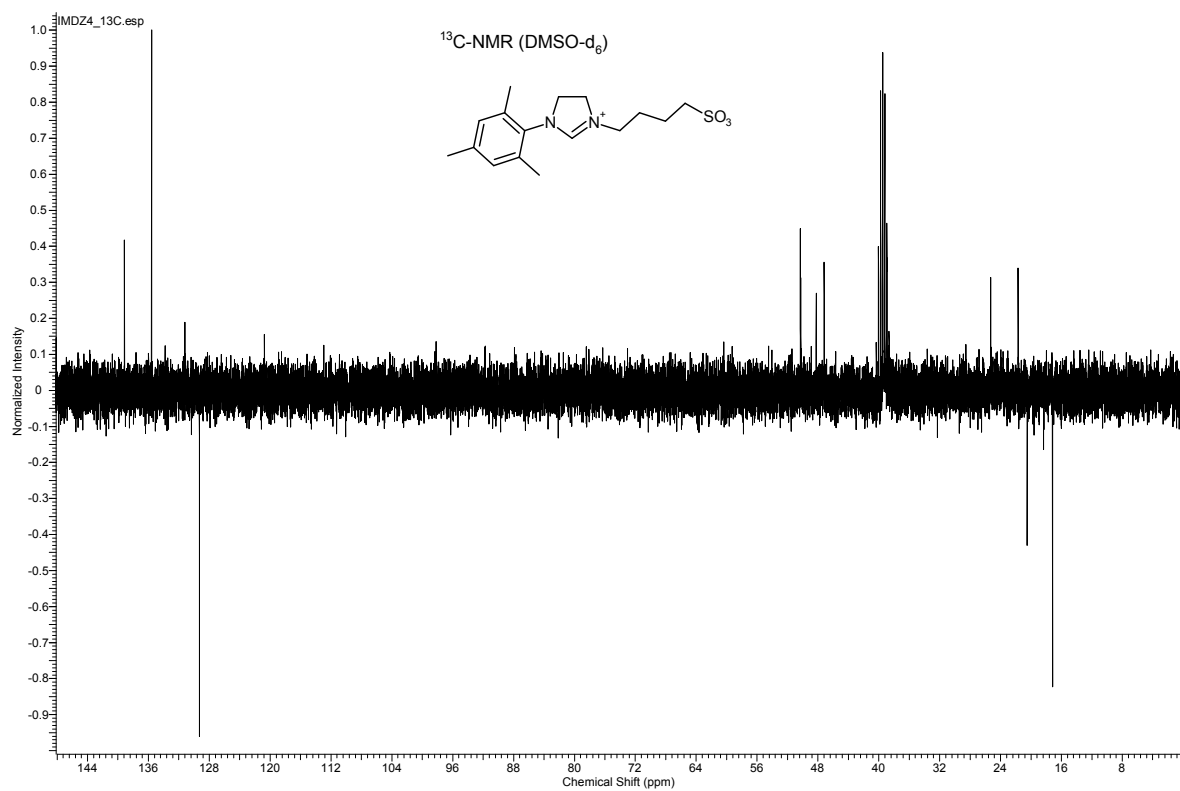


Figure S5: ¹³C-NMR spectrum of **4**.

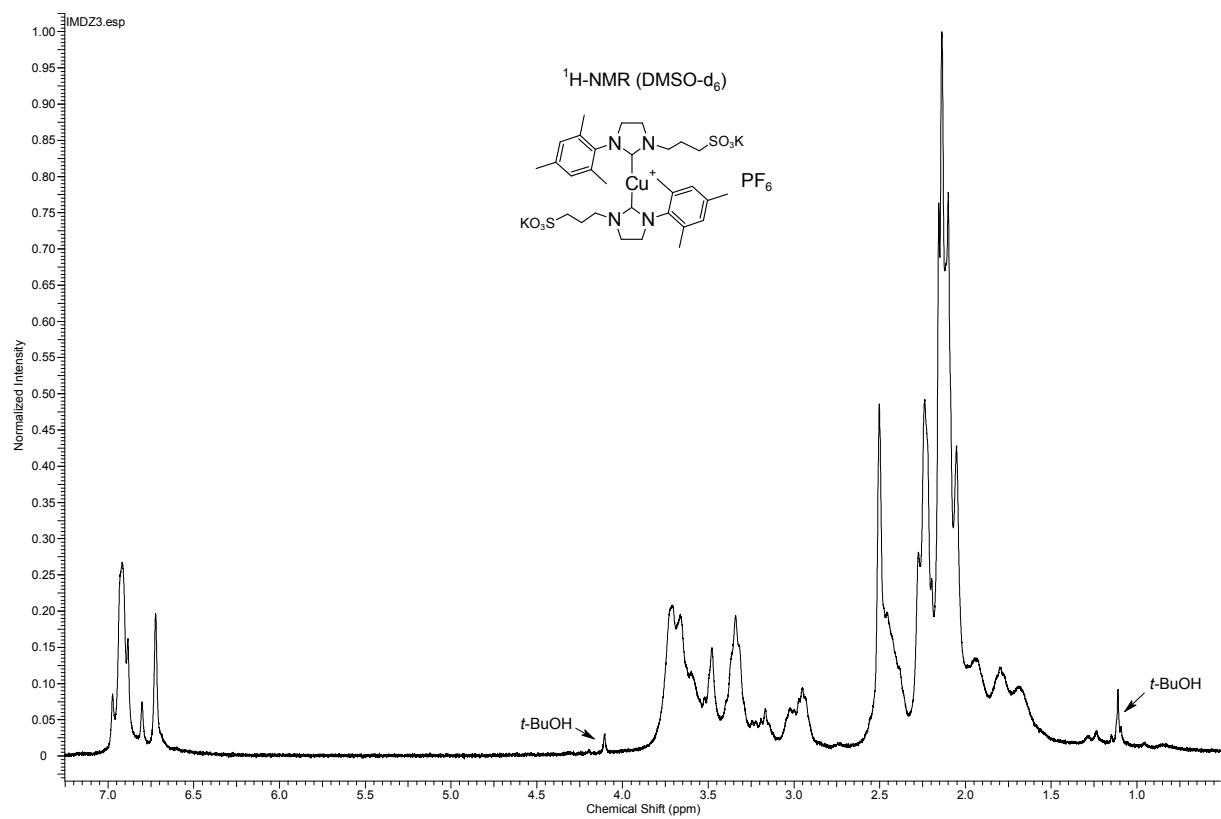


Figure S6: ¹³C-NMR spectrum of 5.

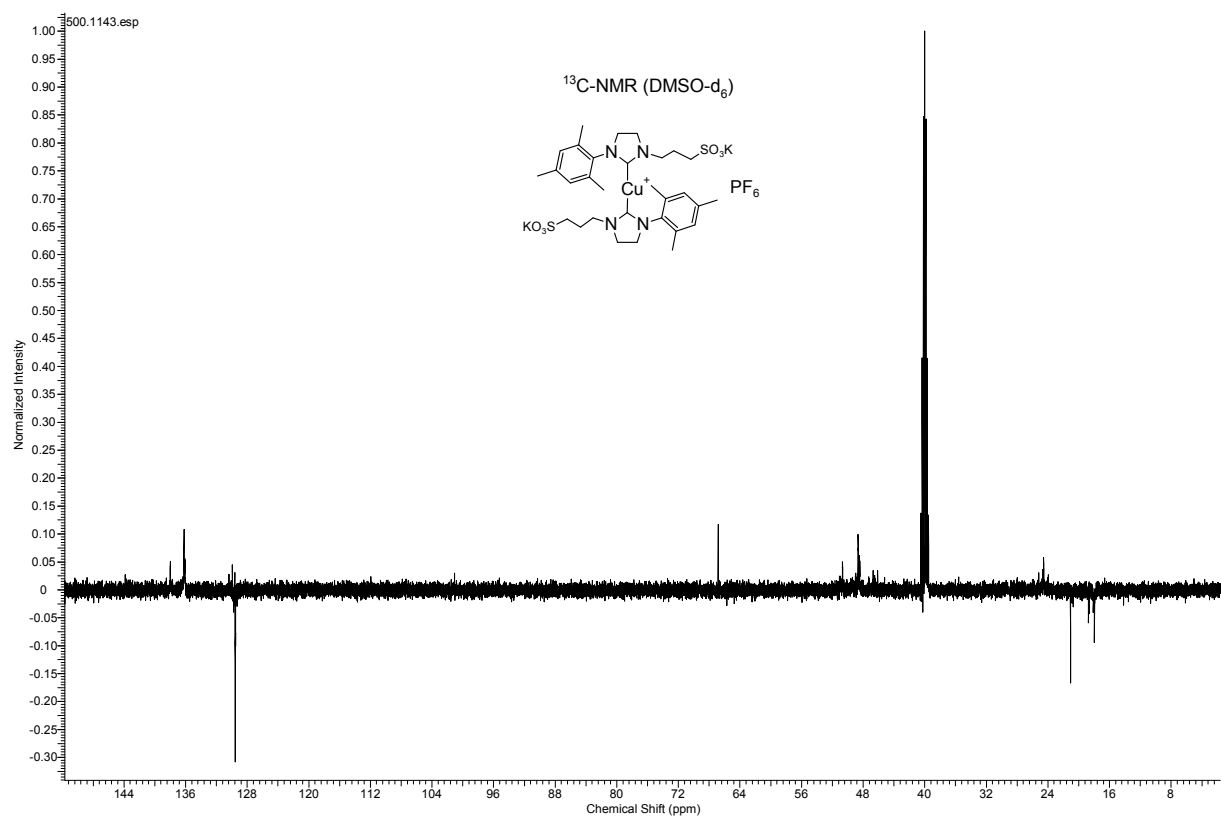


Figure S5-1: ¹³C-NMR spectrum of 5.

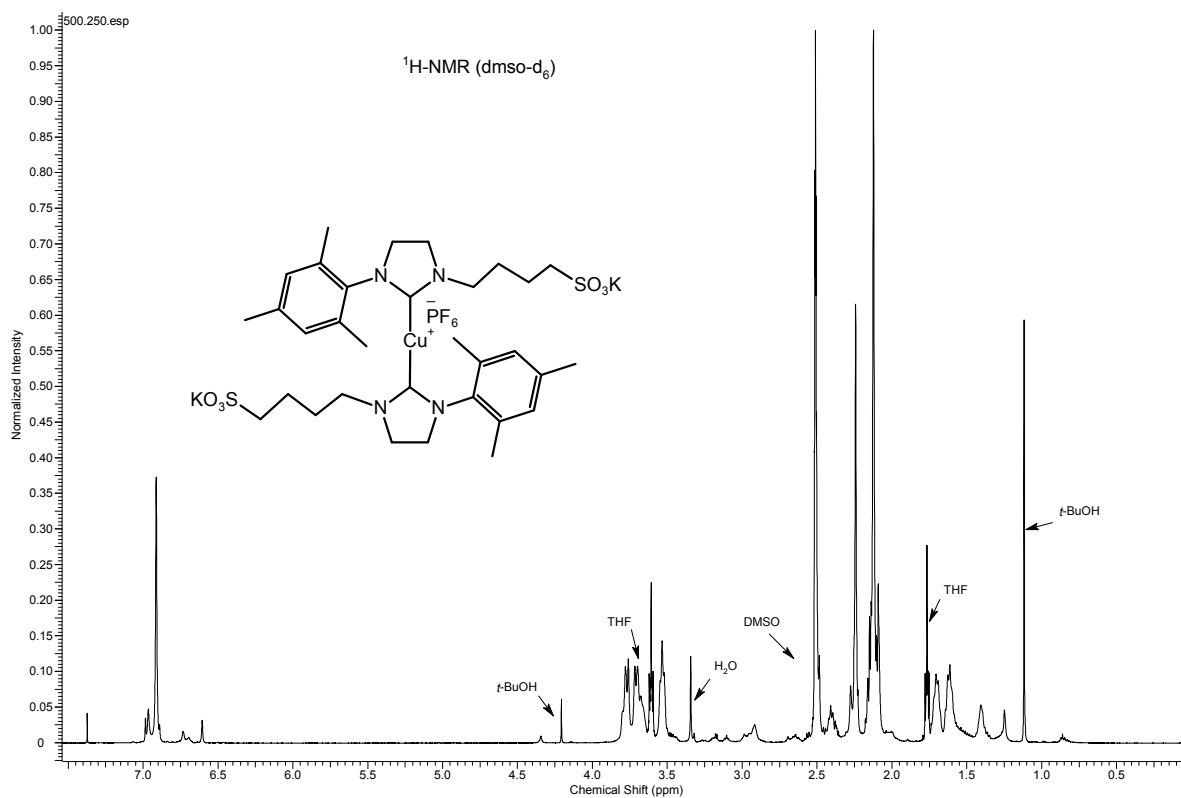


Figure S6: ¹H-NMR spectrum of 6.

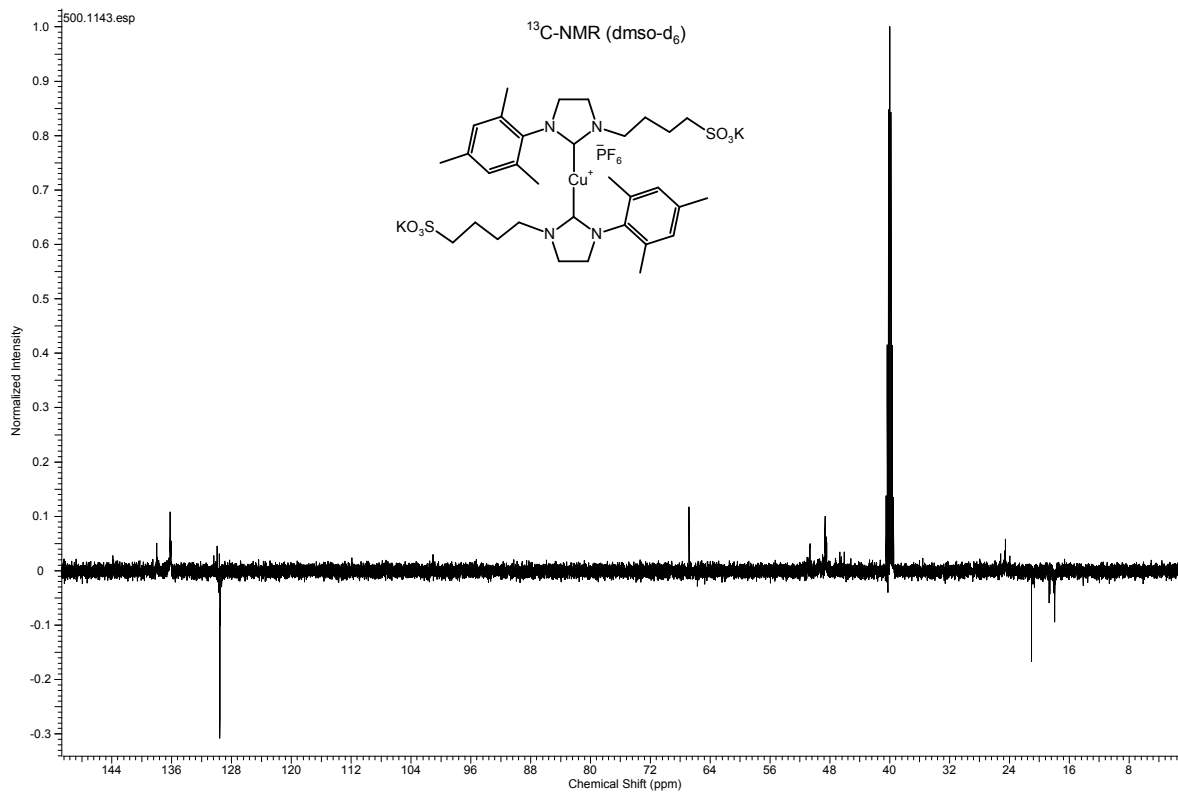


Figure S7: ¹³C-NMR spectrum of 6.

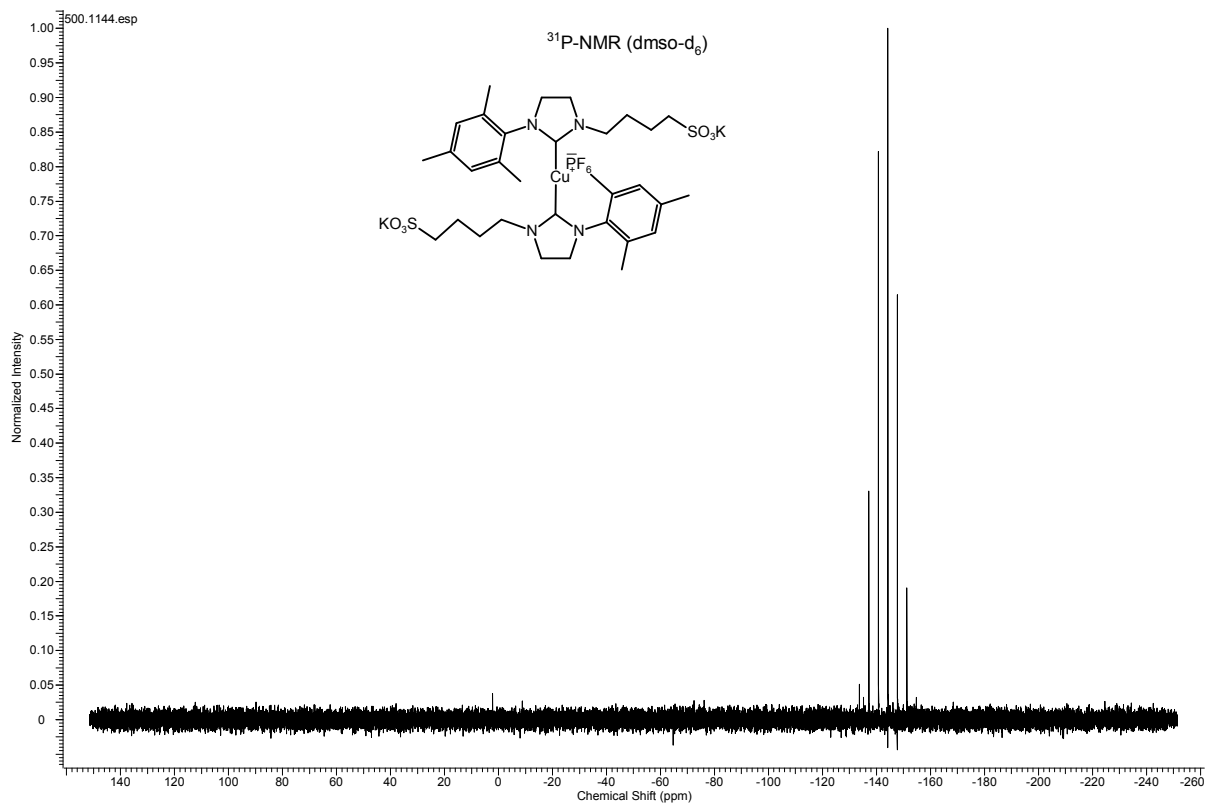


Figure S8: ³¹P-NMR spectrum of **6**.



Figure S9: ¹⁹F-NMR spectrum of **6**.

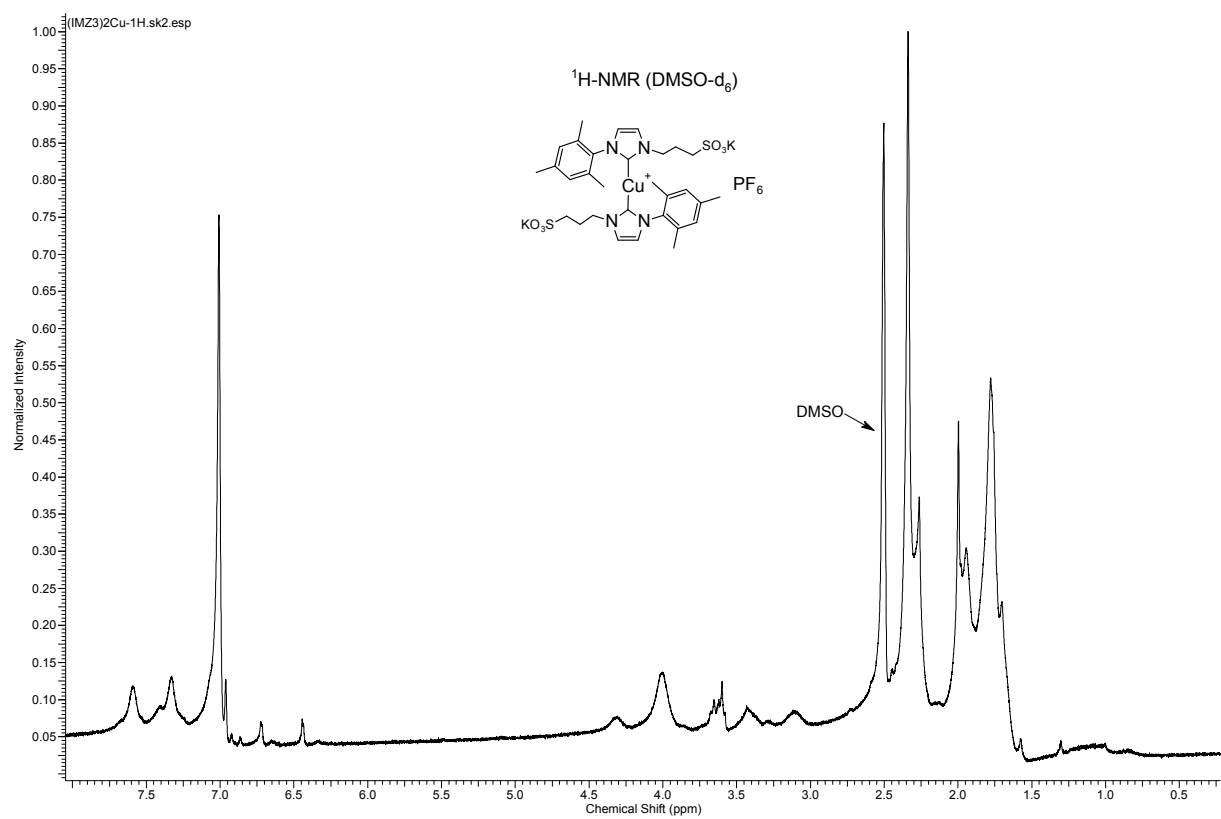


Figure S10: ¹H-NMR spectrum of 7.

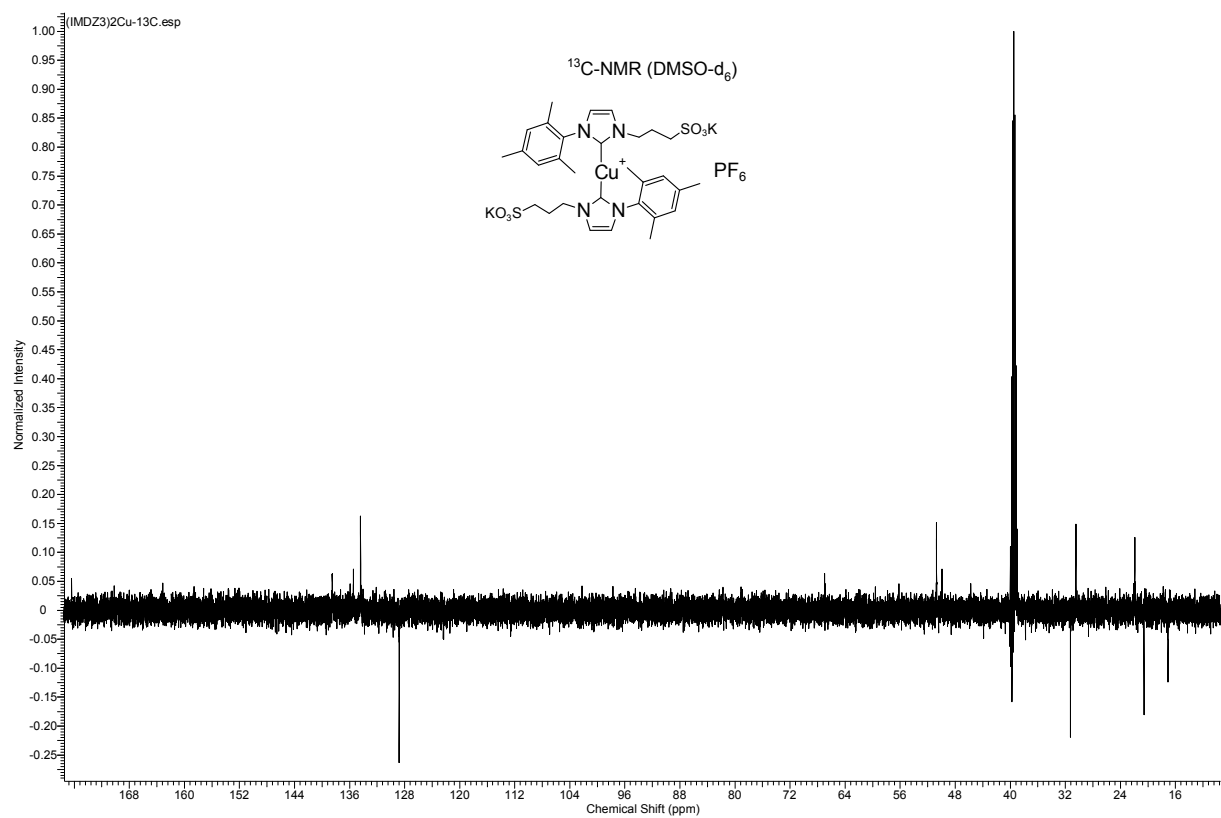


Figure S10-1: ¹³C-NMR spectrum of 7.

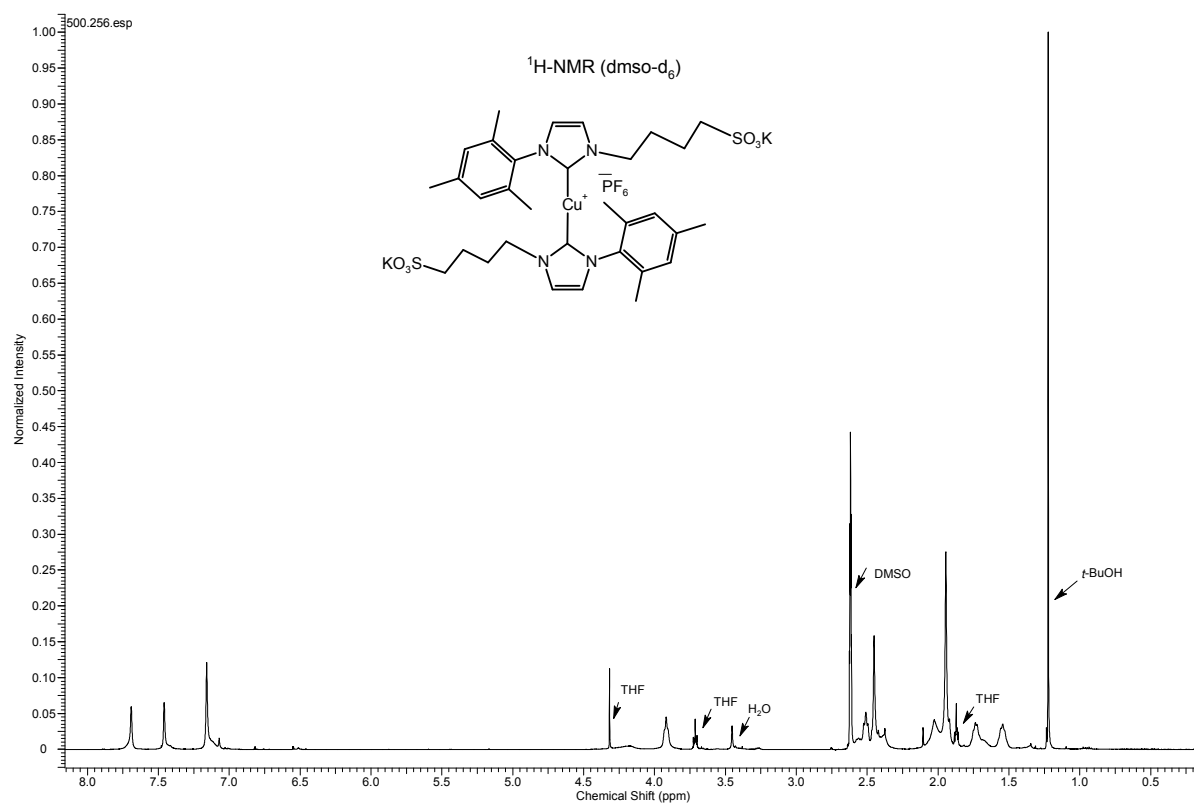


Figure S11: ¹H-NMR spectrum of **8**.

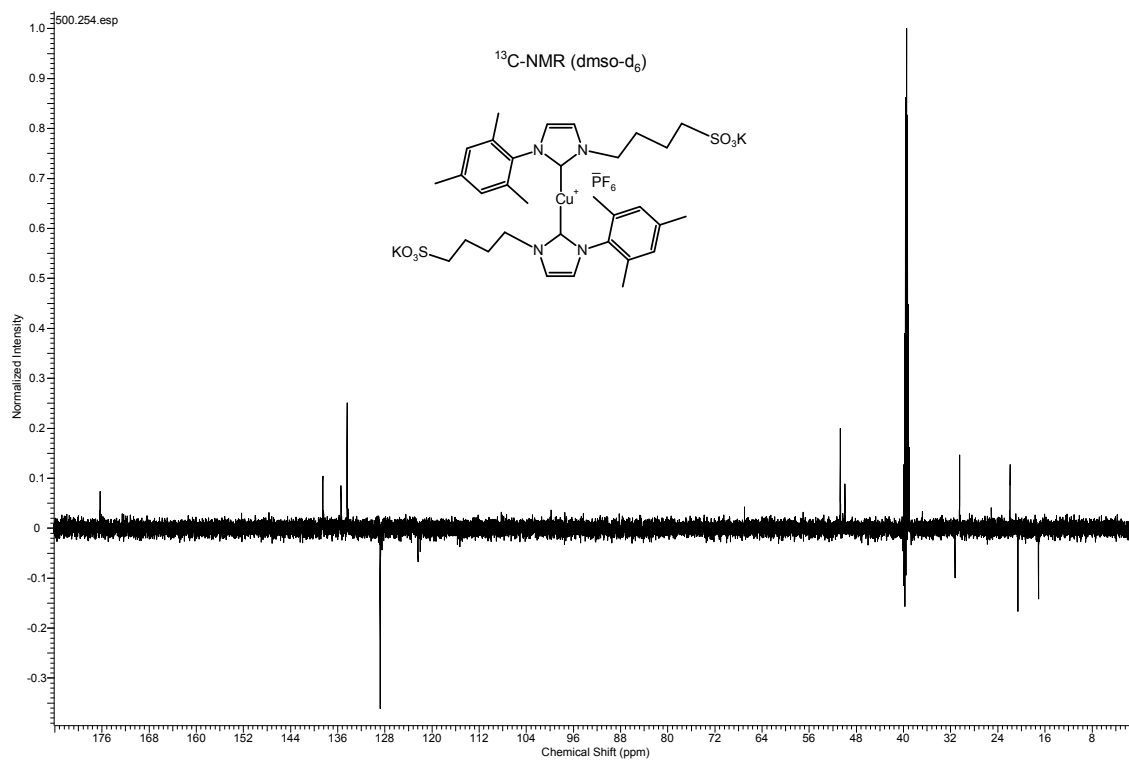


Figure S12: ^{13}C -NMR spectrum of **8**.

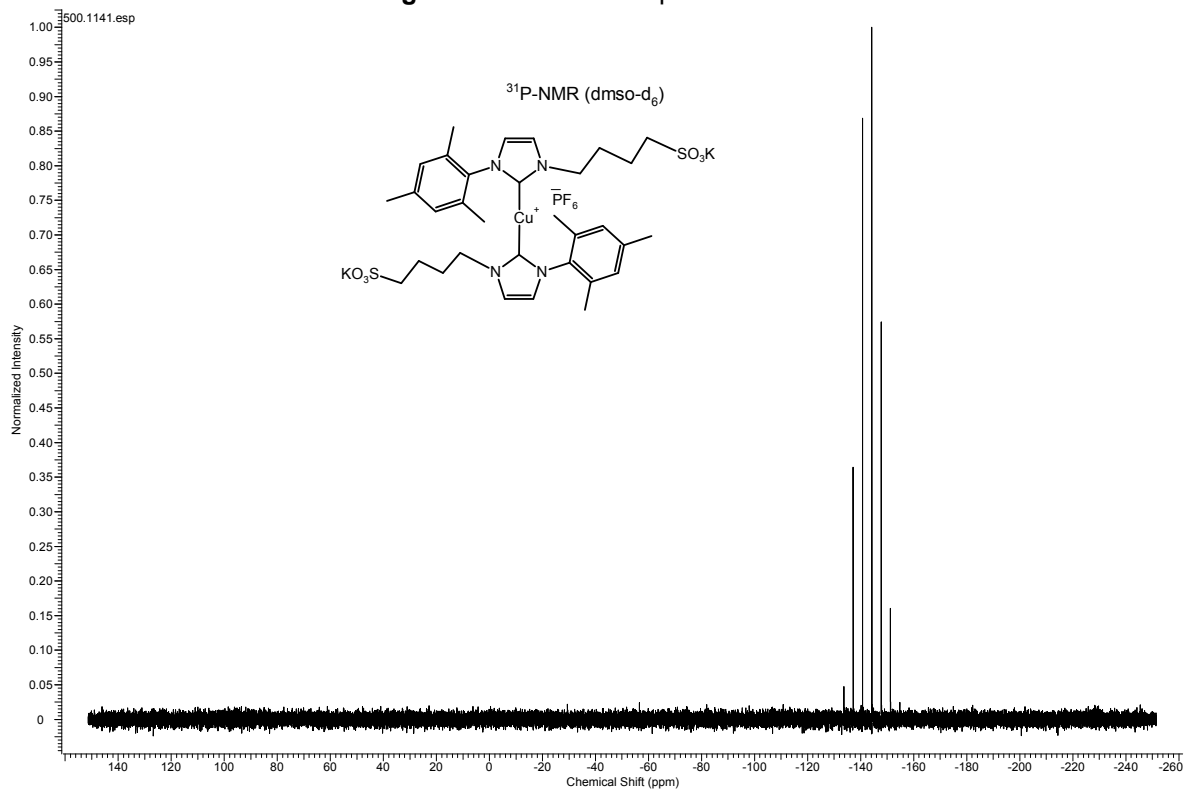


Figure S13: ^{31}P -NMR spectrum of **8**.

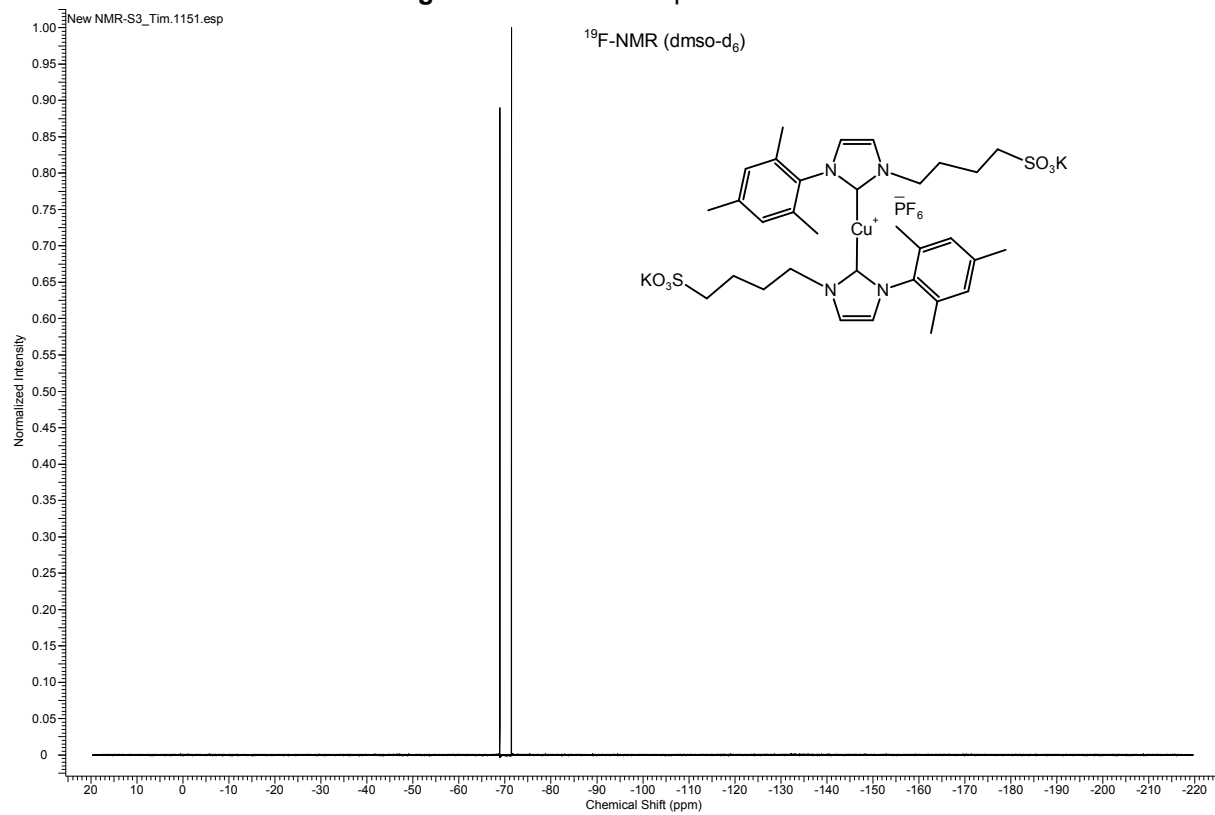


Figure S14: ^{19}F -NMR spectrum of **8**.

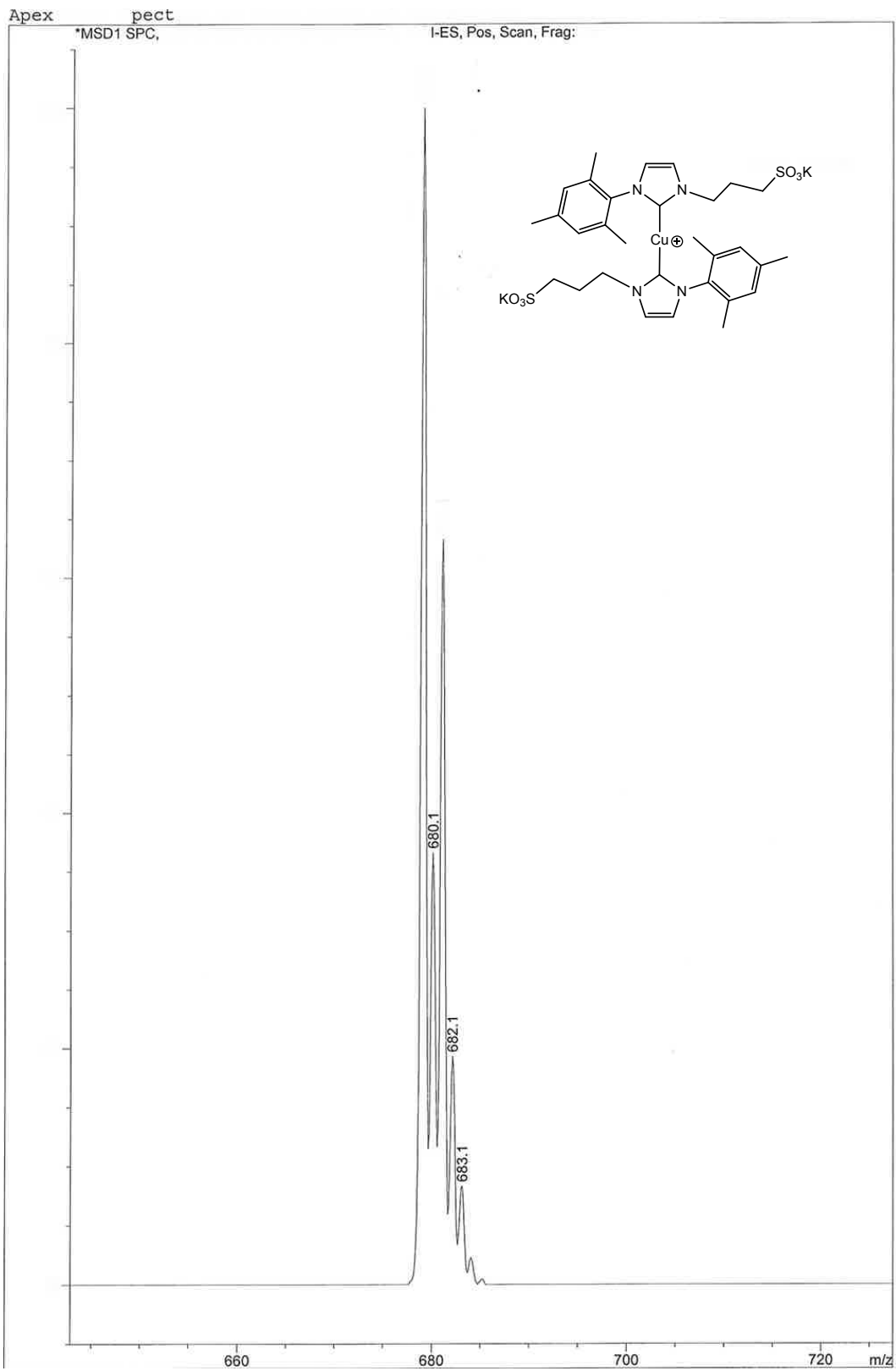


Figure S15: ESI-MS spectrum of 7.

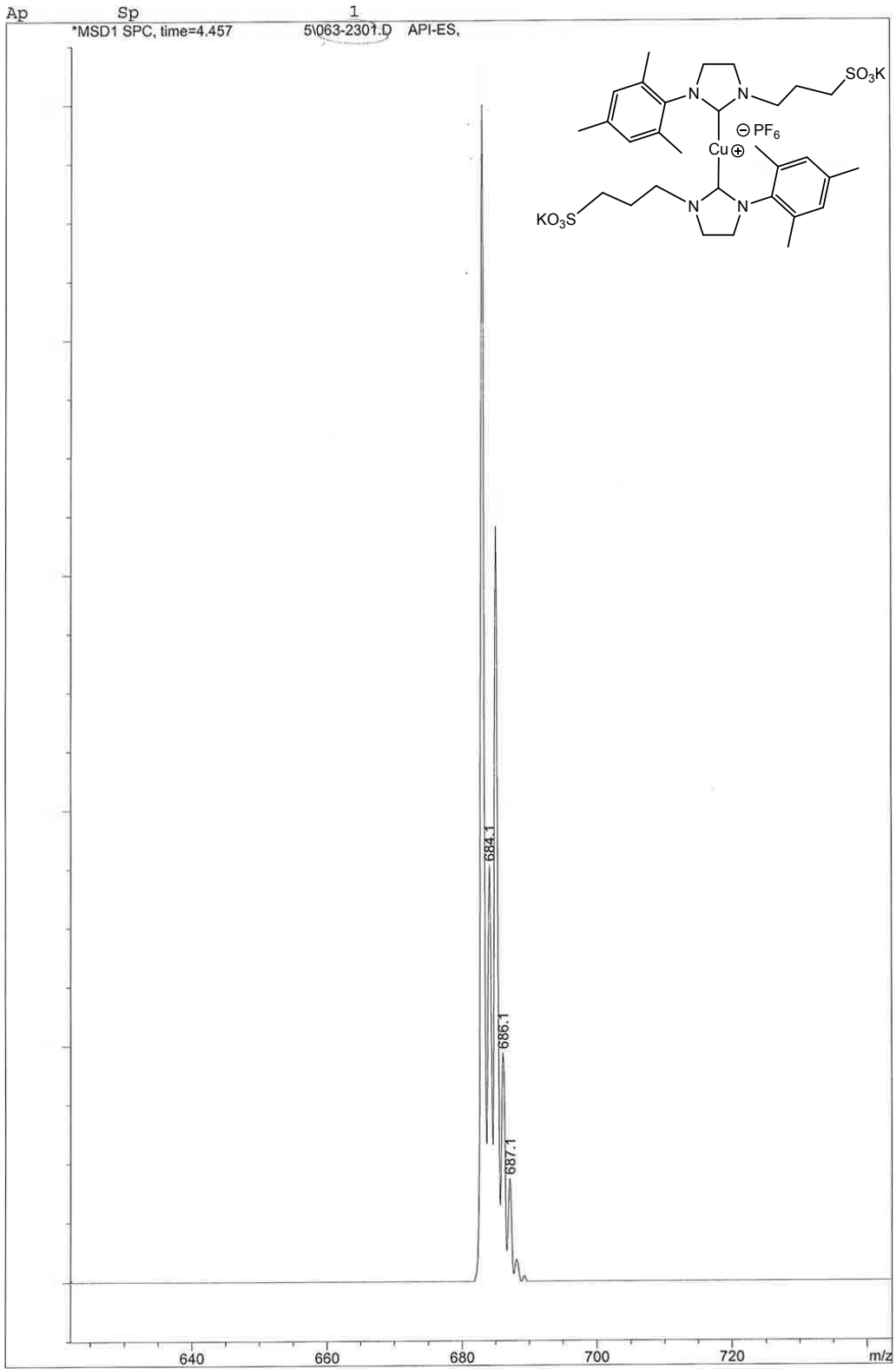


Figure S16: ESI-MS spectrum of 5.

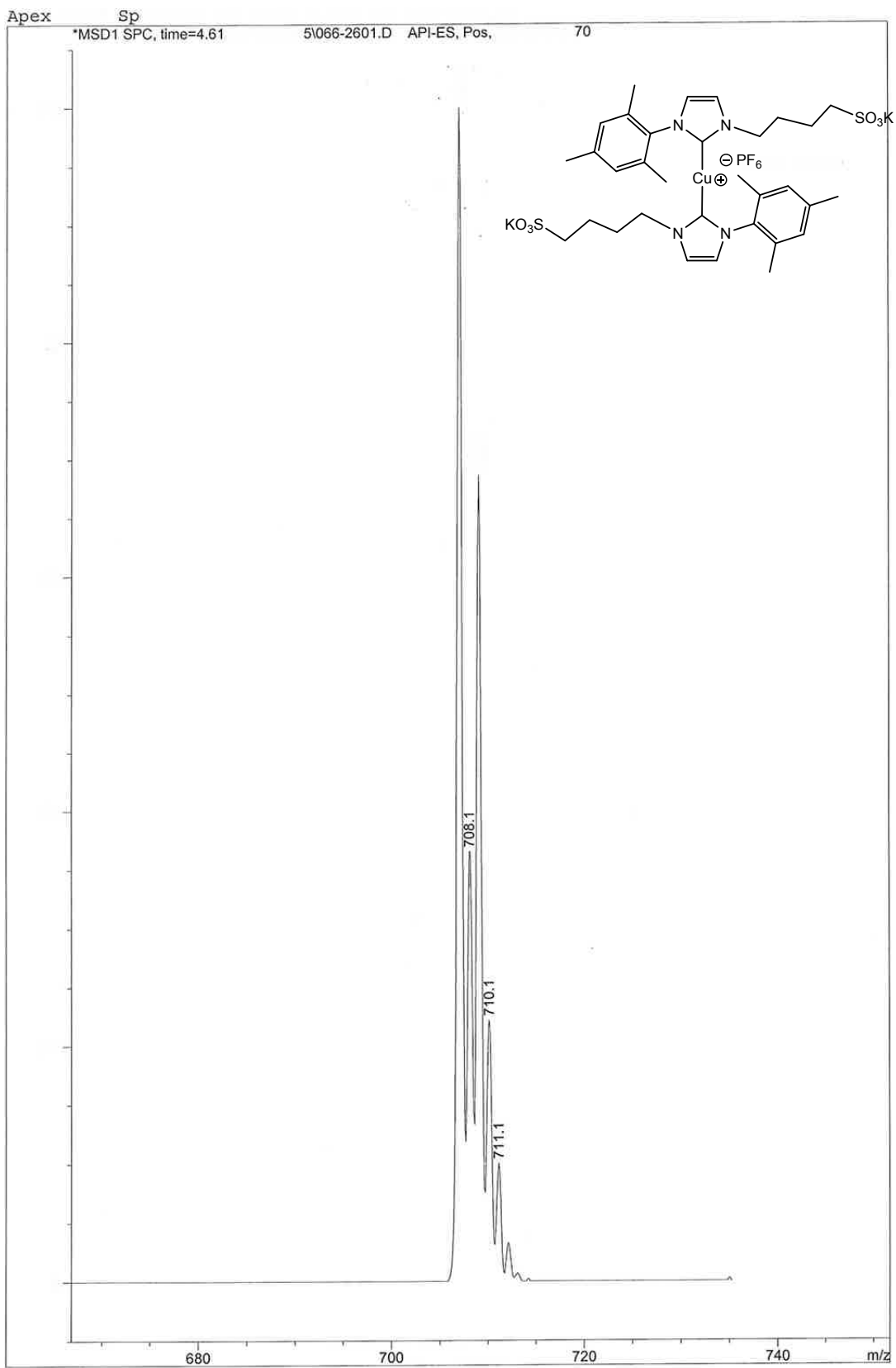


Figure S17: ESI-MS spectrum of 8.

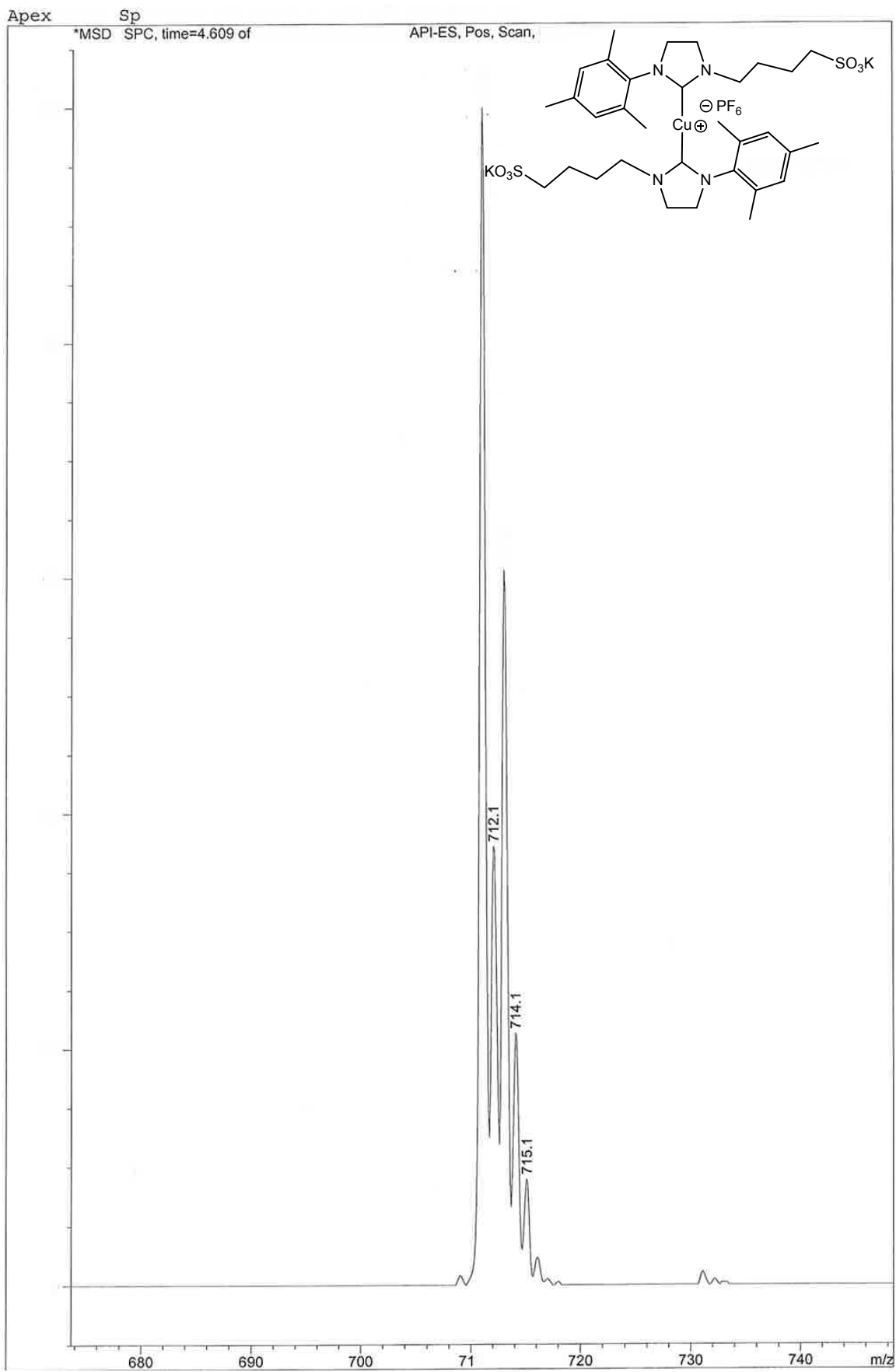
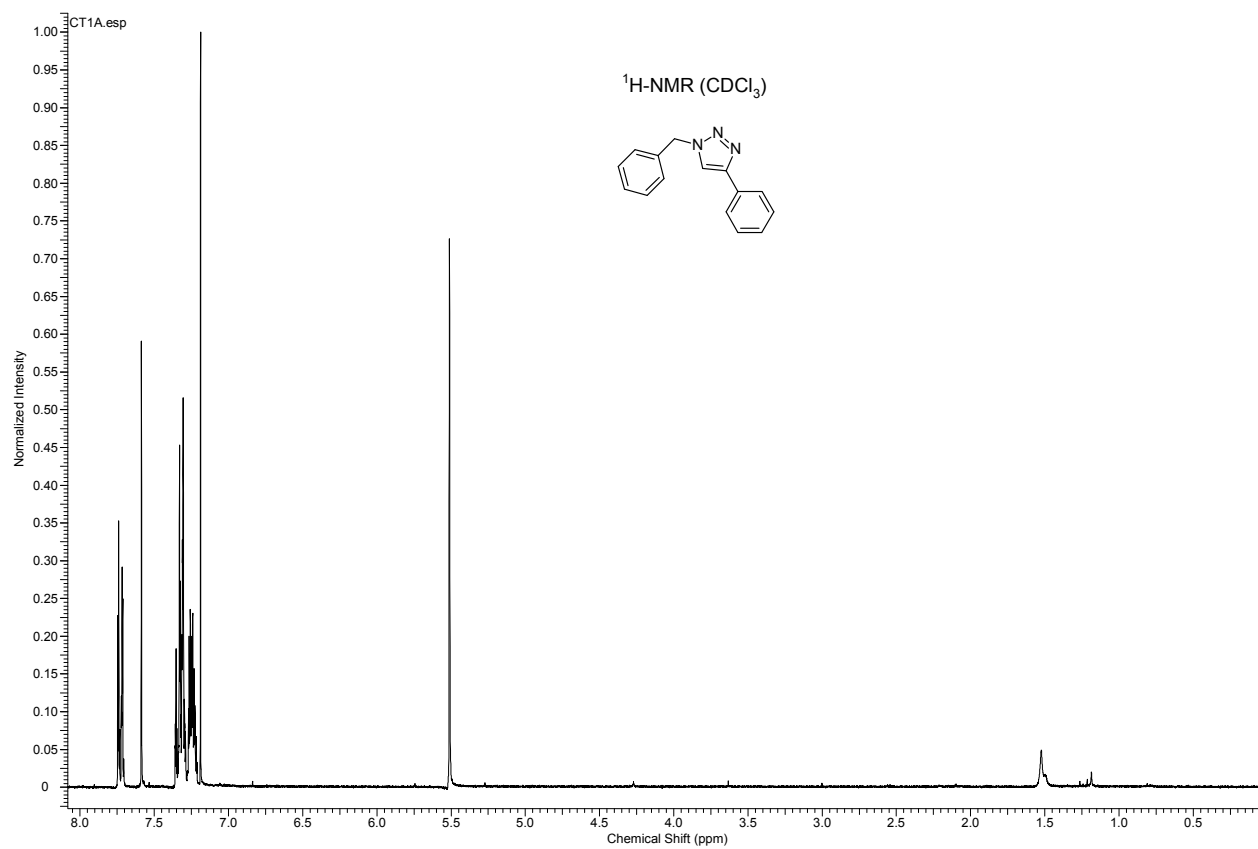
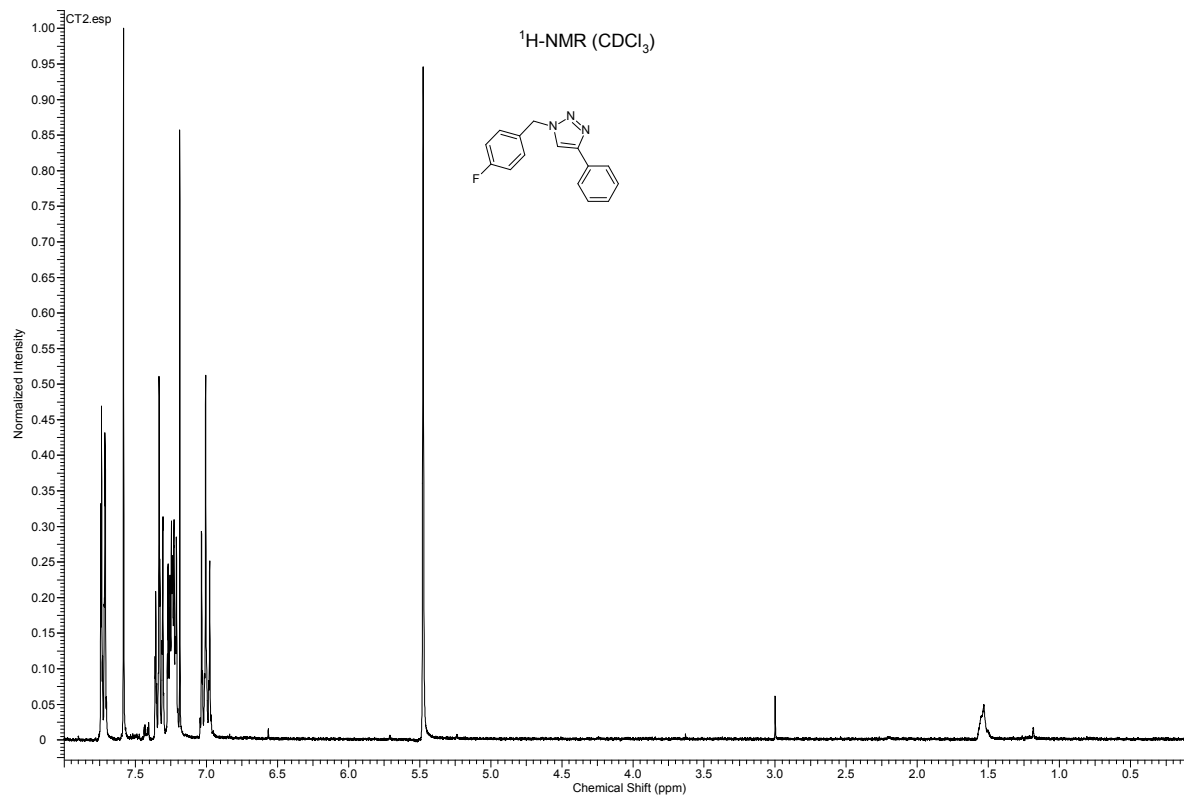


Figure S18: ESI-MS spectrum of 6.

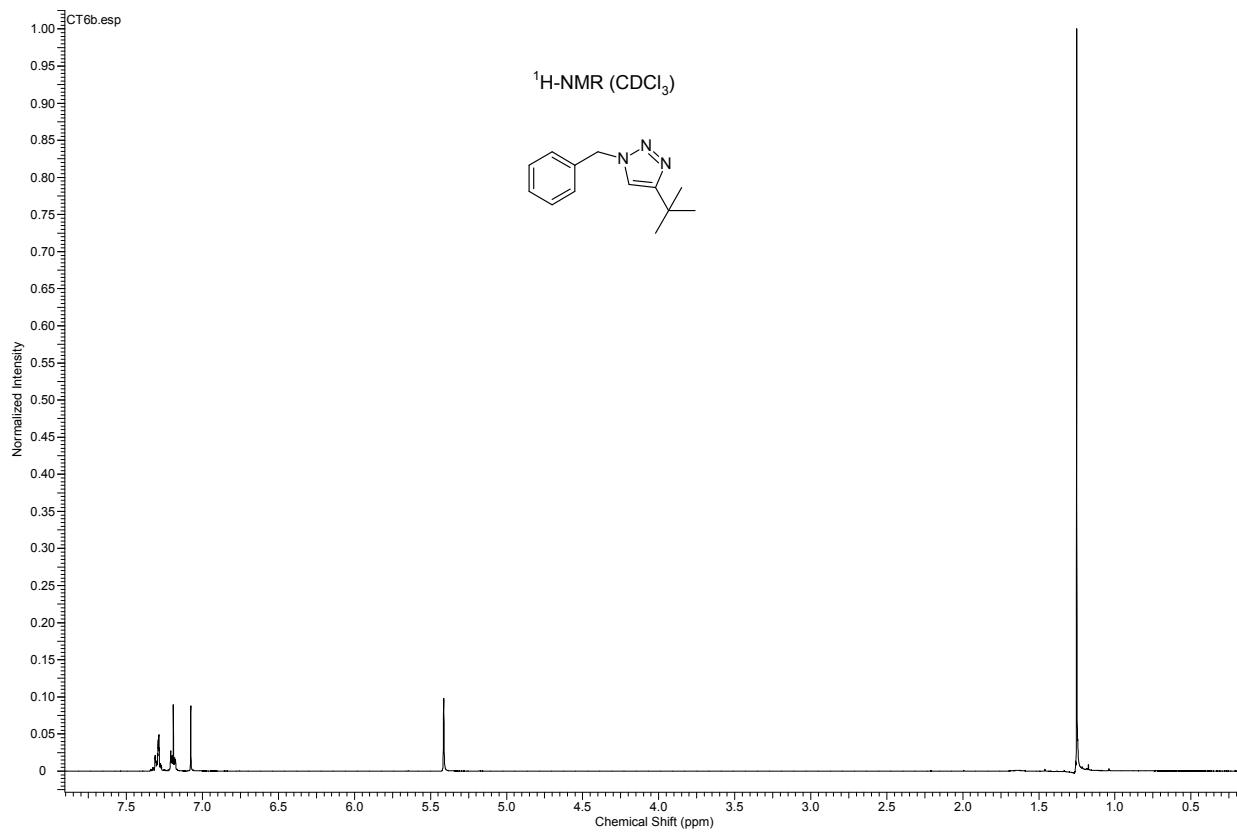
1.6 NMR spectra of synthesized triazoles



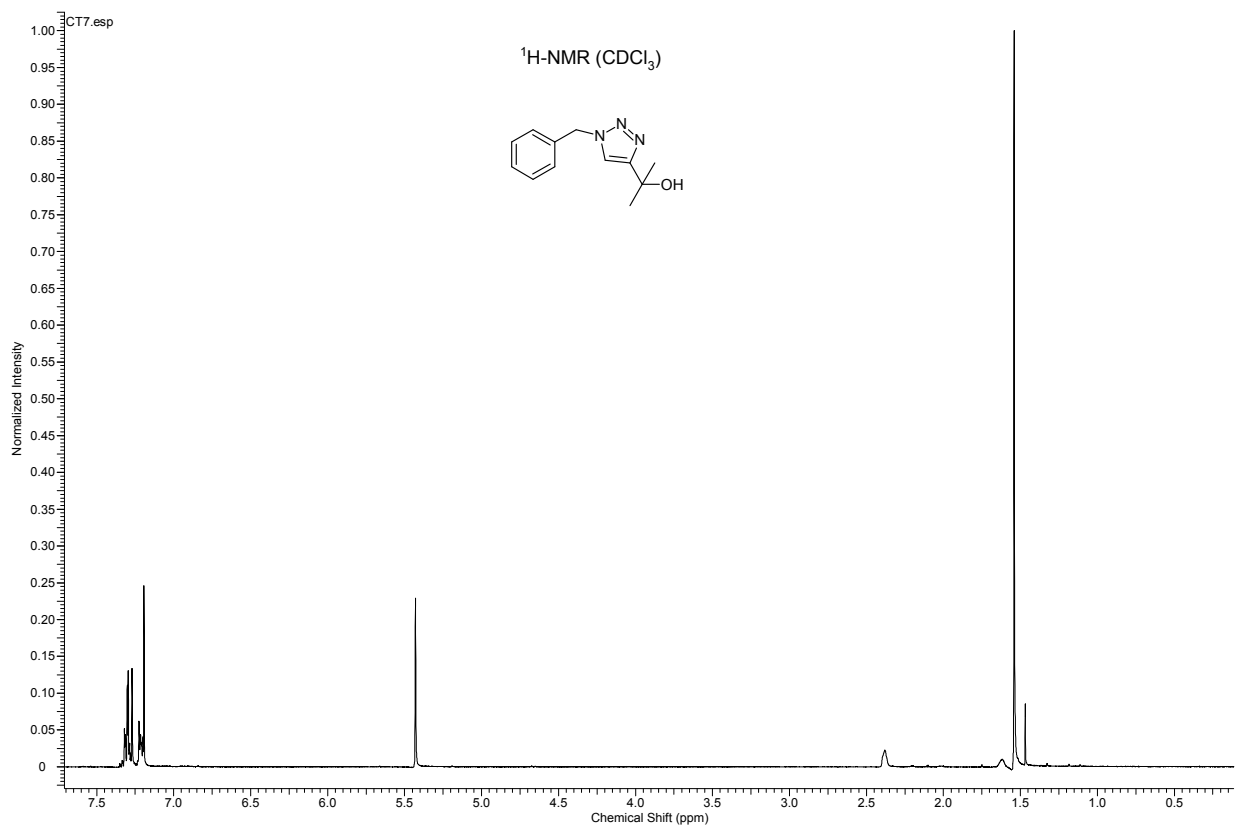
10



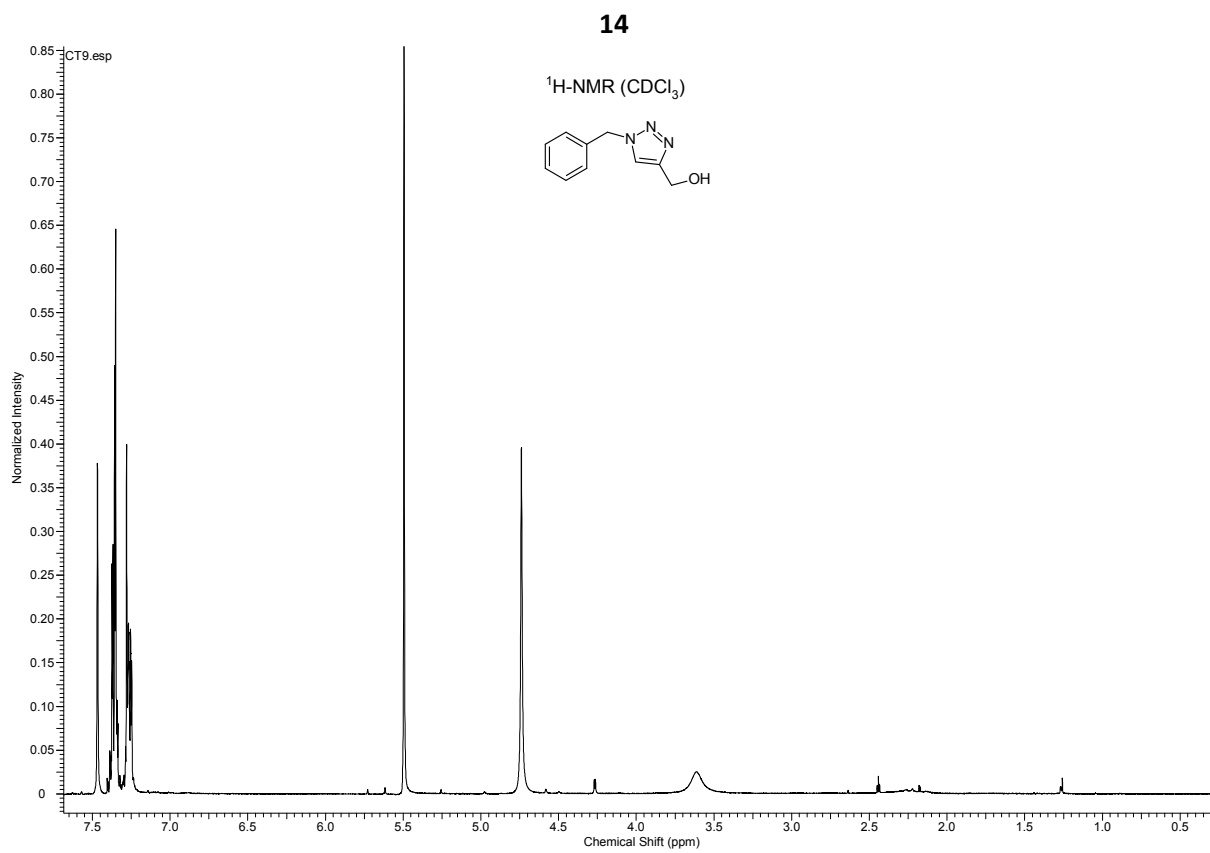
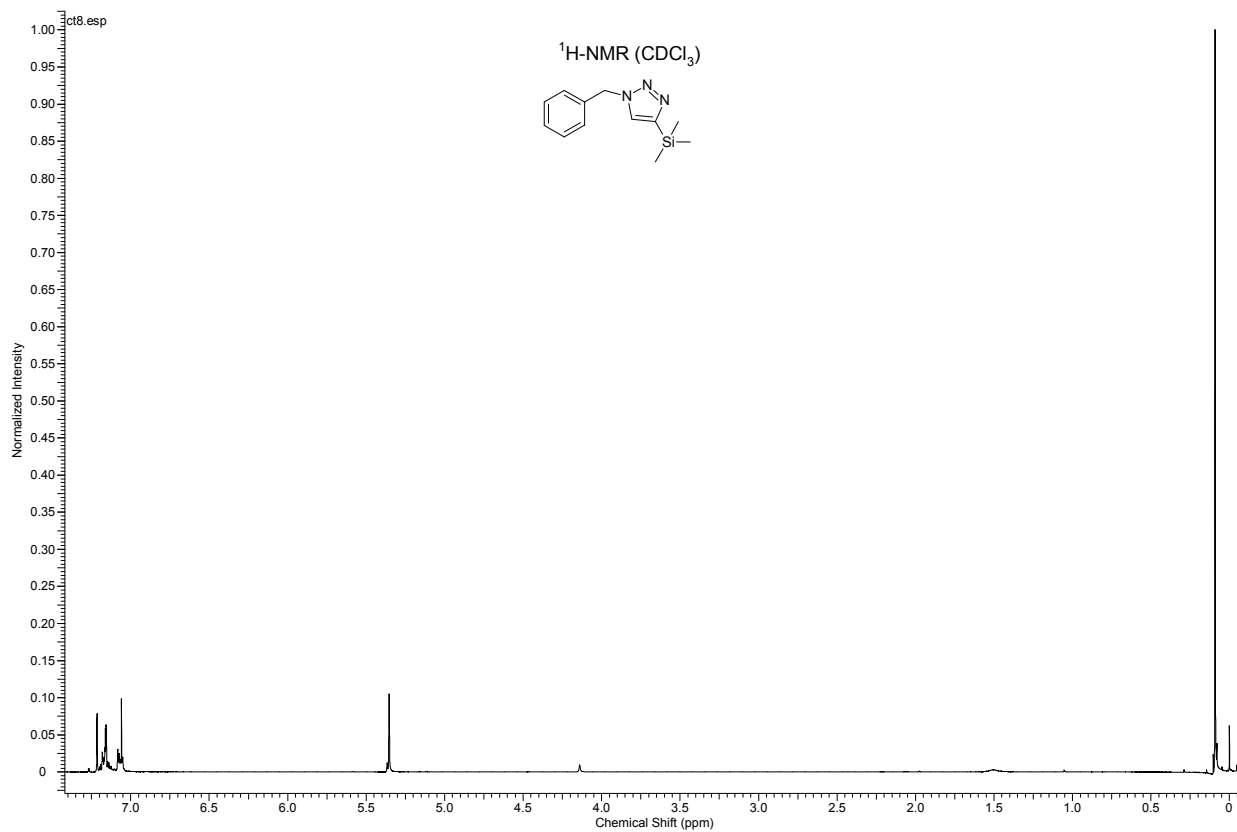
11



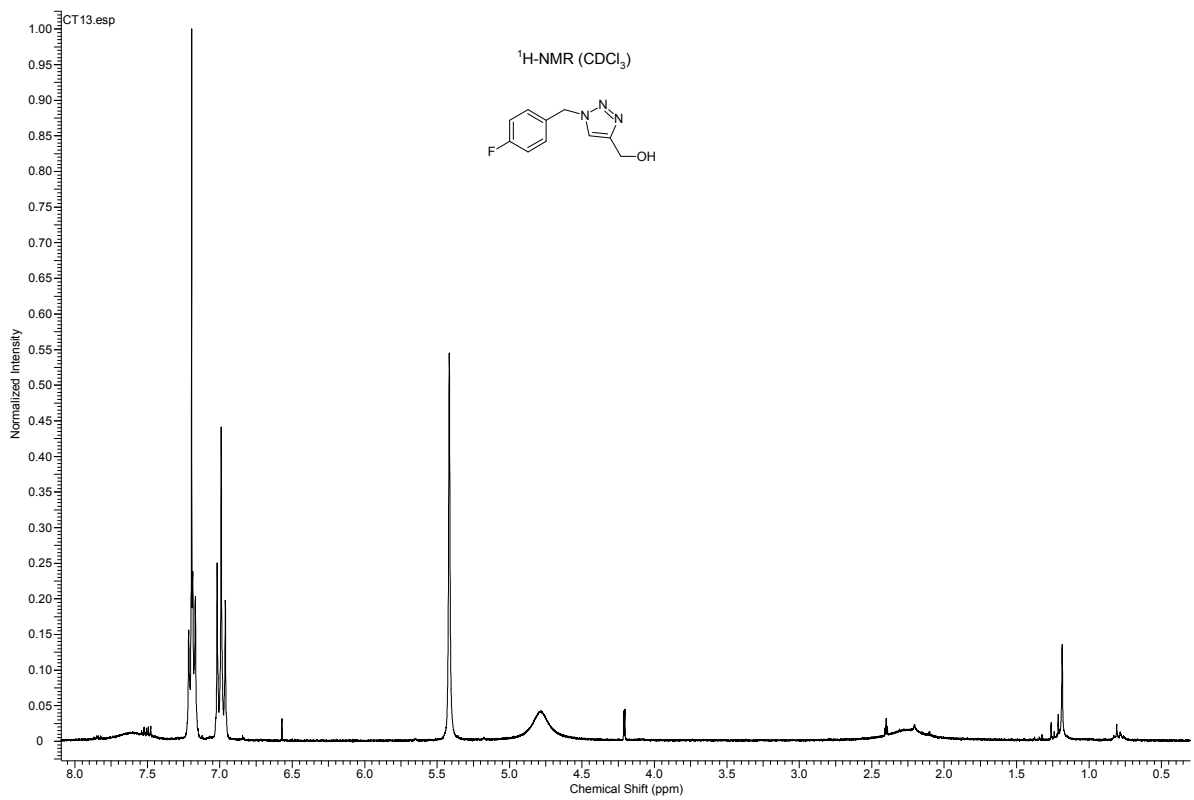
12



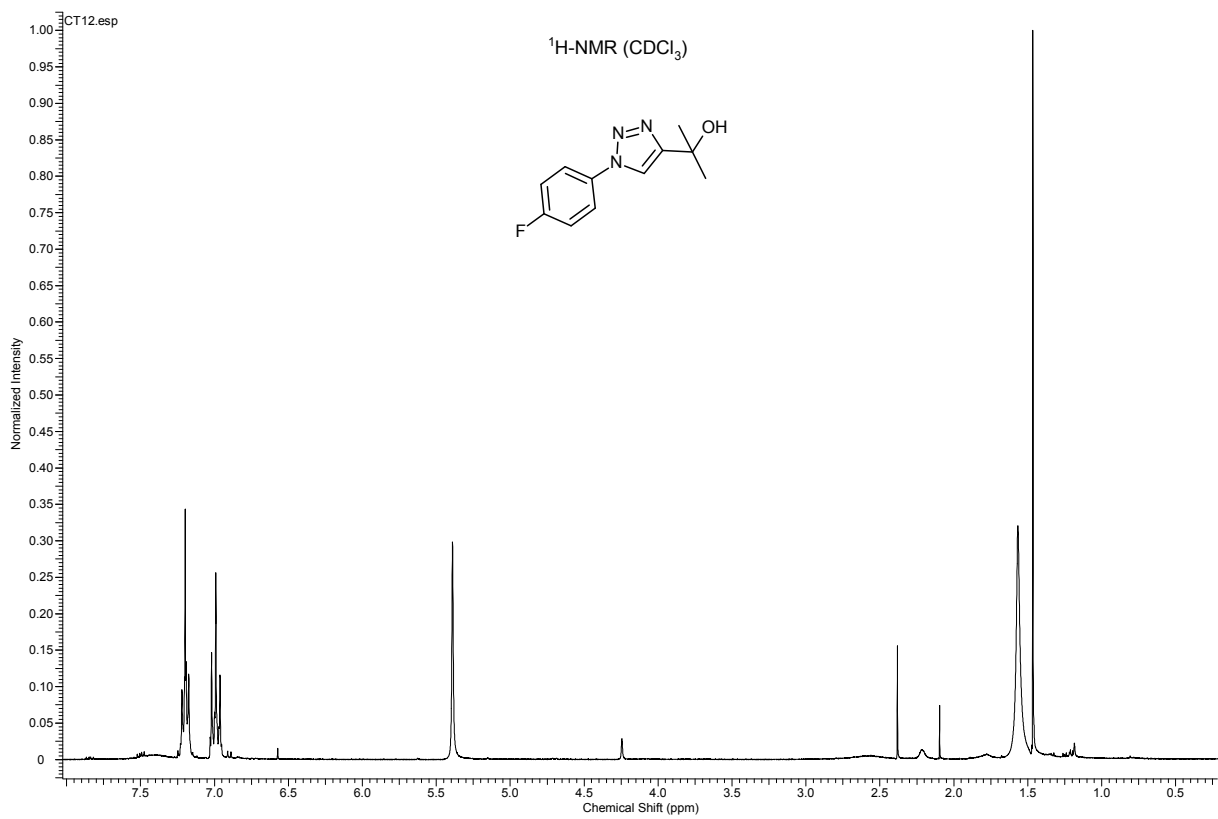
13



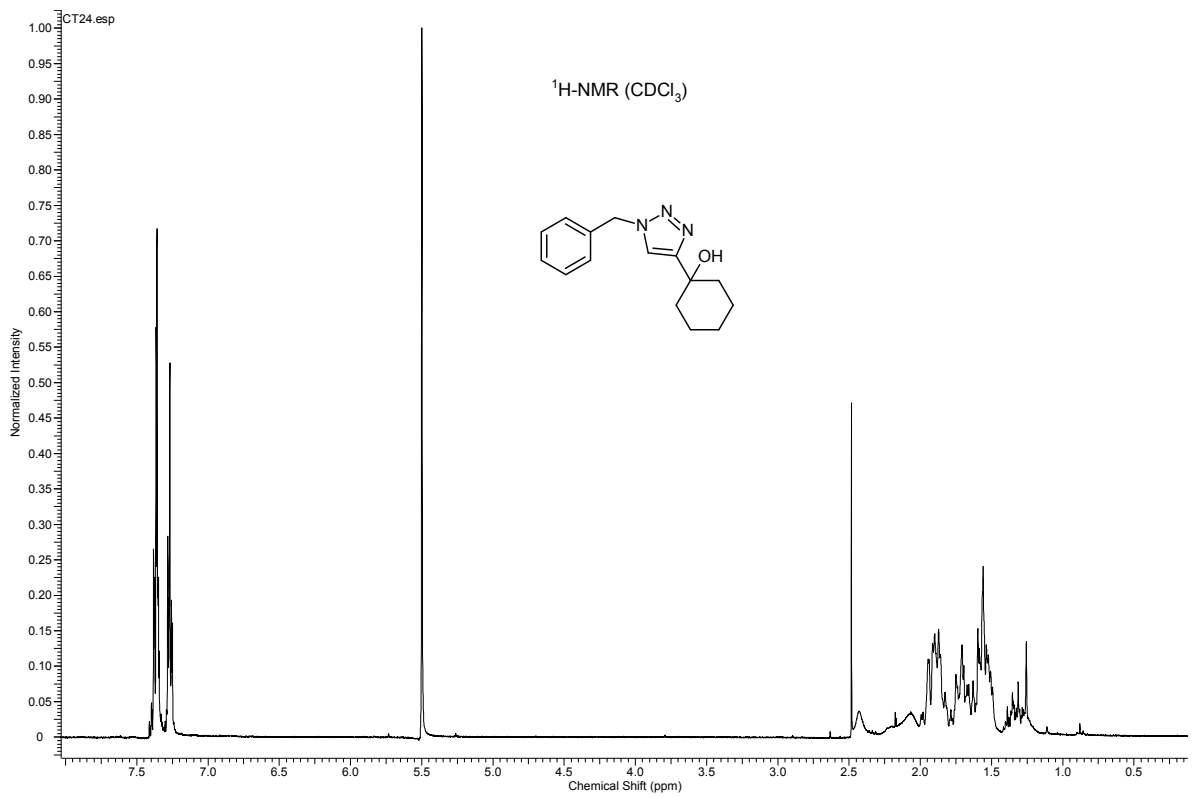
15



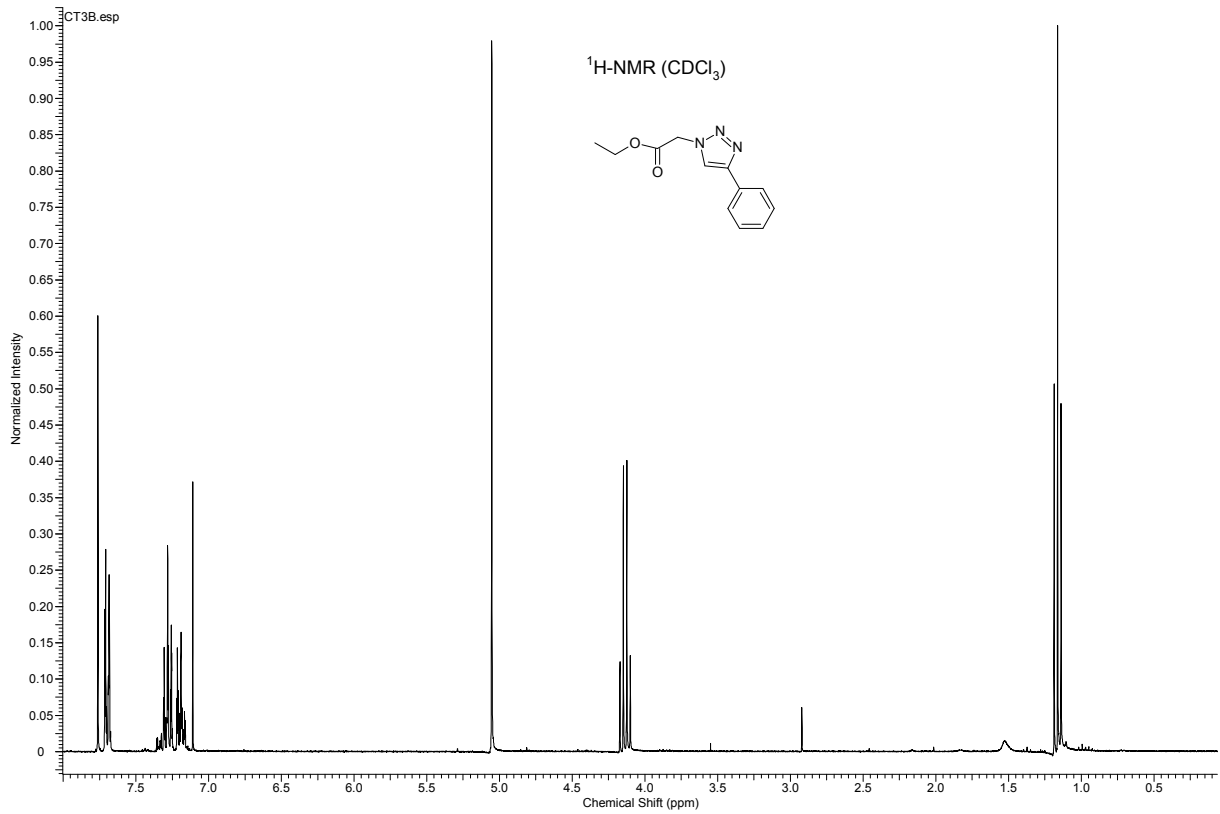
16



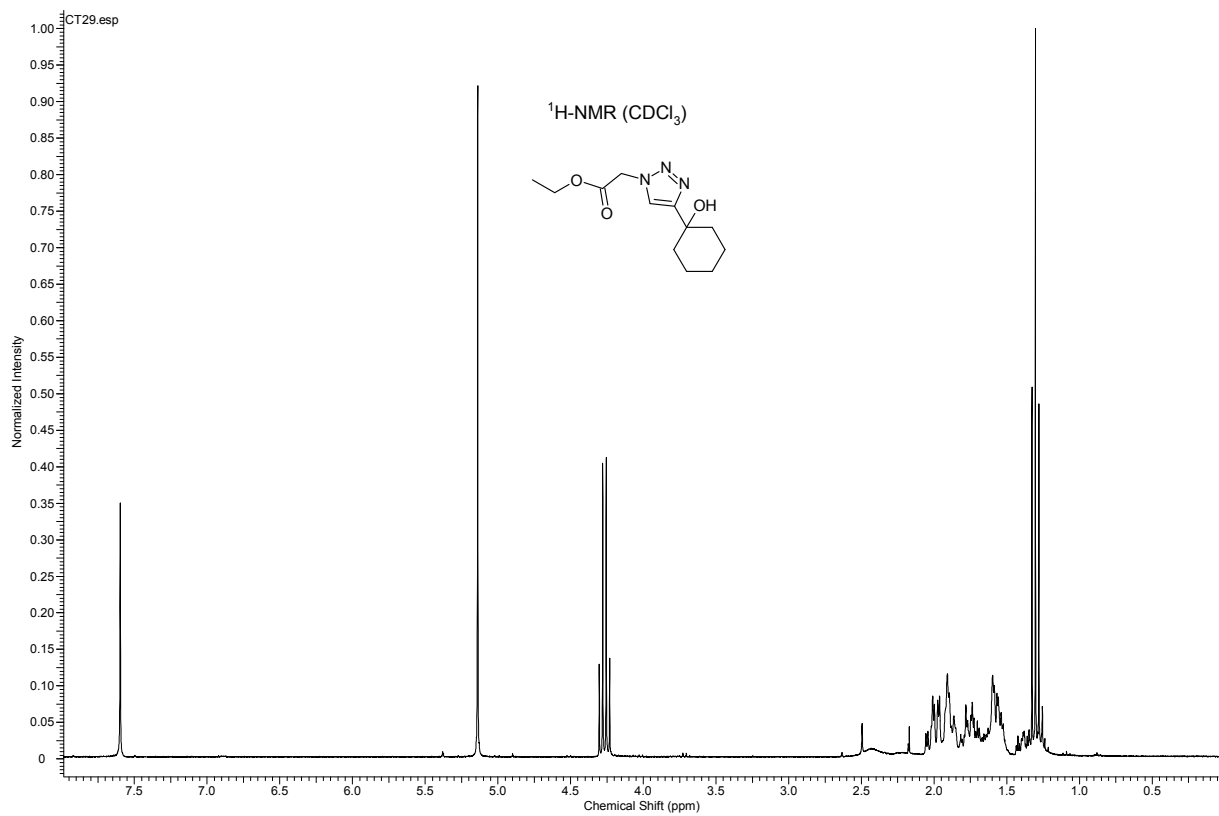
17



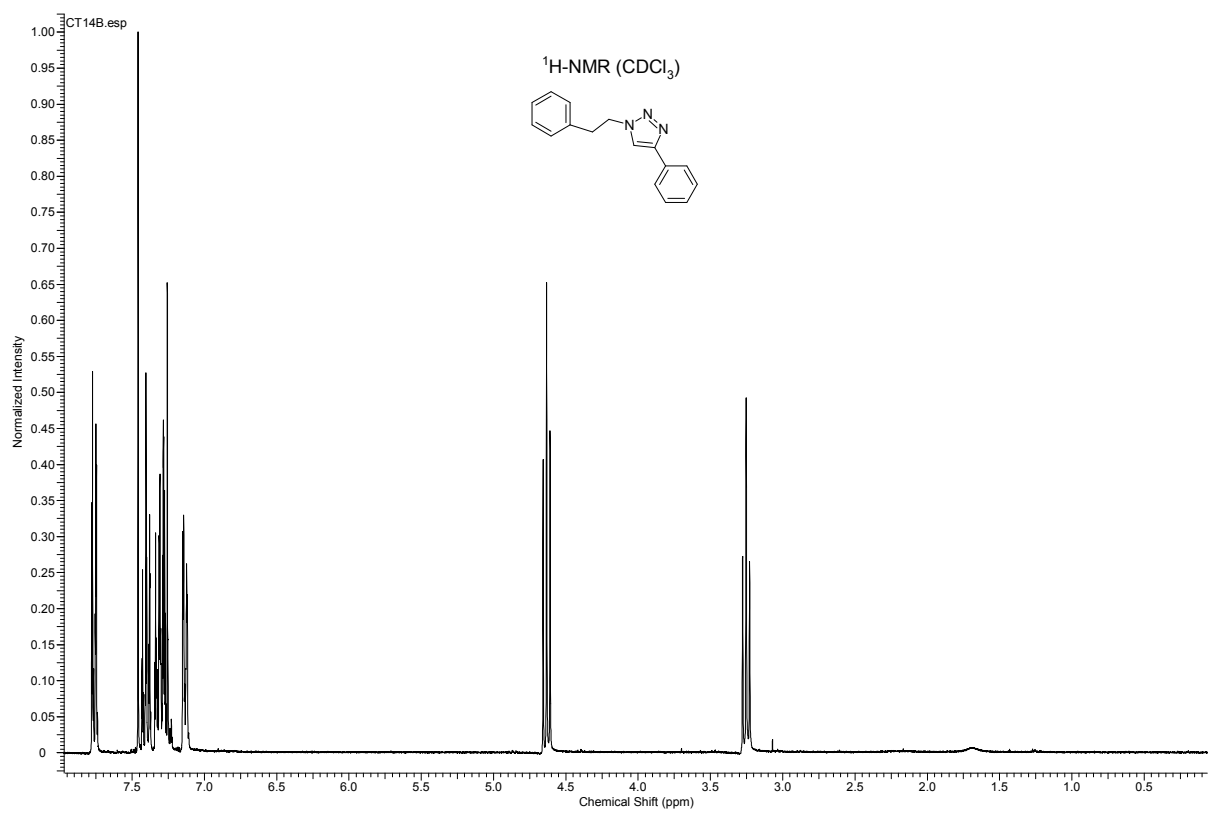
18



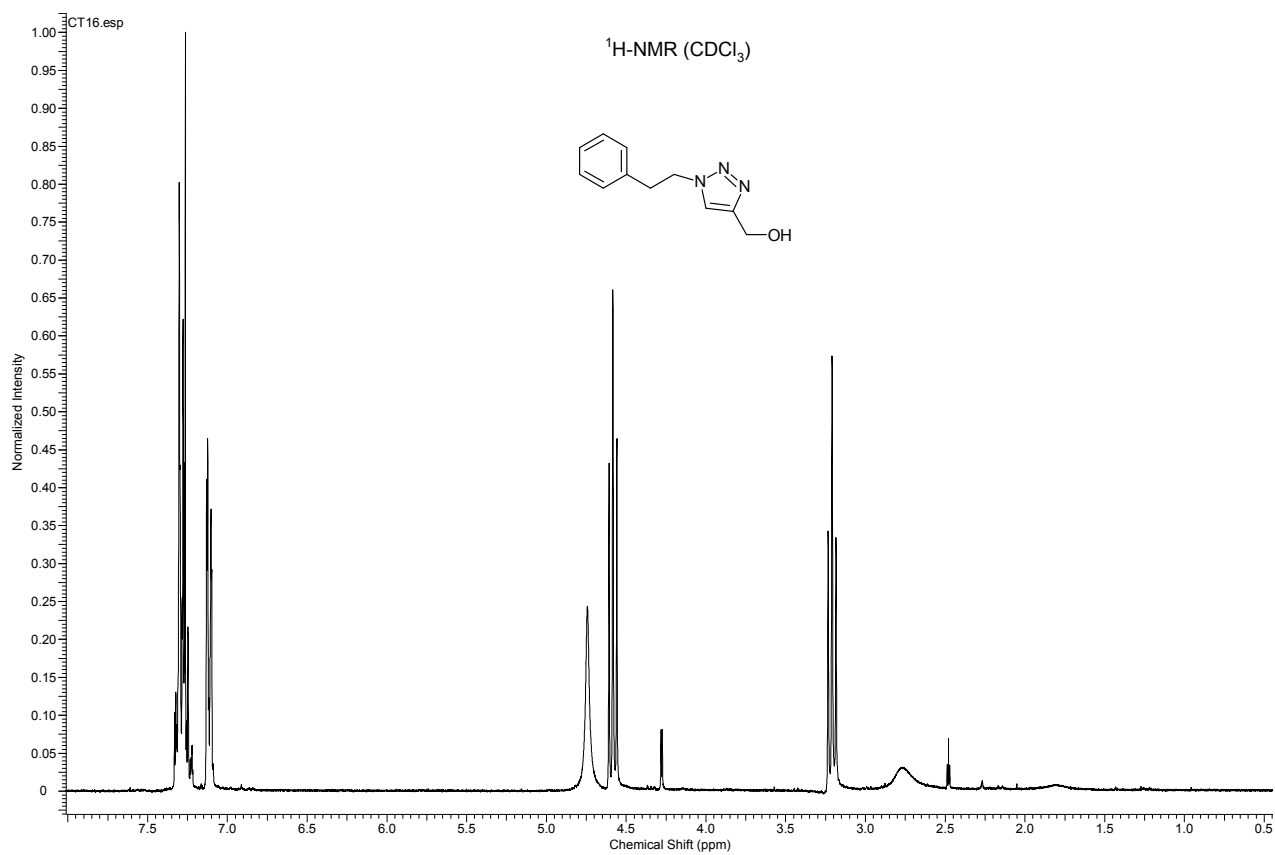
19



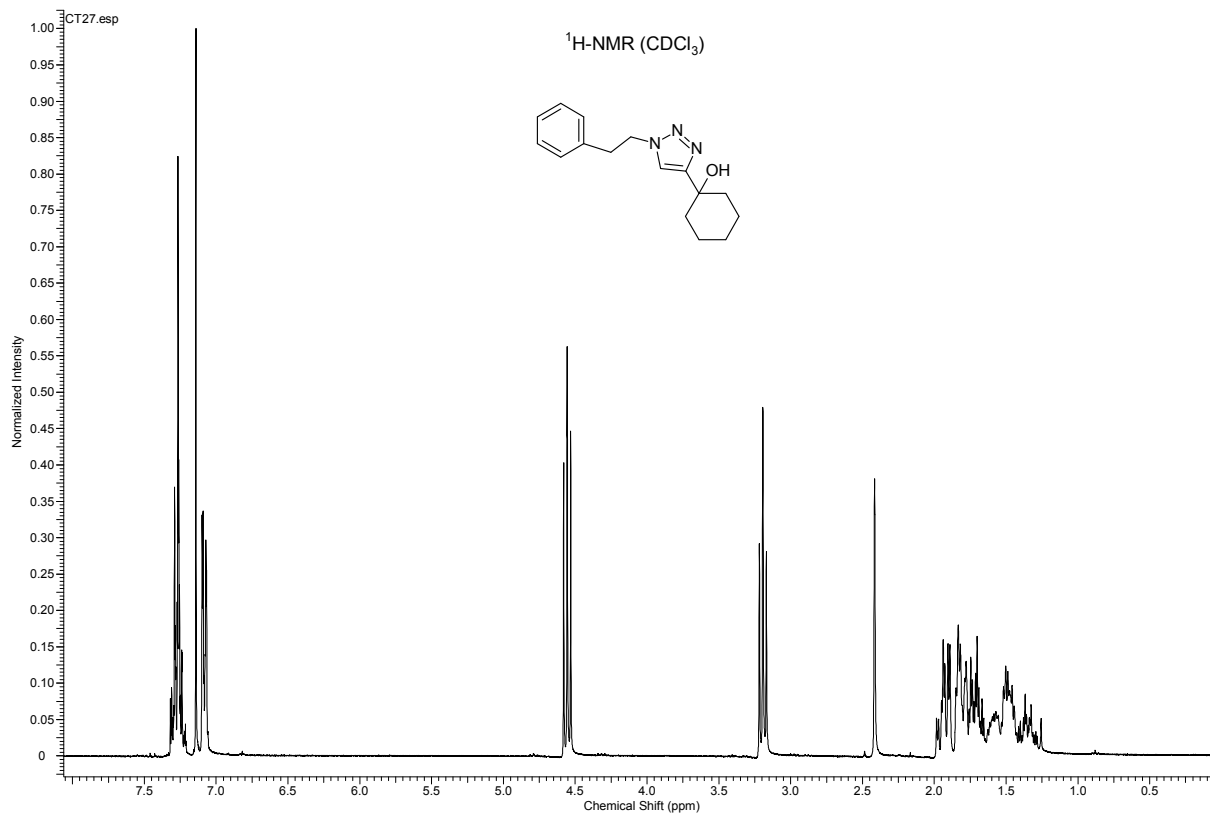
20



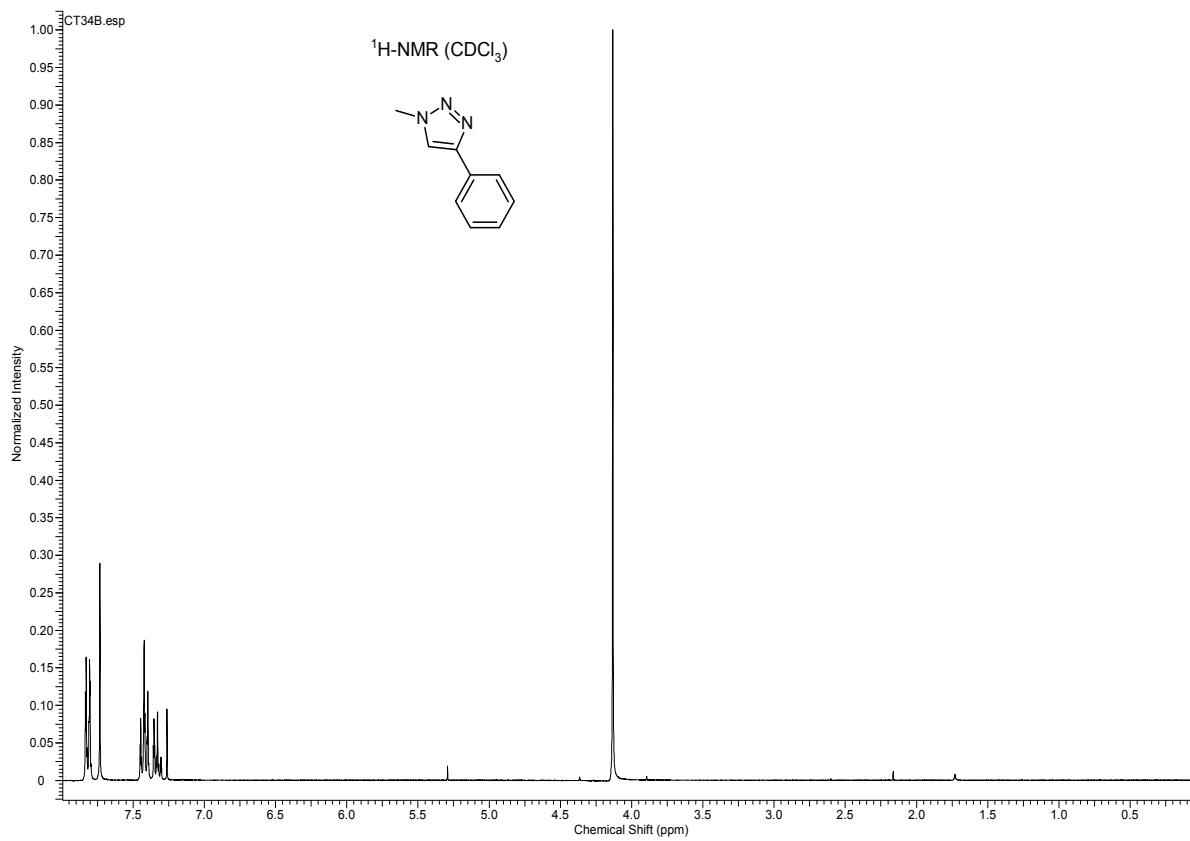
21



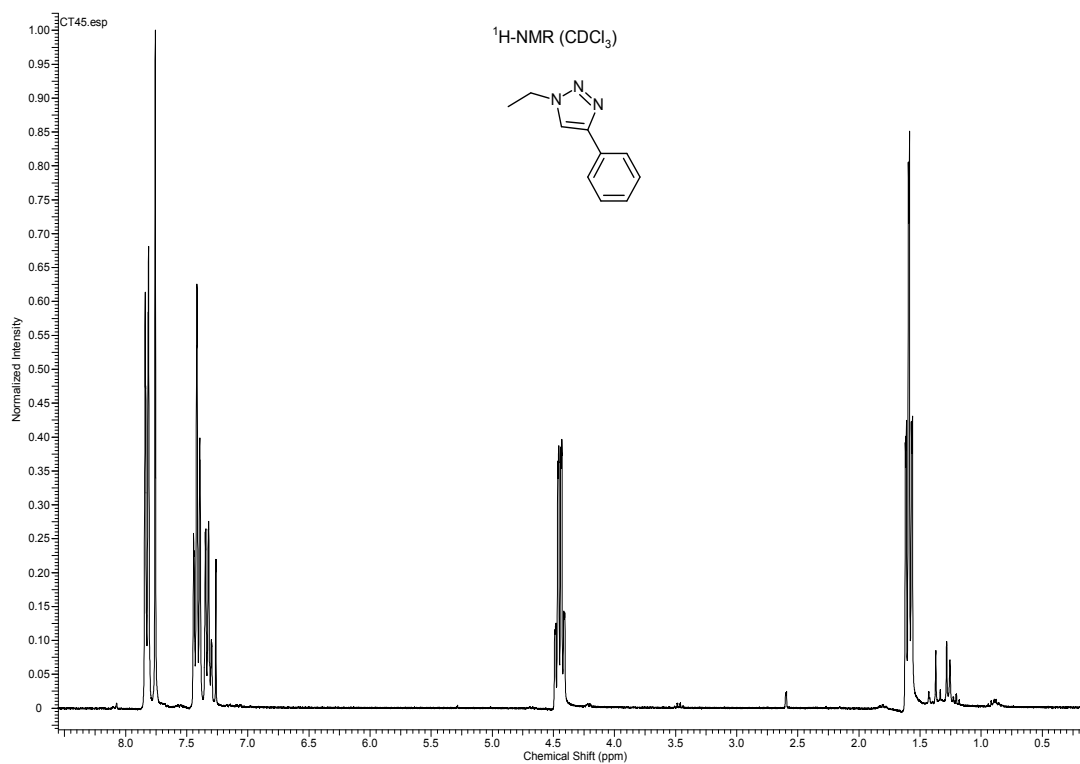
22



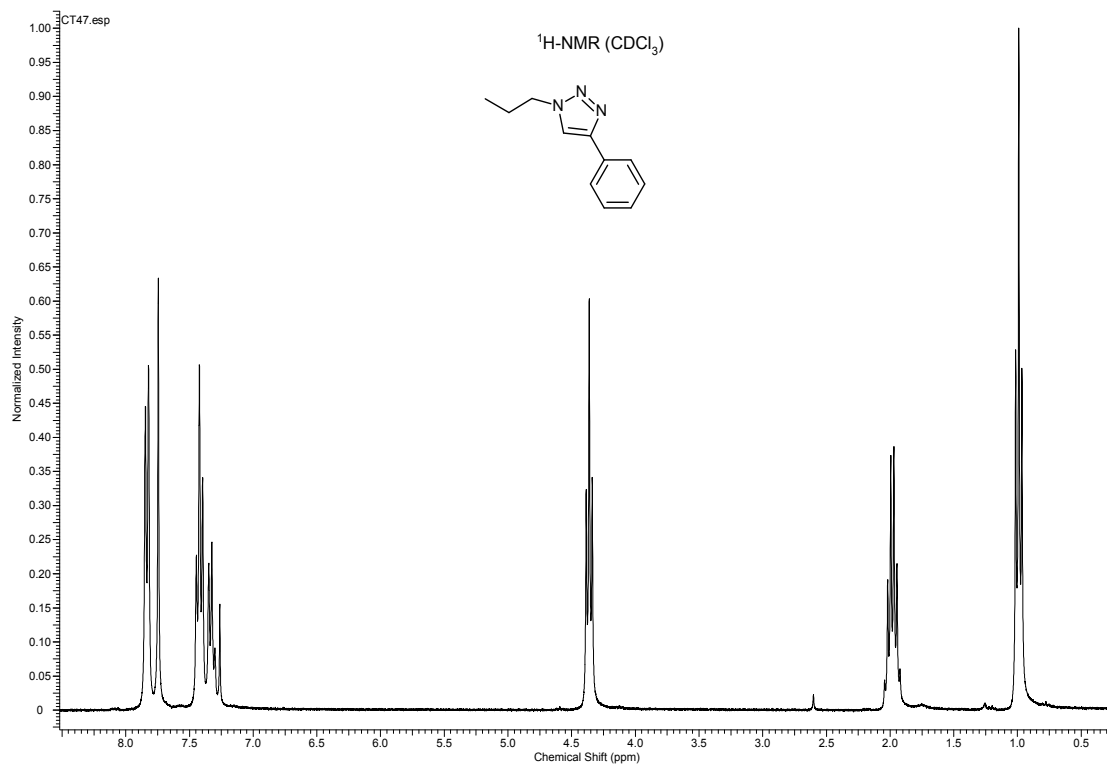
23



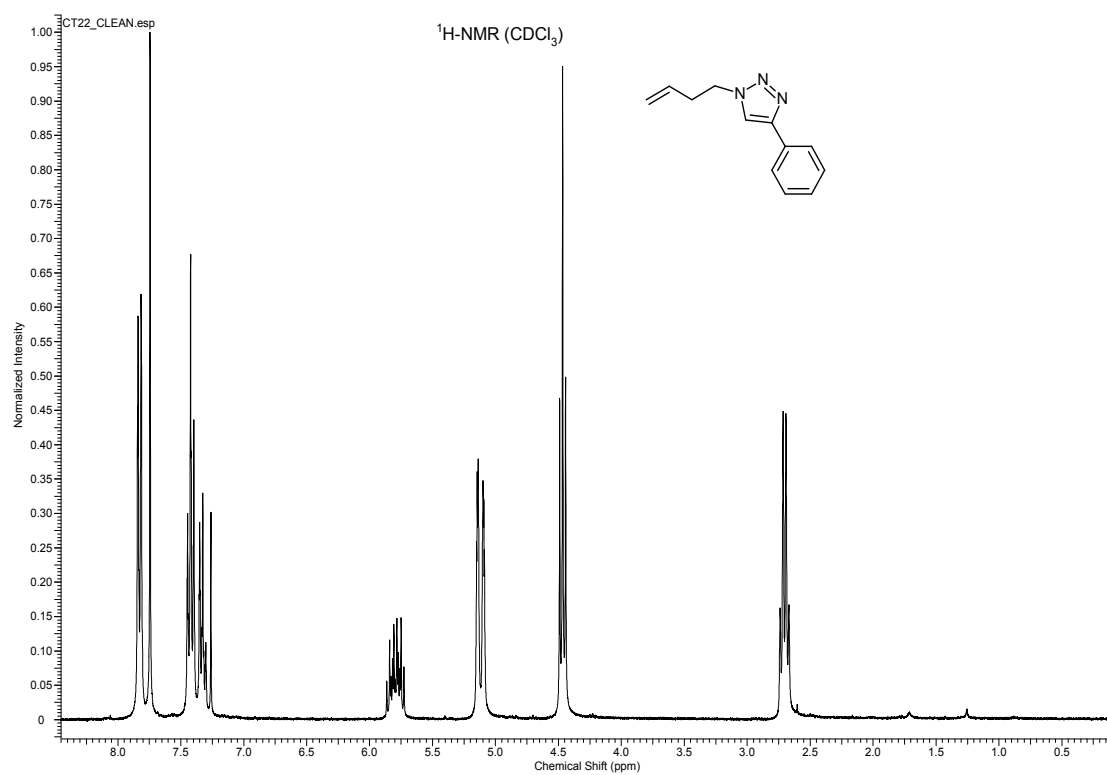
24



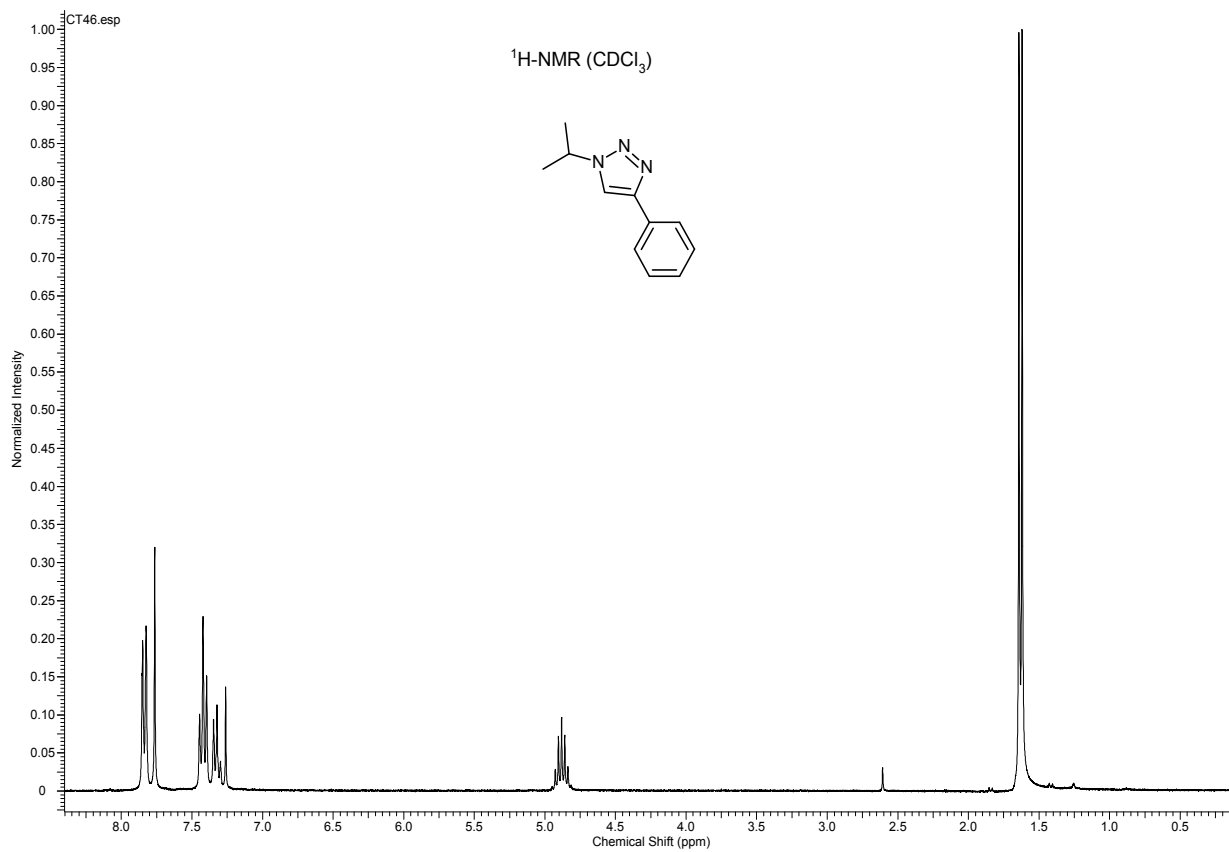
25



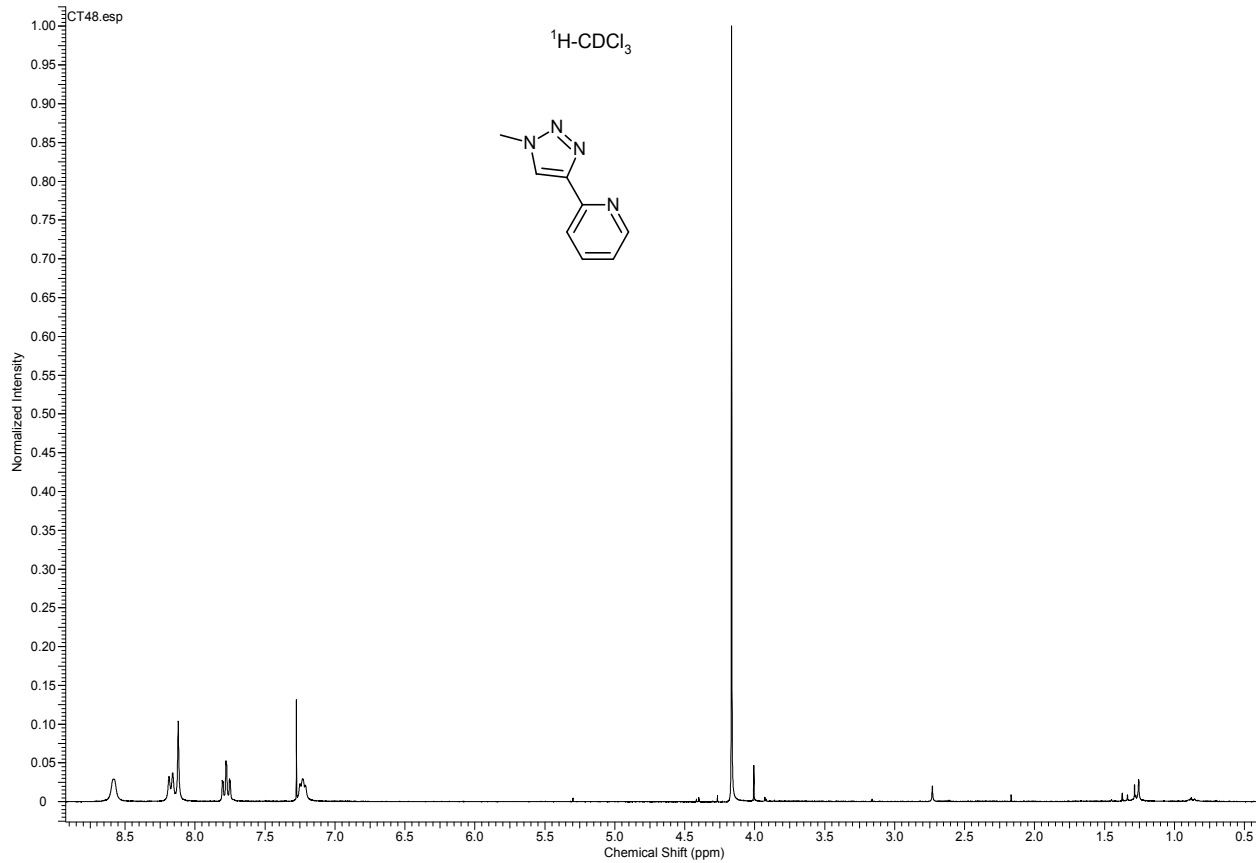
26



27

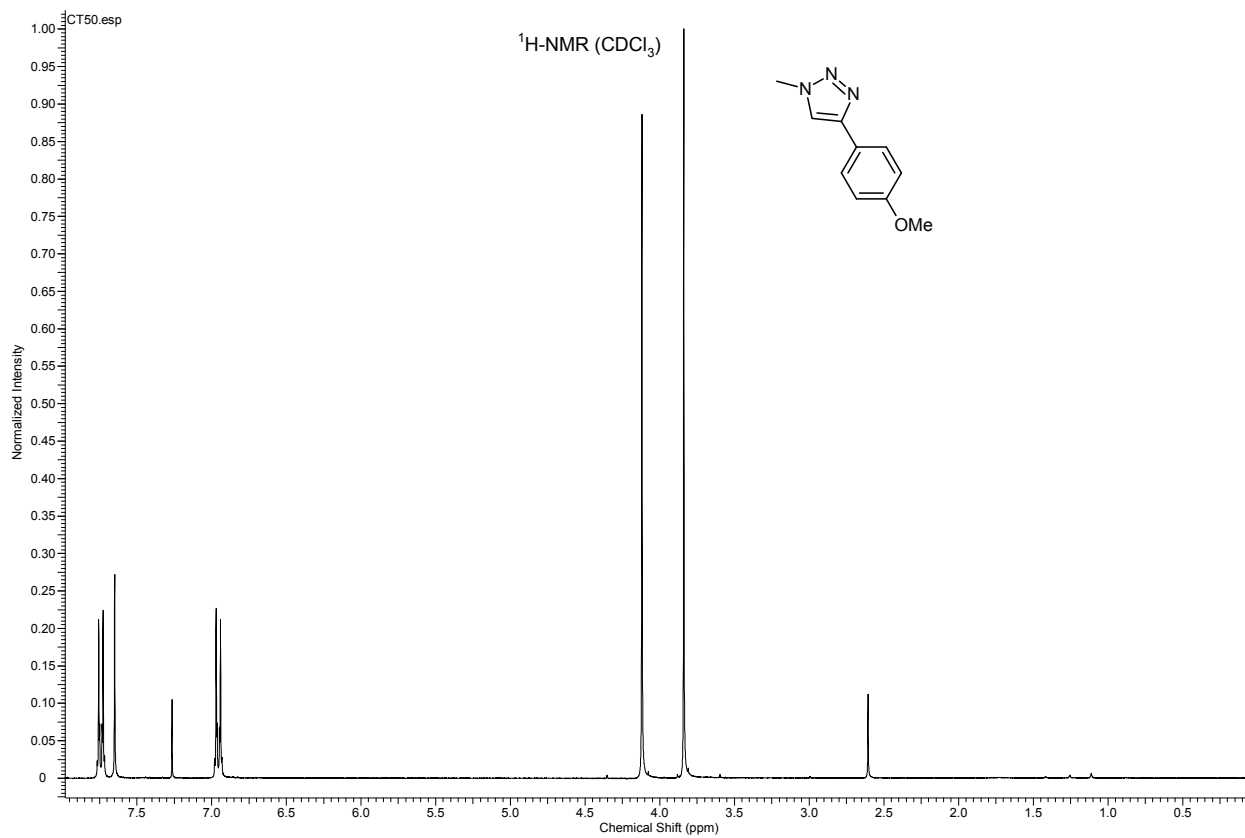


28

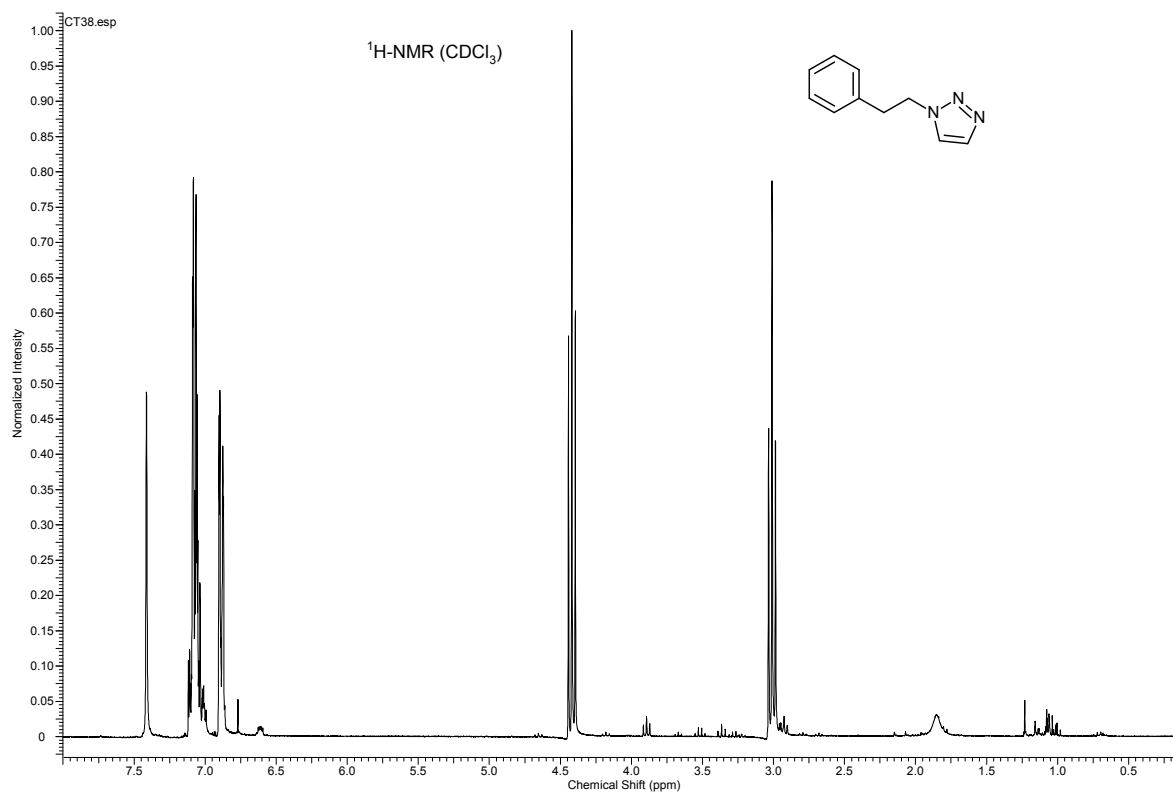


29

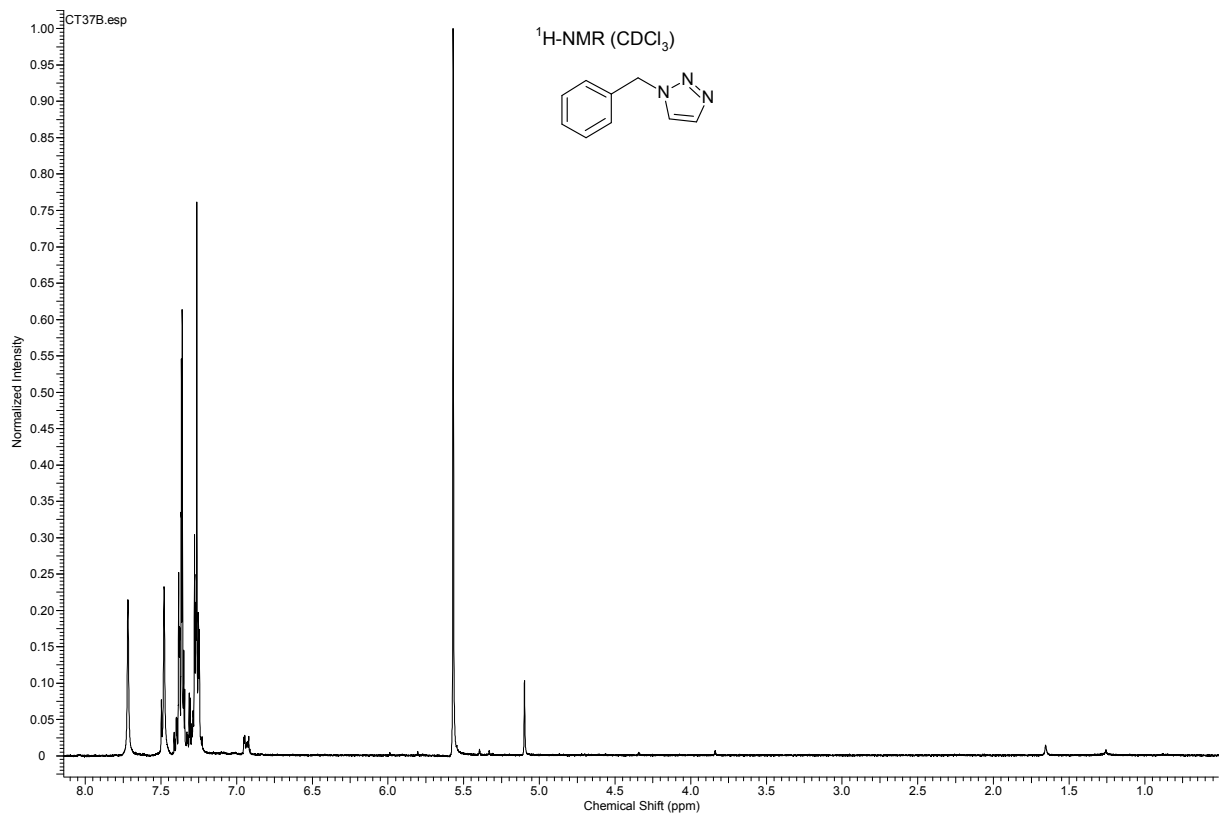
36



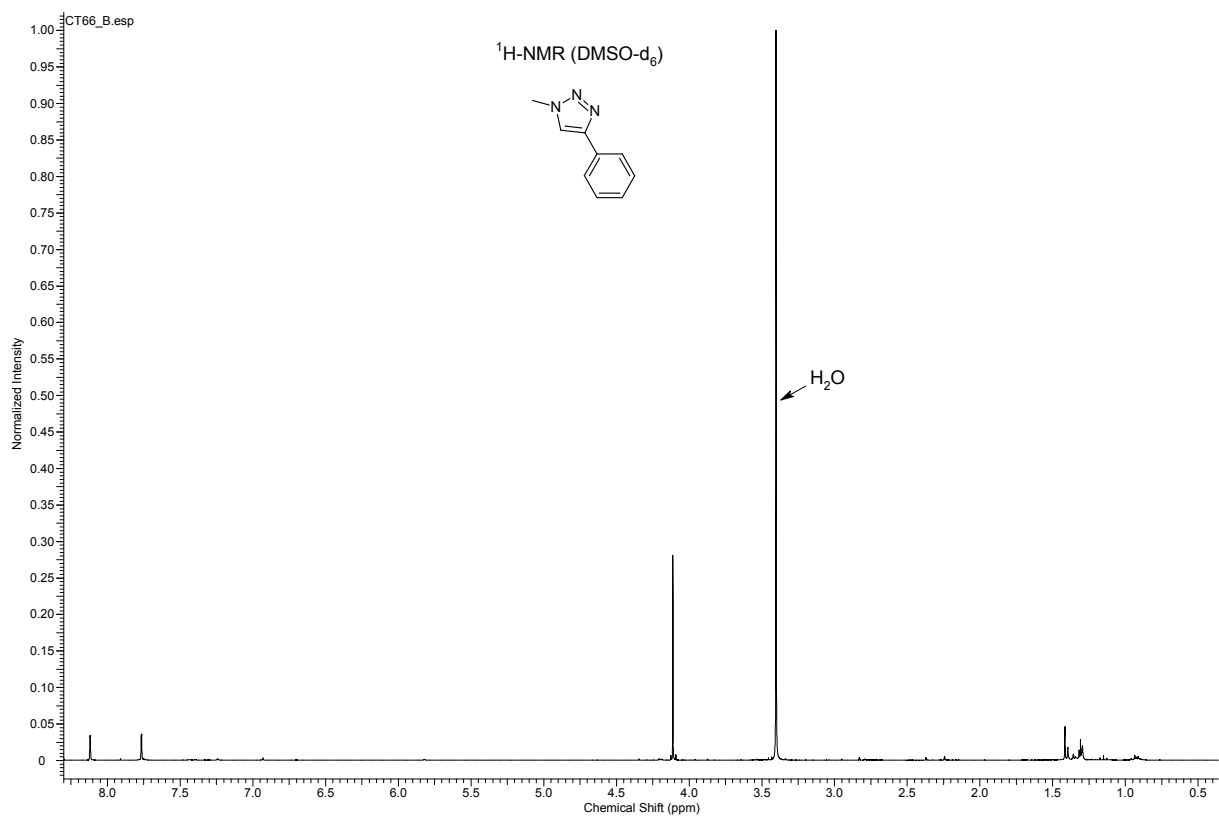
30



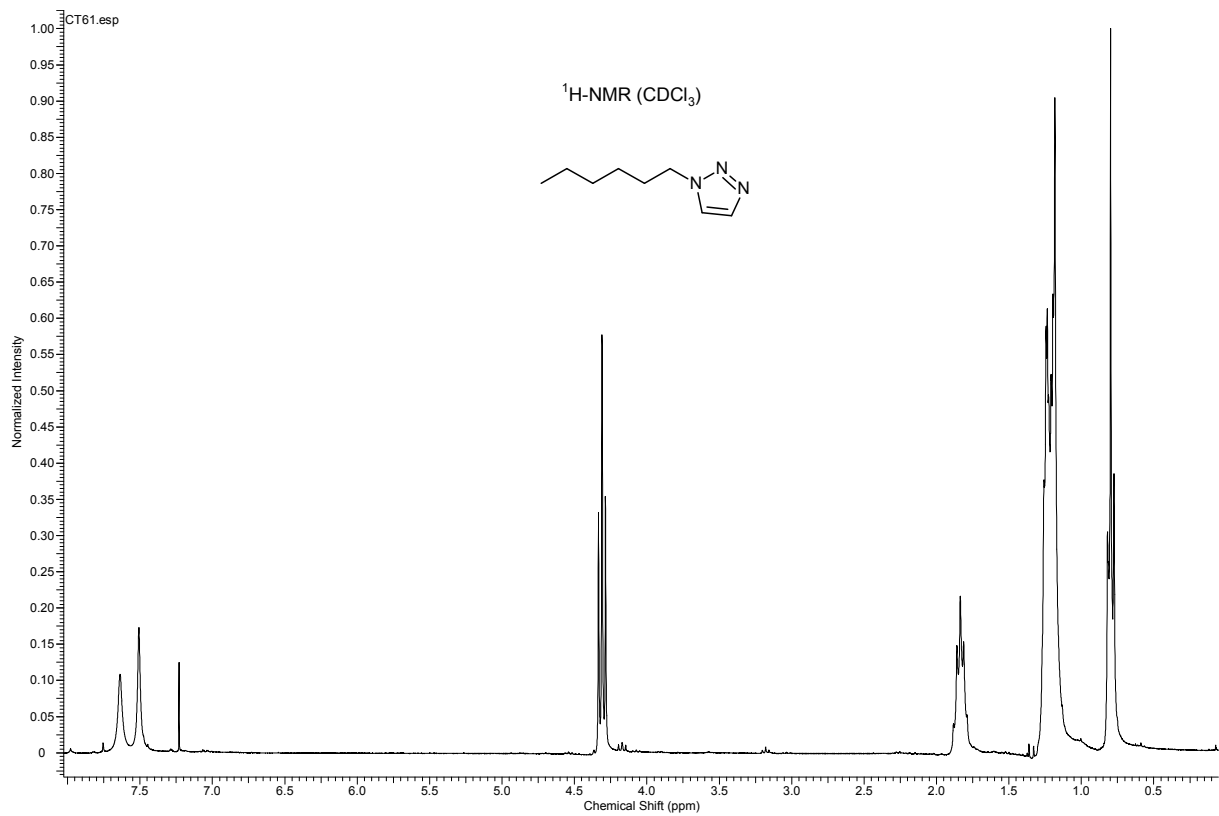
33



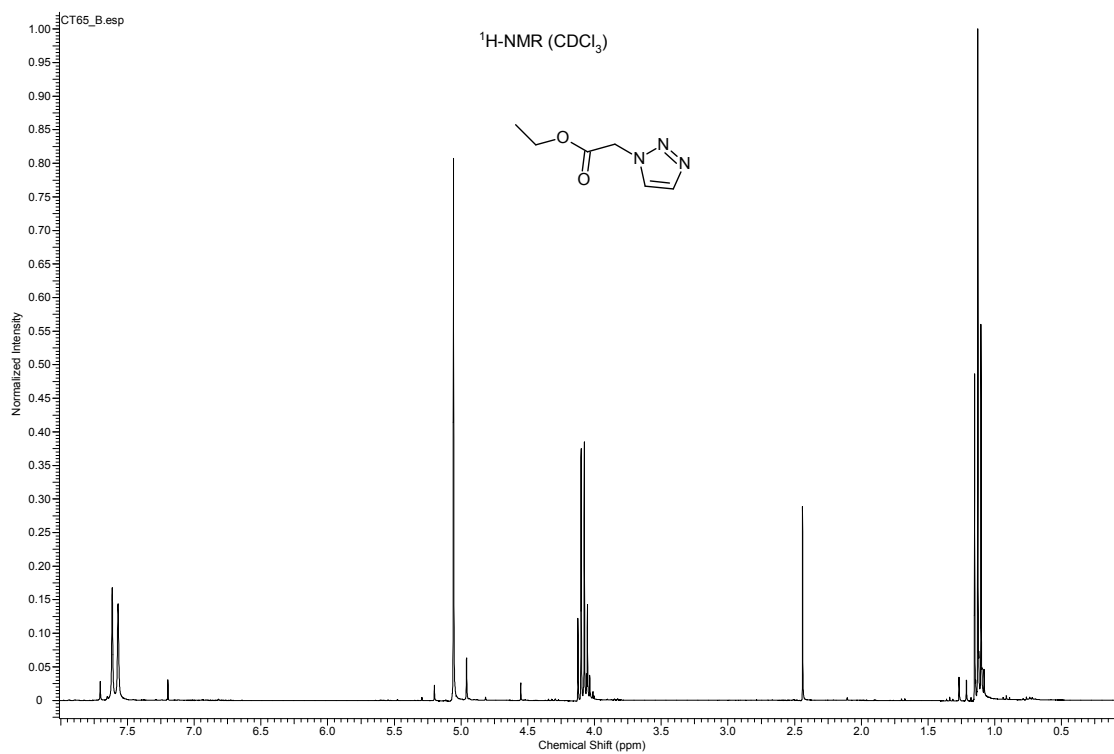
34



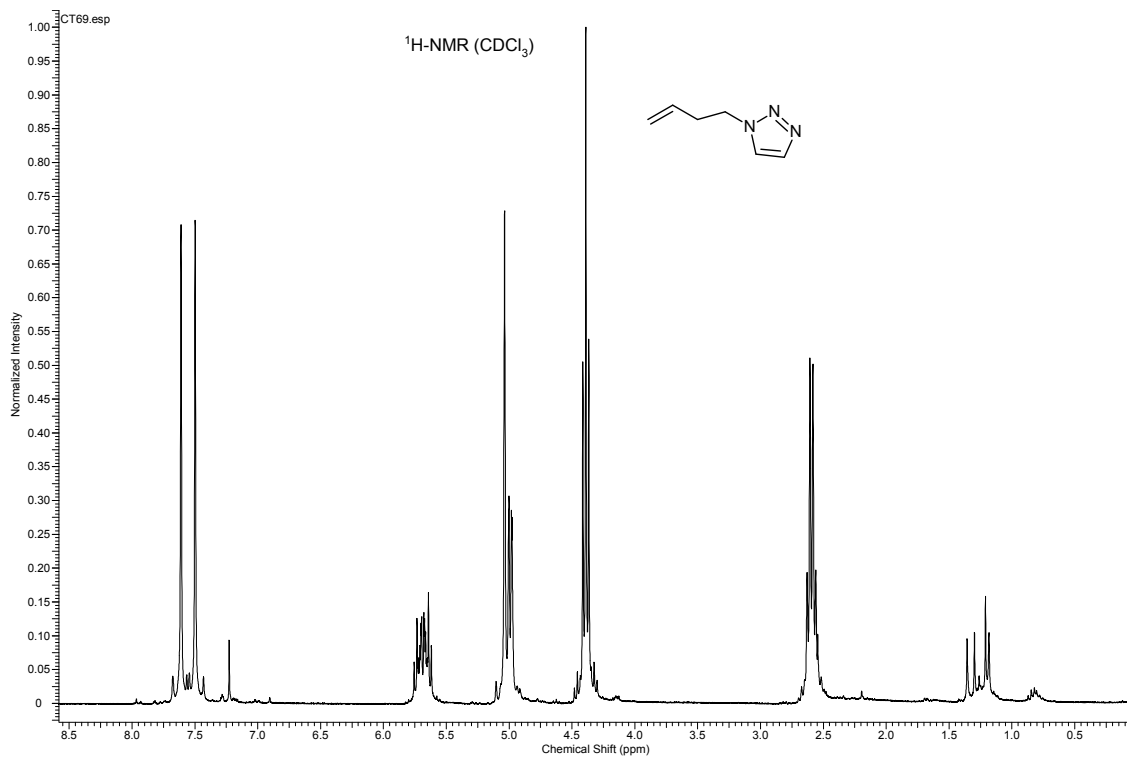
35



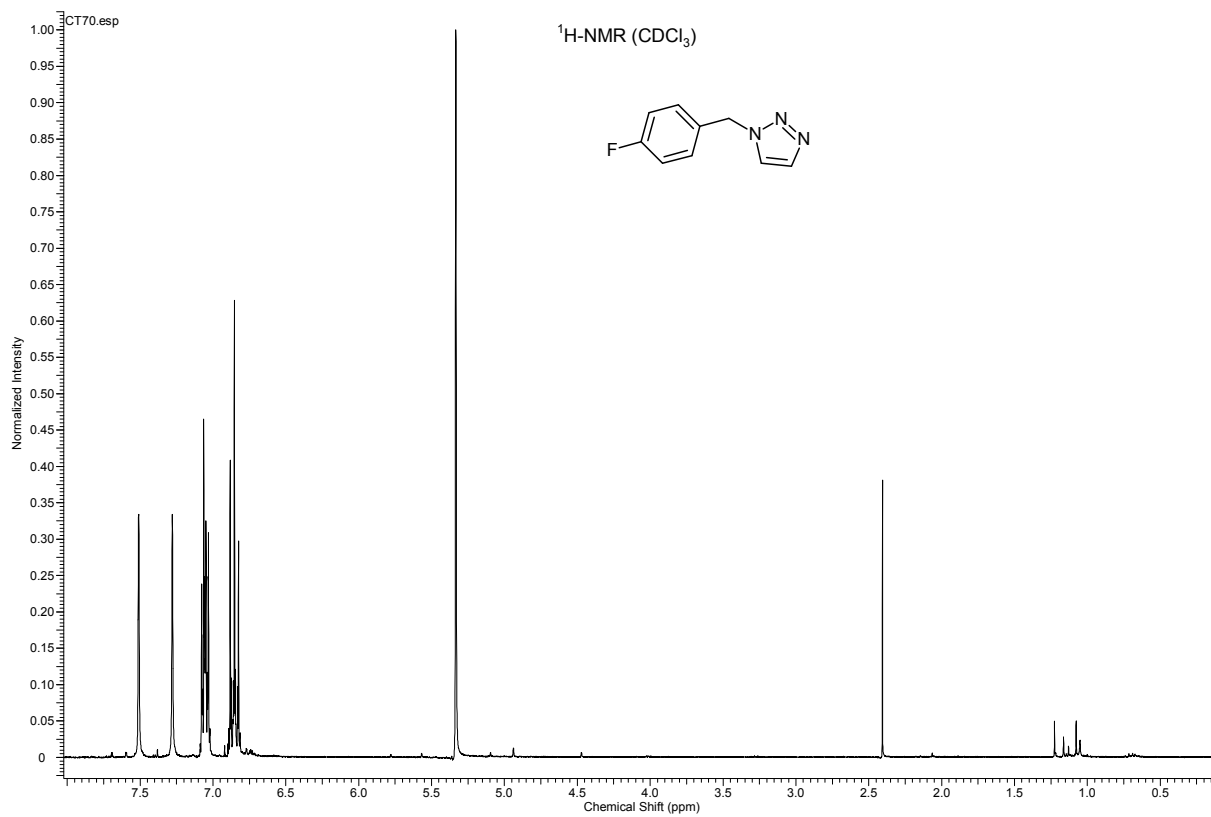
36



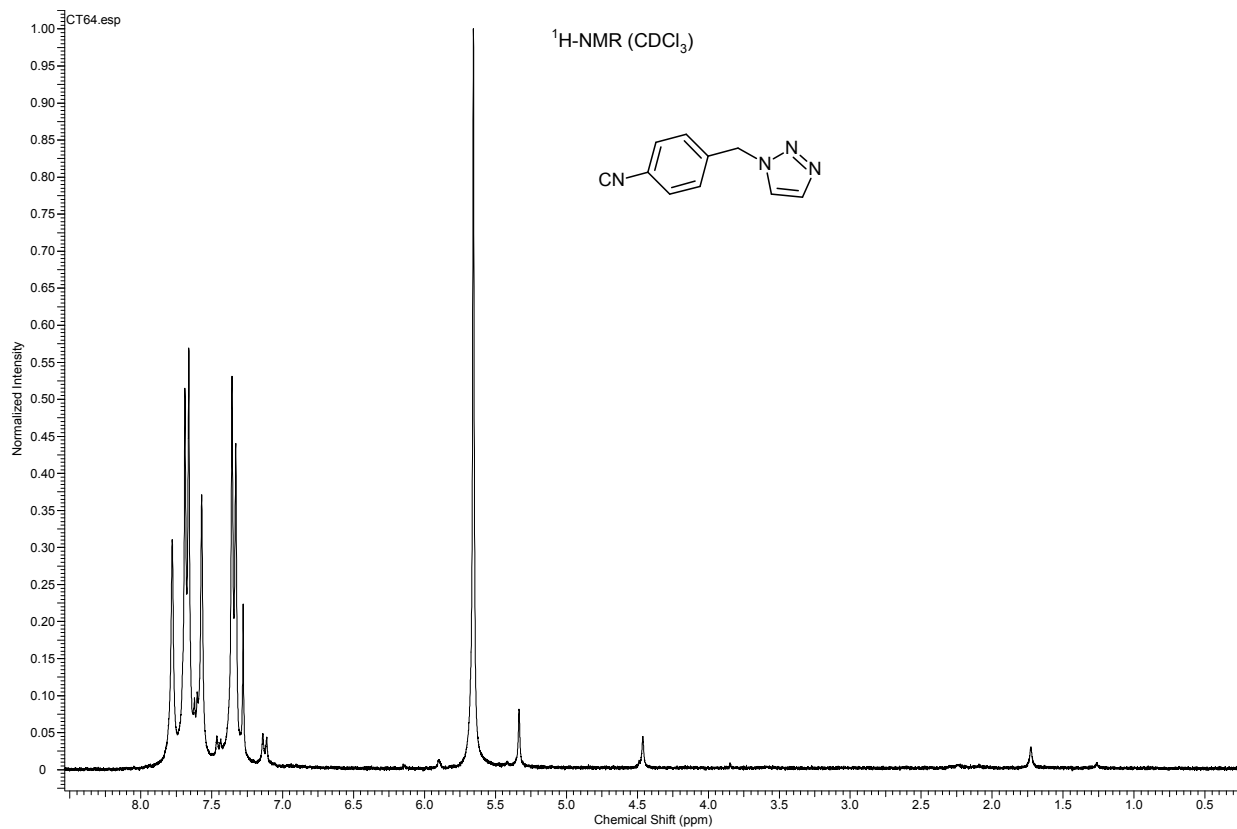
37



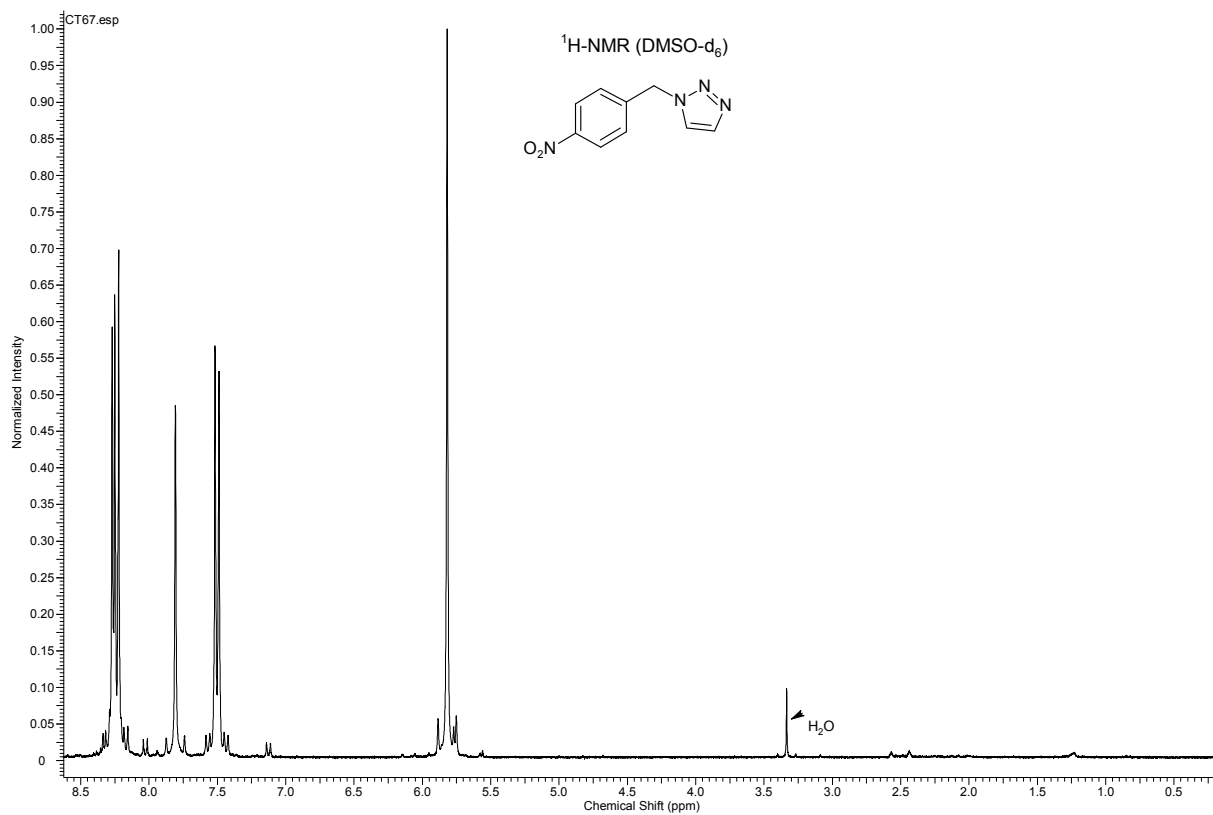
38



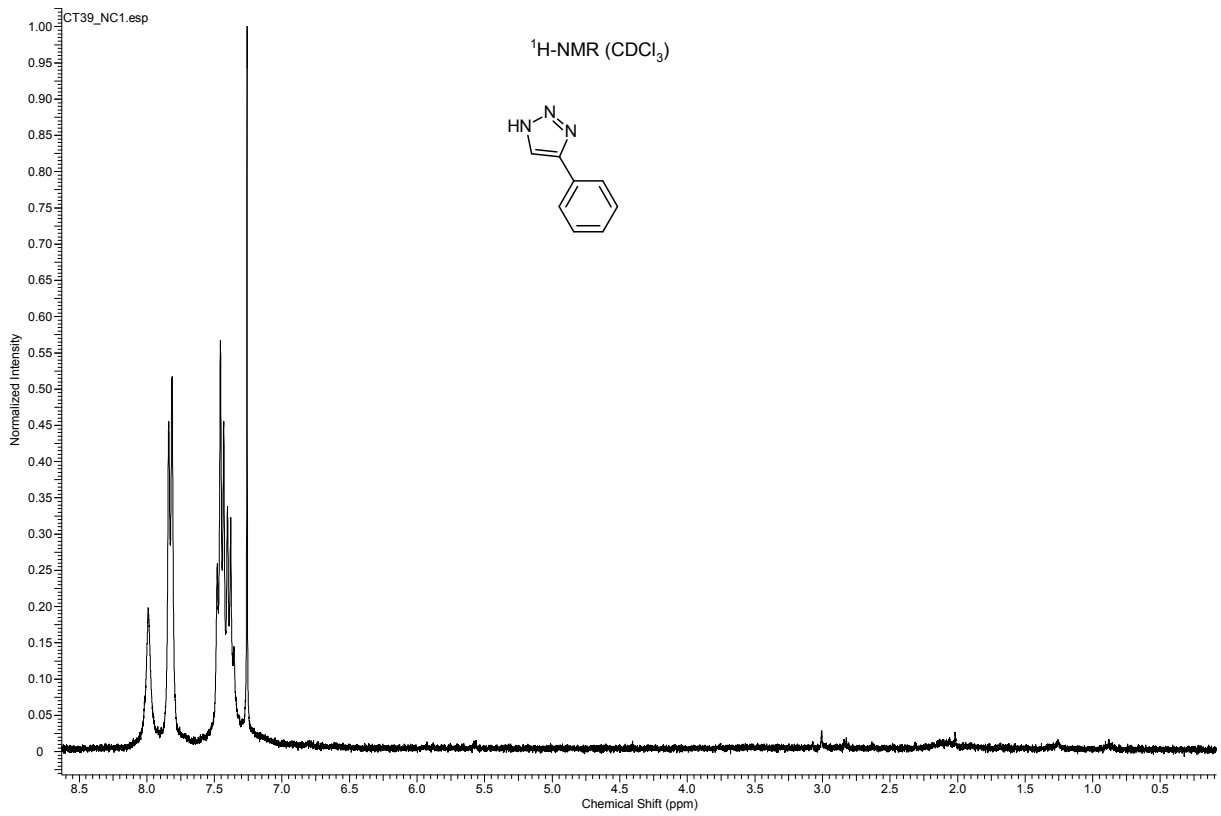
39



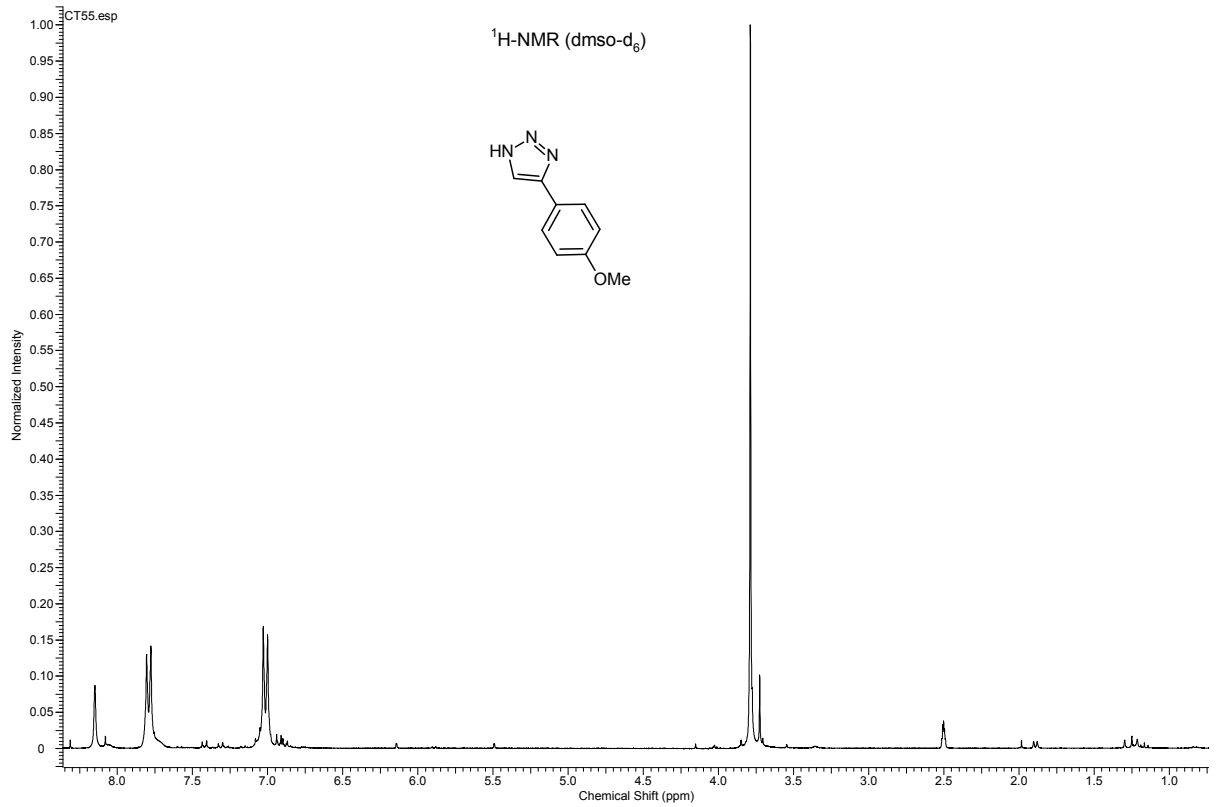
40



41

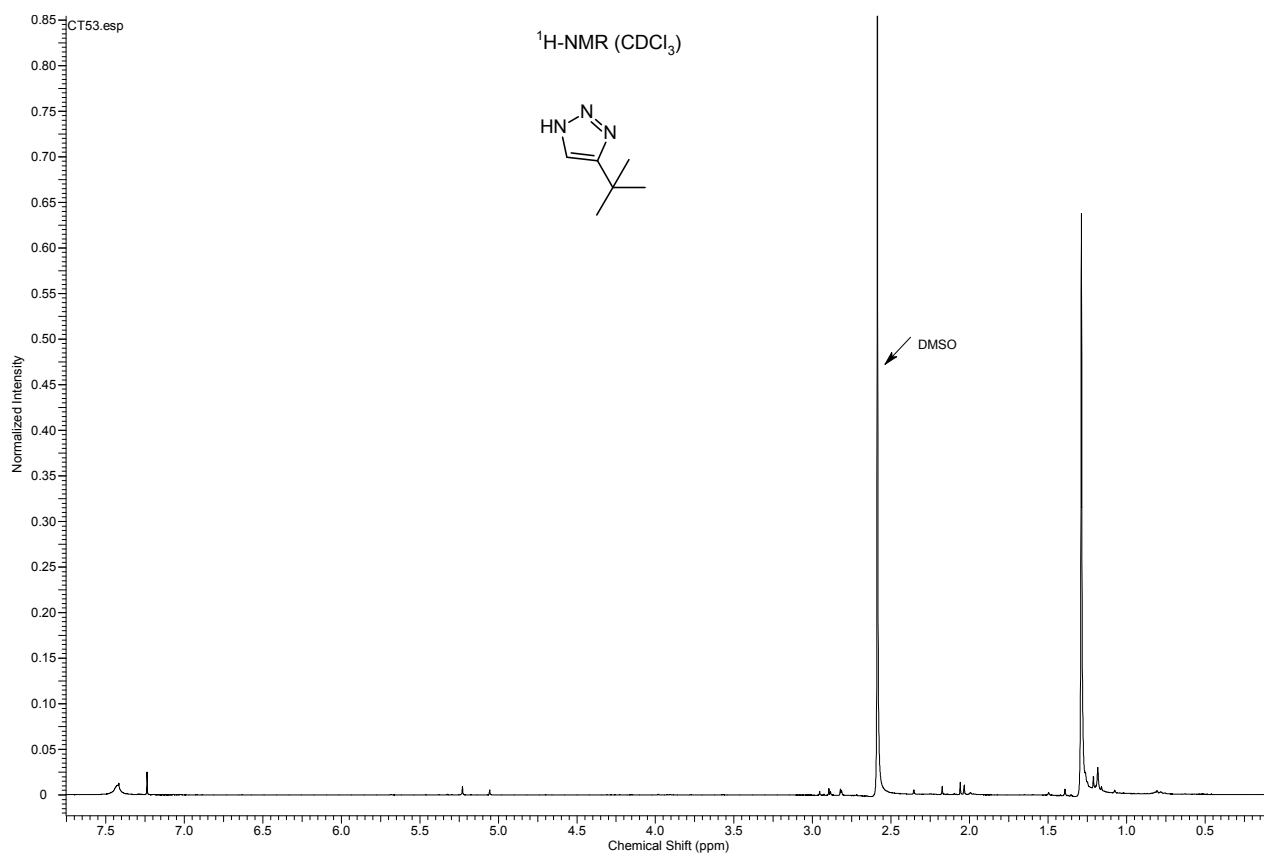


42

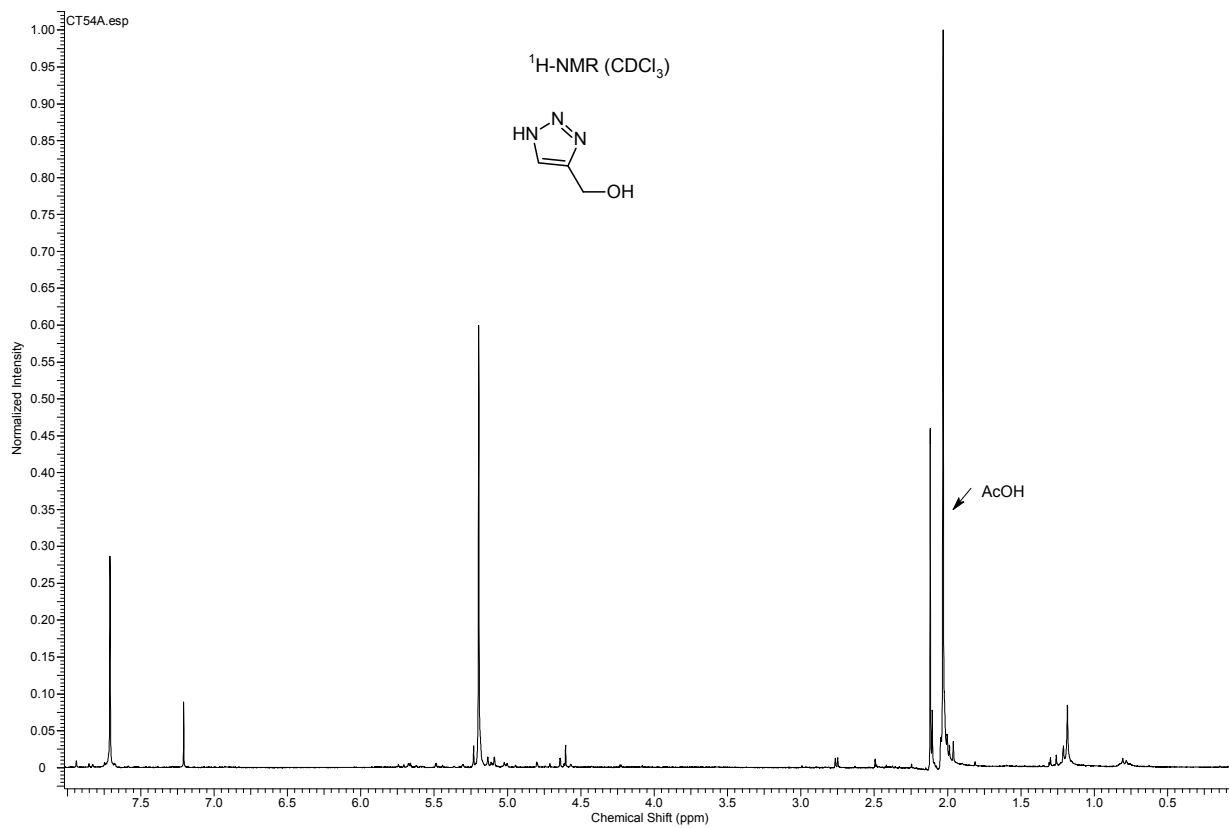


43

42



44



45

2. Bioconjugation experiments

2.1. General information

All organic solvents and chemical reagents were acquired from commercial sources and used without further purification or drying. DMF extra dry (with molecular sieves, water < 50 ppm) was used during manual couplings and manual Fmoc-deprotections. When utilizing this solvent for resin washing and during robot-assisted automated SPPS, peptide synthesis grade was used. The same applies for NMP. HPLC grade quality was employed for all other organic solvents. Water was Milli-Q grade standard. DIPEA was supplied as redistilled (i.e. dry) (Aldrich). 2-chlorotrityl-chloride resin (90 μm , manufacturer's loading: .28 mmol/g) was obtained from Merck Novabiochem. All chiral α -amino acids used in this paper possessed the L-configuration. Throughout this work, N α -Fmoc protected residues with standard acid-sensitive side-chain PGs were used: Asp(OtBu) [D], Glu(OtBu) [E], Lys(Boc) [K], Asn(Trt) [N], Gln(Trt) [Q], Arg(Pbf) [R], Ser(tBu) [S], Thr(tBu) [T].

Automated peptide synthesis was performed on an automated SYRO Multiple Peptide Synthesizer robot, equipped with a vortexing unit for the 24-reactor block (MultiSynTech GmbH). Reactions were open to the atmosphere, executed at ambient temperature and shielded from light.

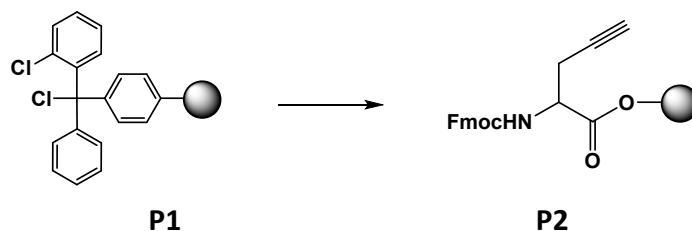
Reversed-Phase HPLC analysis and purification was performed with diode array detection, using a (Phenomenex Jupiter) C4 300 Å column (250 x 4.6 mm, 5 μm , at 35 °C), applying a flow = 1.0 mL/min. Signals at 214, 254, 280, 310 and 360 nm were simultaneously detected. Through a binary solvent system composed of (A =) H₂O + TFA (0.1 %) and (B =) CH₃CN as mobile phases, linear gradient elution has been performed: after injection the column is flushed with x % B for 3 min, followed by a linear increase of B (versus A) to 100 % in y min, finishing by flushing with 100 % B for 5 min, after which the gradient returns to x % B in 0.5 min, concluding the cycle by flushing with x % B for 3 min. Gradient 1 refers therein to (x,y) = (0, 15), or a 0 to 100 % linear increase of B (versus A) in 15 min.

ESI-MS spectra were recorded on a quadrupole ion trap LC mass spectrometer, equipped with electrospray ionization. MeOH/H₂O (4/1 \pm 0.1 % formic acid) was used as carrier solution. All data were collected in the positive mode, at 250 °C.

MALDI-TOF-MS spectra were acquired with a high performance nitrogen laser (337 nm), using the positive and reflector mode with delayed extraction. All measurements were calibrated against MePEOH (Mn \approx 2000, PD = 1.06), spotted from a MeOH (2 mg/mL) solution. Following matrix solutions were utilized (made in microtubes, stored in freezer, carefully defrosted and homogenized upon use): DHB: 2,5-dihydroxybenzoic acid (98.0 % pure, 10 mg) + CH₃CN (500 μL) + H₂O (470 μL) + TFA_{aq} (30 μL , 3 %); α -CHCA: α -cyano-4-hydroxycinnamic acid (99 % pure, 10 mg) + CH₃CN (500 μL) + H₂O (400 μL) + TFA_{aq} (100 μL , 3 %).

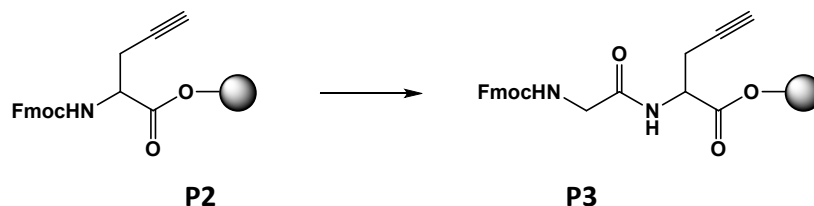
2.2. Peptide synthesis:

2.2.1. Immobilization of Fmoc-Pra-OH on 2-chlorotrityl chloride resin



To a suspension of 2-chlorotrityl chloride resin **P1** (0.150 g, 1.55 mmol/g) in dry DCM (10 mL/g resin), were added Fmoc-Pra-OH (Fmoc-Propargylglycine) (48 mg, 0.288 mmol) and DIPEA (0.1 mL, 0.576 mmol). The mixture was shaken at room temperature for 3 h. After the reaction, the resin was washed with DCM and Et₂O. Fmoc determination was performed to calculate the yield. The loading was calculated to be 0.56 mmol/g, indicating a coupling yield of 90%. The resin was then capped with MeOH/DIPEA in DCM (3 mL) 3 times for 2 min.

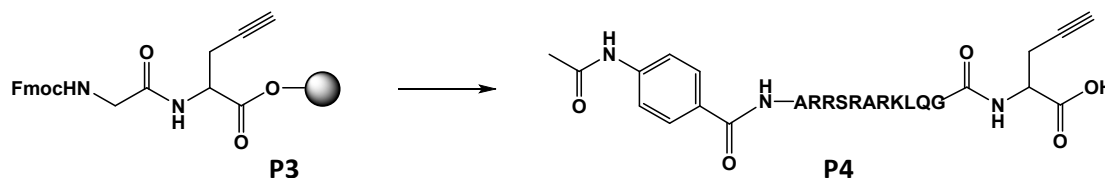
2.2.2. Fmoc deprotection and coupling of Fmoc-Gly-OH:

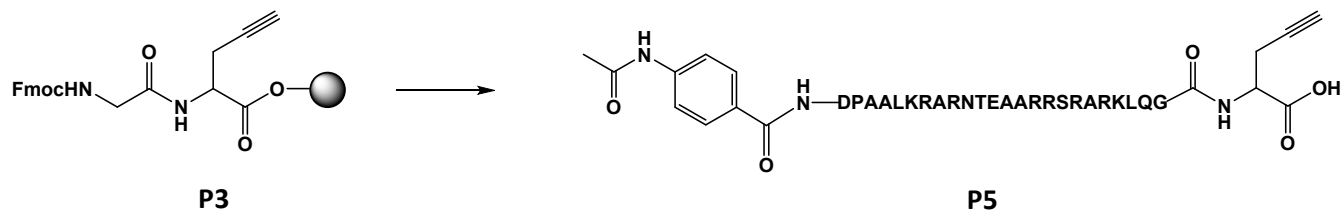


NHFmoc deprotection of compound **P2**. After an initial DMF washing step, resin **P2** (0.125 mmol) was successively treated twice for 30 min with a piperidine solution in DMF (40 % v/v, 3 mL) at ambient temperature, applying intermediate filtration under reduced pressure and washing with DMF, while the final resin is additionally washed with CH₃CN and DCM.

After Fmoc deprotection, Fmoc-Gly-OH (0.150 g, 0.502 mmol, 0.5 M), PyBOP (0.26 g, 0.502 mmol, 0.5 M) and DIPEA (0.087 mL, 0.502 mmol, 2 M) were added to a suspension of resin in dry DMF (3 mL). The mixture was shaken at room temperature for 3 h. After the reaction, the resin was washed again with DMF/MeOH/DCM/Et₂O/DMF successively.

2.2.3. Automated synthesis of linear peptide





Before automated peptide synthesis, resin **P3** was manually NHFmoc-deprotected using the procedure described above.

Automated solid phase peptide synthesis was carried out on a Syro synthesizer from Biotage using standard Fmoc/tBu chemistry with HBTU as coupling reagent and 20% piperidine in NMP as deprotection reagent.

Fmoc deprotected resin (0.125 mmol) was subjected to automated synthesis where solutions of Fmoc-N_α-protected amino acids (0.5 M in NMP) were prepared. Each coupling reaction was repeated twice for 40 min (amino acids 0.625 mmol; HBTU 0.625 mmol in DMF, 0.5 M; DIPEA 0.625 mmol 2 M) and followed by Fmoc deprotection with 20% piperidine in NMP. The N-terminus was capped manually with 4-acetamidobenzoic acid (1.25 mmol, 0.5 M), PyBOP (1.25 mmol, 0.5 M), DIPEA (2.50 mmol, 2 M) in dry DMF. The peptide was then cleaved from the resin and deprotected with a cocktail of TFA:TIS:water (95: 2.5: 2.5). After precipitation in cold ether, the peptide was analyzed by RP-HPLC and MALDI.

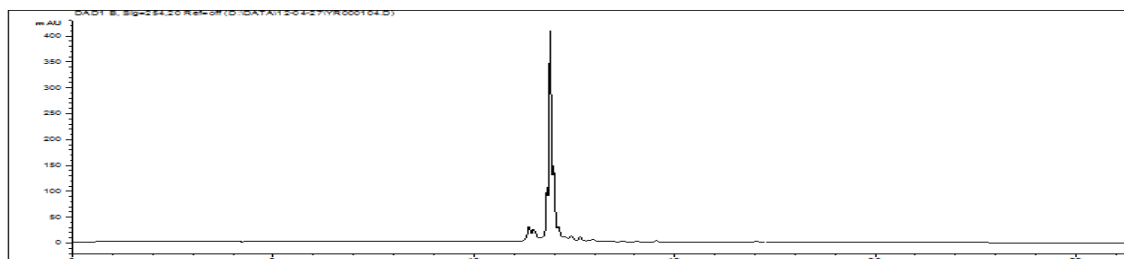


Figure S19. RP-HPLC Chromatogram of crude compound **P4** (C4, 300Å column using a gradient from 0 to 100 % CH₃CN in 15 minutes)

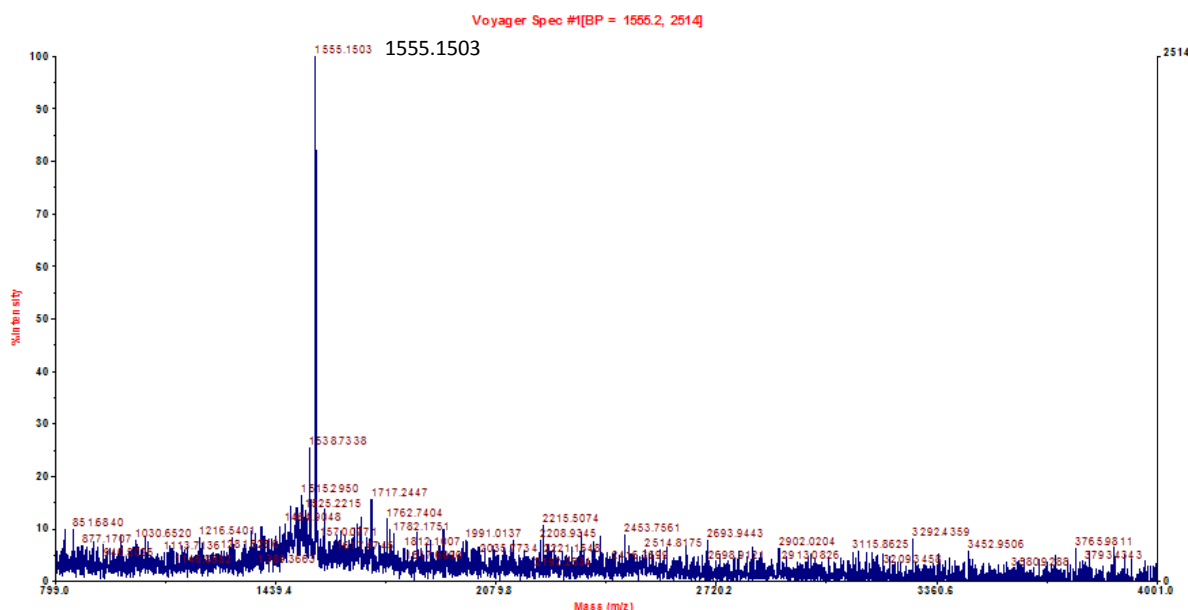


Figure S20: MALDI-TOF Spectrum of crude compound **P4**. M = 1584.88. Found [M+H]⁺ = 1585.15.

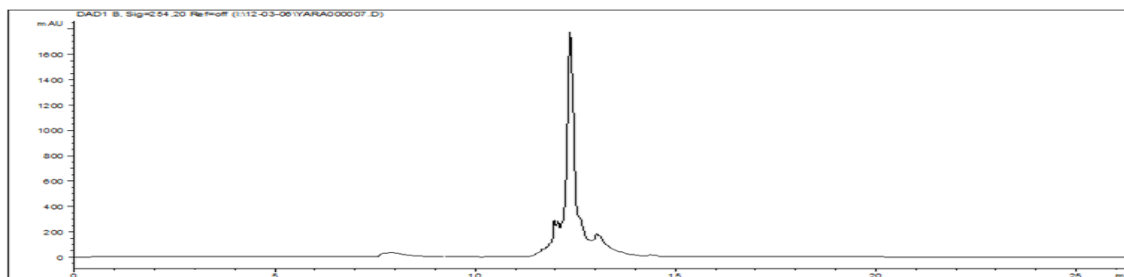


Figure S21. RP-HPLC Chromatogram of crude compound **P5**. (C4, 300Å column using a gradient from 0 to 100 % CH₃CN in 15 minutes).

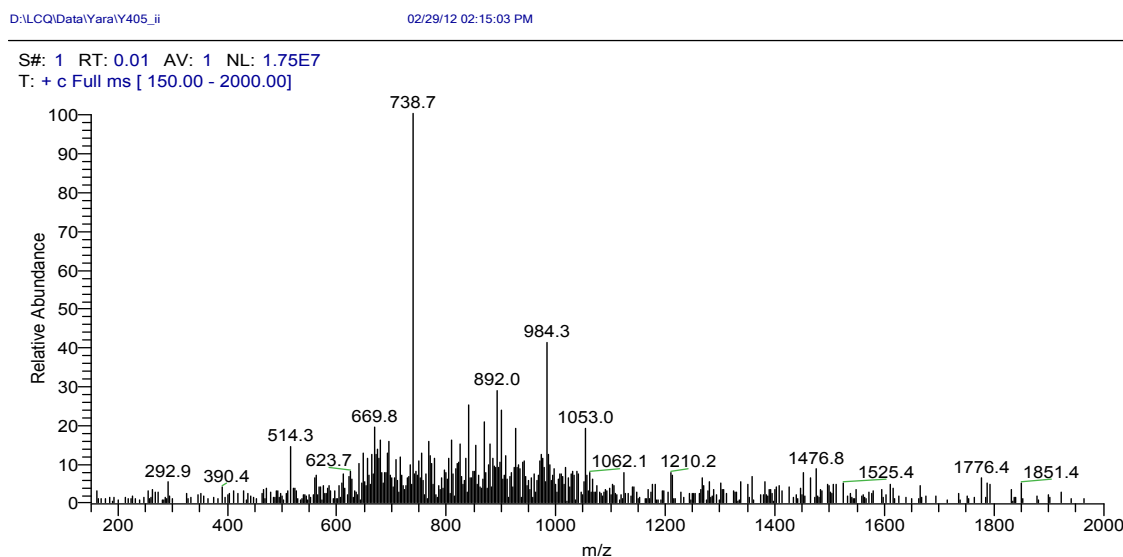
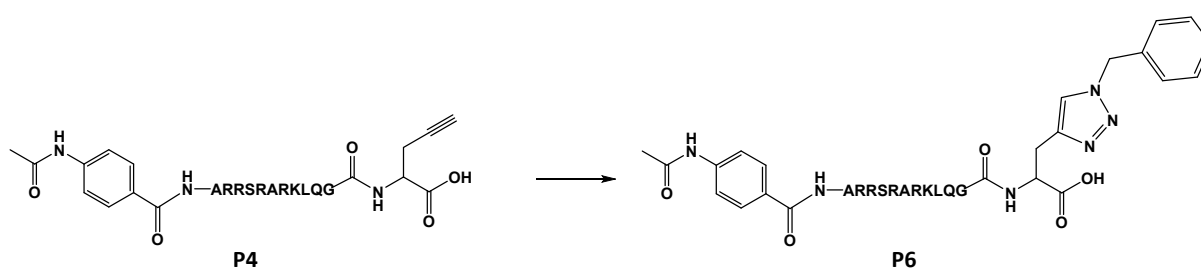


Figure S22. MS(EI) Spectrum of crude compound **P5**. $M = 2949.29$. Found $[M+4H]^+/4 = 738.7$; $[M+3H]^+/3 = 984.3$; $[M+2H]^+/2 = 1476.8$.

2.3. Bioconjugation via CuAAC



12mer GCN4 peptide bearing an alkyne functionality (**P4**) ($3.86 \cdot 10^{-3}$ mmol) was dissolved in 1 mL deoxygenated water. The solution was transferred to a reaction vial under argon and the catalyst ($4.006 \cdot 10^{-3}$ mmol) was added under stirring. Then, a solution of benzylazide in DCM (0.5 M, $2.12 \cdot 10^{-2}$ mmol) was added. An extra 2.26 mL of deoxygenated water was added followed by 0.670 mL of HFIP. The reaction mixture is stirred overnight at room temperature. Analysis and purification of the final peptide are done on reverse-phase C4 HPLC.

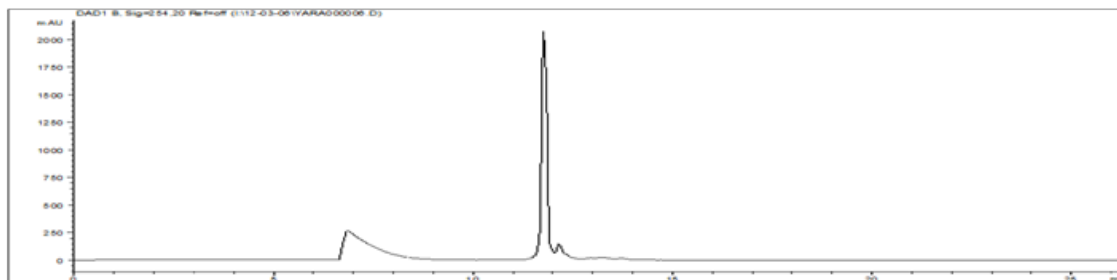


Figure S23: RP-HPLC Chromatogram of compound **P6**. (C4, 300Å column using a gradient from 0 to 100 % CH₃CN in 15 minutes).

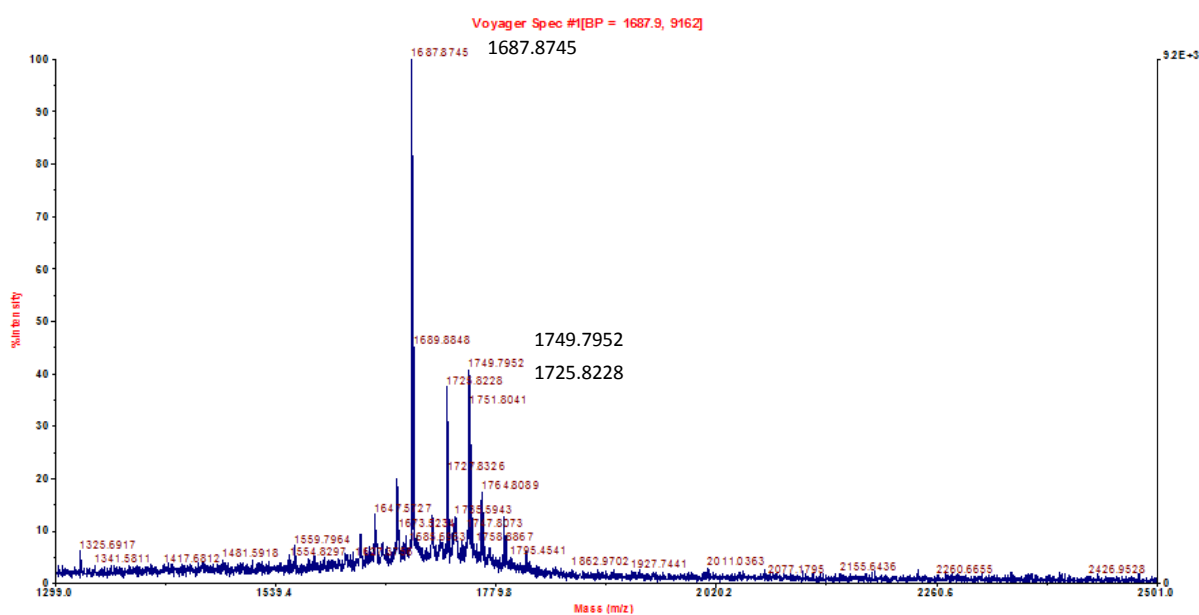
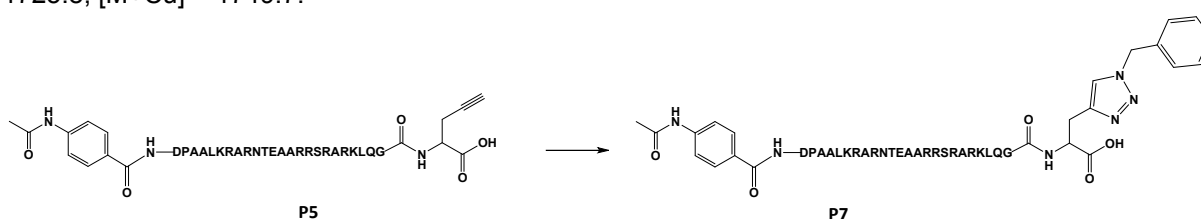


Figure S24. MALDI-TOF Spectrum of compound **P6**. $M = 1686.93$. Found $[M+H]^+ = 1687.8$; $[M+K]^+ = 1725.8$; $[M+Cu] = 1749.7$.



23mer GCN4 peptide bearing an alkyne functionality (**P5**) ($8.477 \cdot 10^{-4}$ mmol) was dissolved in 0.250 mL deoxygenated water. The solution was transferred to a reaction vial under argon and the catalyst ($9.325 \cdot 10^{-4}$ mmol) was added under stirring. Then, a solution of benzylazide in DCM (0.5 M, $4.66 \cdot 10^{-3}$ mmol) was added. An extra 0.250 mL of deoxygenated water was added followed by 50 μ L of HFIP. The reaction mixture is stirred overnight at room temperature. Analysis and purification of the final peptide are done on reverse-phase C18 HPLC.

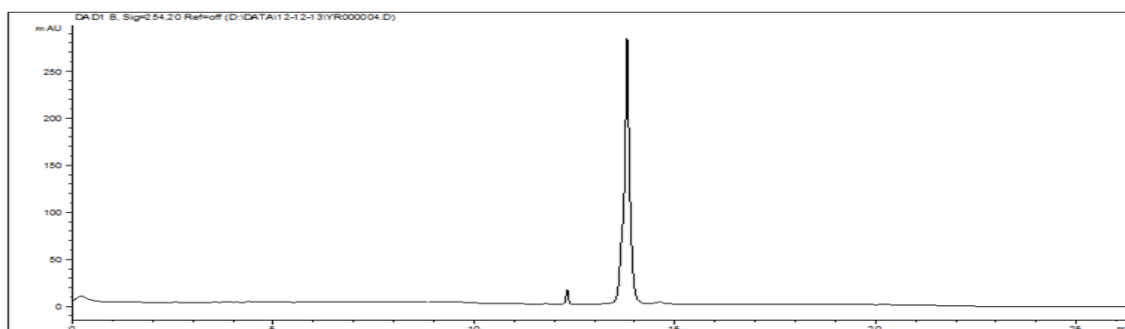


Figure S25: RP-HPLC Chromatogram of compound **P7**. (C4, 300Å column using a gradient from 0 to 100 % ACN in 15 minutes).

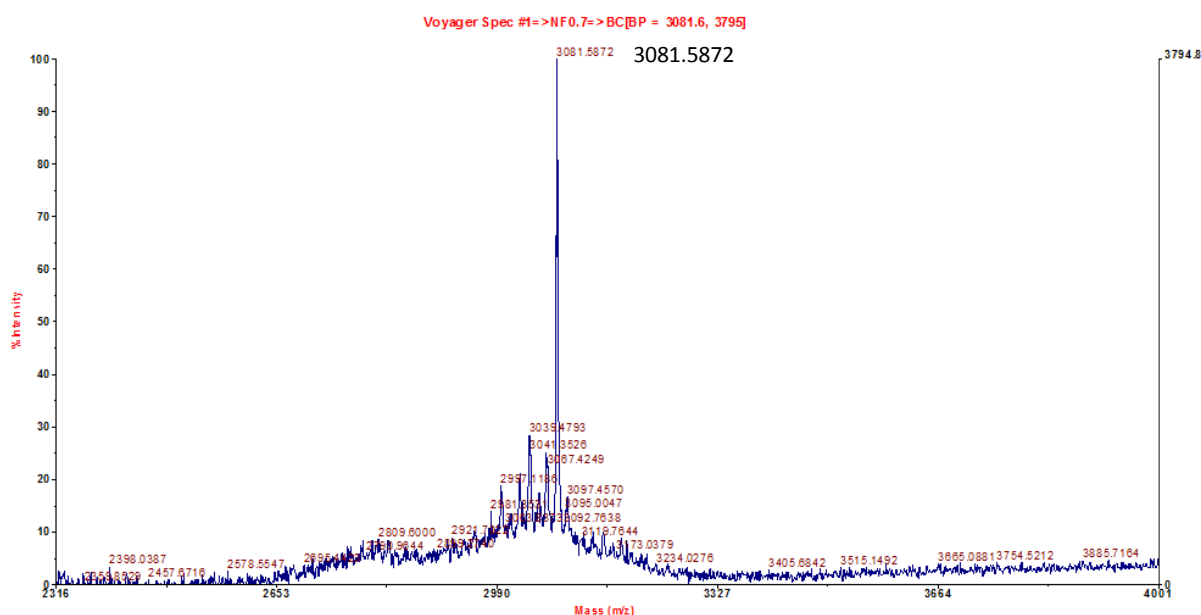
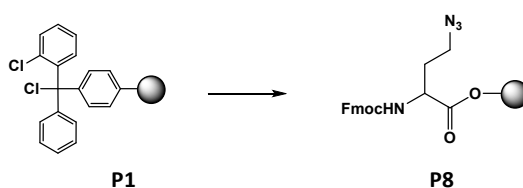


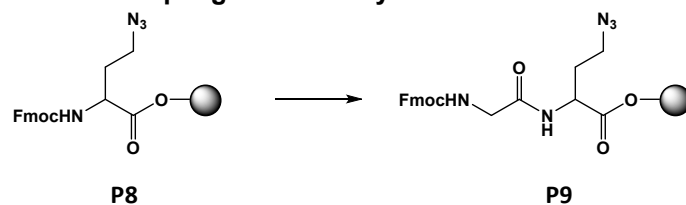
Figure S26: MALDI-TOF Spectrum of compound **P7**. $M = 3080.67$. Found $[M+H]^+ = 3081.58$.

2.3.1. Immobilization of Fmoc-Aha-OH on 2-chlorotrityl resin

To a suspension of resin **P1** (0.150 g, 1.55 mmol/g) in dry DCM (10 mL/g resin), were added Fmoc-Aha-OH (Fmoc-azidohomoalanine) (51 mg, 0.140 mmol) and DIPEA (0.050 mL, 0.279 mmol). The mixture was shaken at room temperature for 3 h. The loading was calculated to be 0.65 mmol/g, indicating a coupling yield of 91%. The resin was then capped with MeOH/DIPEA in DCM 3 times for 2 min.



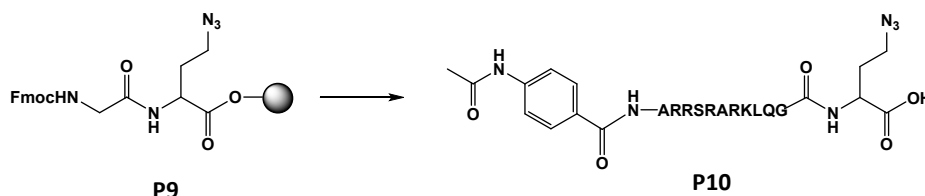
2.3.2. Fmoc deprotection and coupling of Fmoc-Gly-OH:



NHFmoc deprotection of construct **P8**. After an initial DMF washing step, resin **P8** (0.127 mmol) was successively treated twice for 30 min with a piperidine solution in DMF (40 % v/v, 3 mL) at ambient temperature, applying intermediate filtration under reduced pressure and washing with DMF, while the final resin is additionally washed with CH₃CN and DCM.

Fmoc deprotected resin (0.127 mmol). Fmoc-Gly-OH (0.151 g, 0.508 mmol, 0.5 M), PyBOP (0.264 mg, 0.508 mmol, 0.5 M) and DIPEA (0.088 mL, 0.508 mmol, 2 M) were added to a suspension of resin in dry DMF (3 mL). The mixture was shaken at room temperature for 3 h.

2.3.3. Automated synthesis of linear peptide



Before automated peptide synthesis, resin **P9** was manually NHFmoc-deprotected using the procedure described above.

Automated solid phase peptide synthesis was carried out on a Syro synthesizer from Biotage using standard Fmoc/tBu chemistry with HBTU as coupling reagent and 20% piperidine in NMP as deprotection reagent.

The resin X (0.127 mmol) was subjected to automated synthesis where solutions of Fmoc-N_α-protected amino acids (0.5 M in NMP) were prepared. Each reaction coupling was repeated twice for 40 min long (amino acids 0.635 mmol; HBTU 0.635 mmol in DMF, 0.5 M; DIPEA 0.635 mmol 2 M) and followed by Fmoc deprotection with 20% piperidine in NMP. The N-terminus was capped manually with 4-acetamidobenzoic acid (1.27 mmol), PyBOP (1.27 mmol), DIPEA (2.54 mmol) in dry DMF (3 mL) for 4 hours. The peptide was then cleaved for the resin and deprotected with a cocktail of TFA:TIS:water (95: 2.5: 2.5). After precipitation in cold ether, the peptide was analyzed by LC-MS(ESI) and MALDI.

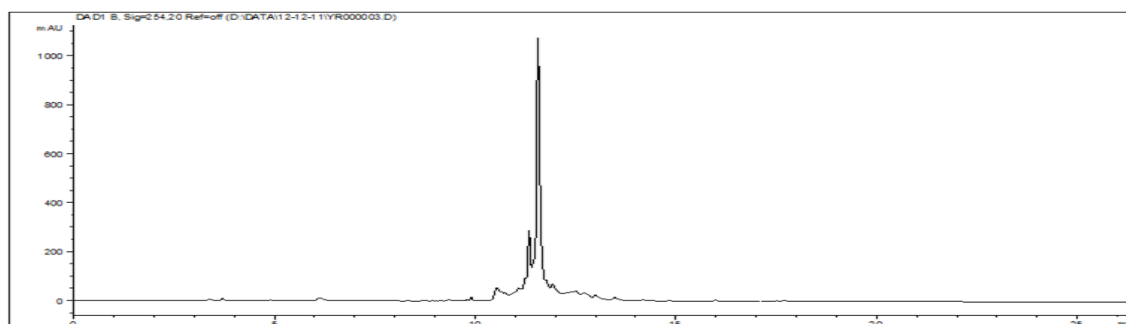


Figure S27: RP-HPLC Chromatogram of crude compound **P10**. (C4, 300 Å column using a gradient from 0 to 100 % CH₃CN in 15 minutes).

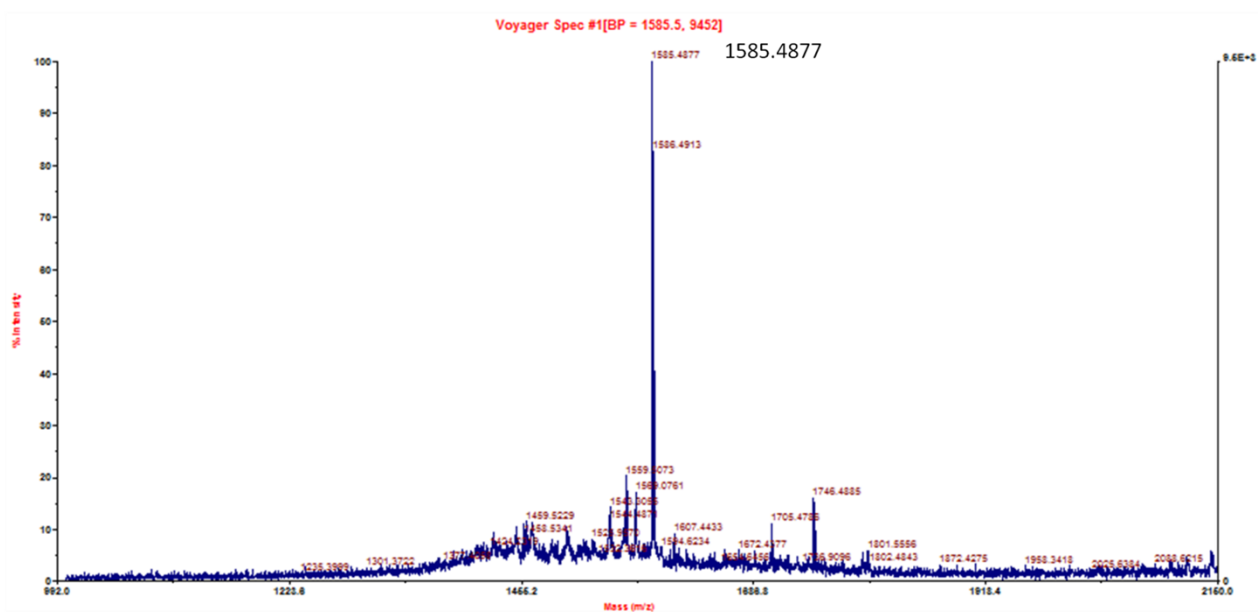
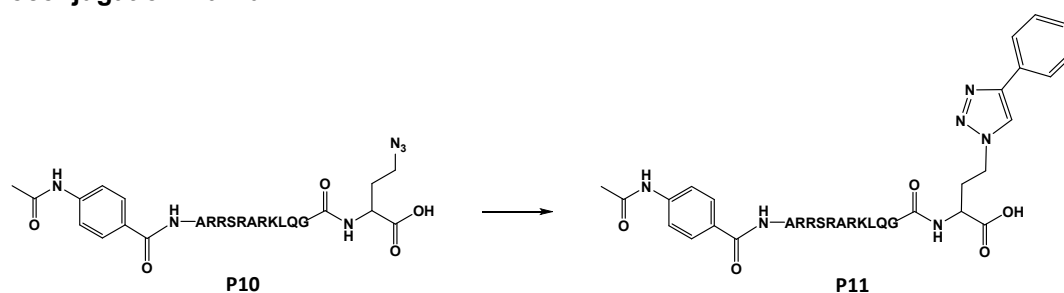


Figure S28: MALDI-TOF Spectrum of crude compound **P10**. $M = 1584.88$. Found $[M+H]^+ = 1585.48$.

2.4. Bioconjugation via CuAAC



12mer GCN4 peptide bearing an alkyne functionality ($3.86 \cdot 10^{-3}$ mmol) was dissolved in 1 mL deoxygenated water. The solution was transferred to a reaction vial under argon and the catalyst ($4.006 \cdot 10^{-3}$ mmol) was added under stirring. Then, a solution of benzylazide in DCM (0.5 M, $2.12 \cdot 10^{-2}$ mmol) was added. An extra 2.26 mL of deoxygenated water was added followed by 0.670 mL of HFIP. The reaction mixture is stirred overnight at room temperature. Analysis and purification of the final peptide are done on reverse-phase C4 HPLC

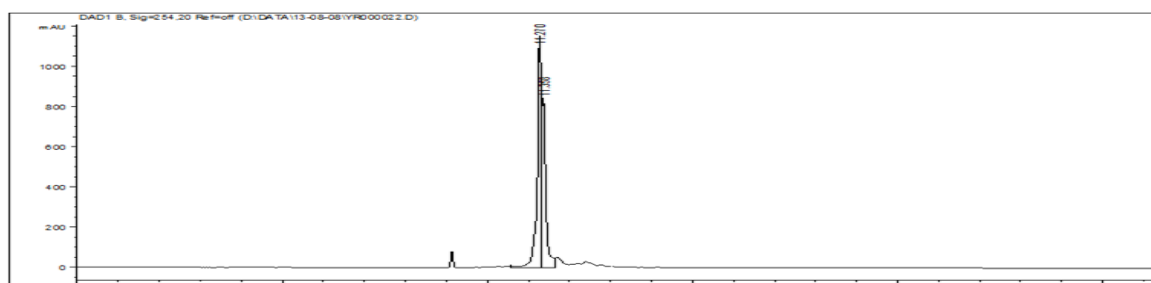


Figure S29: RP-HPLC Chromatogram of crude compound **P11**. (C4, 300Å column using a gradient from 0 to 100 % CH_3CN in 15 minutes).

Presence of compound **P10** at 11.270 min shows incompleteness of the reaction.

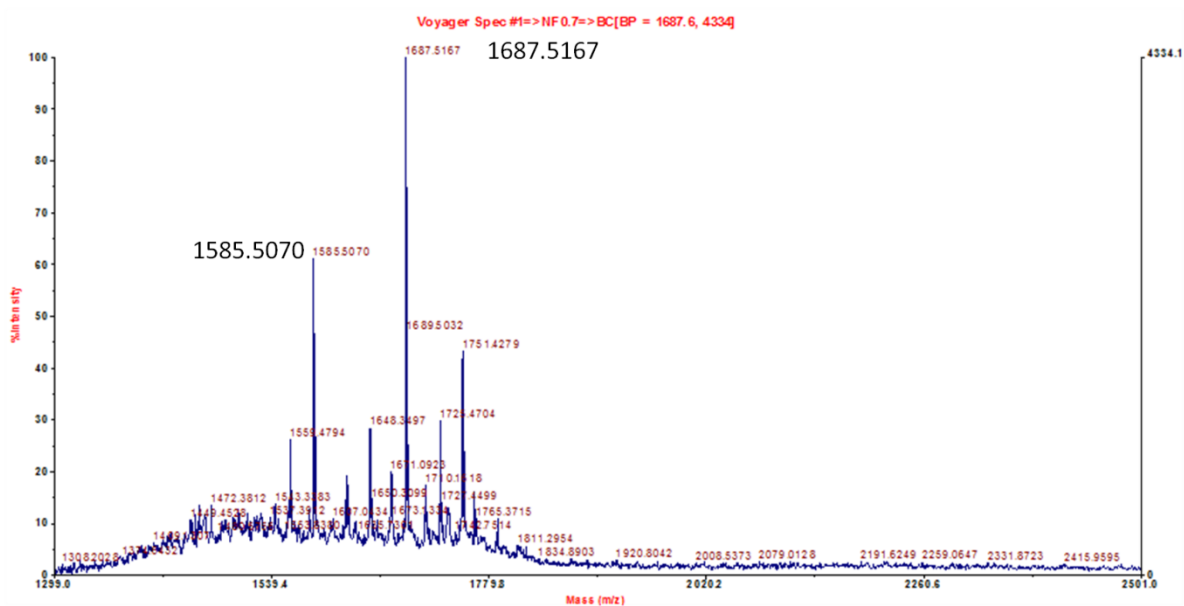
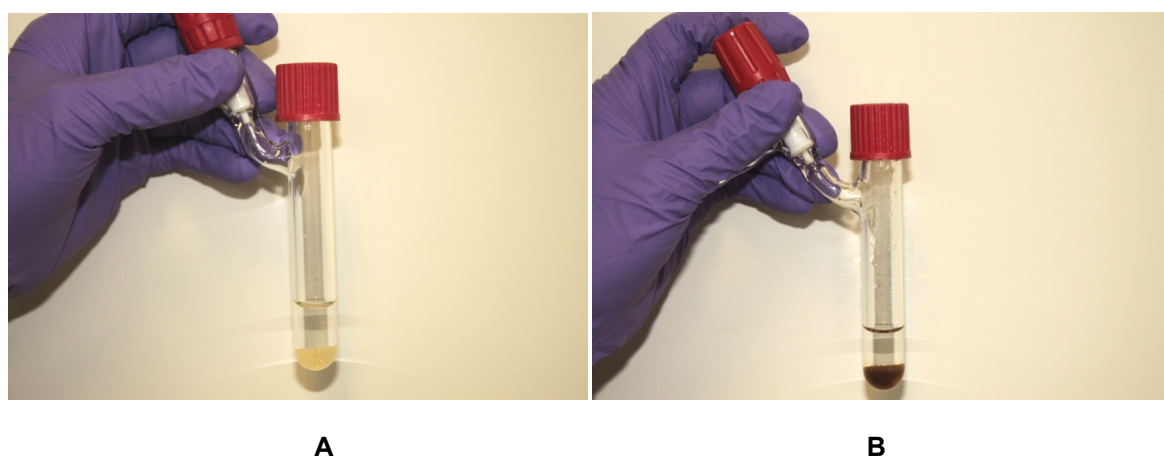


Figure S30: MALDI-TOF Spectrum of compound **P11**. $M = 1686.93$. Found $[M+H]^+ = 1687.51$. Presence of starting compound **P10**. $M = 1584.88$. Found $[M+H]^+ = 1585.51$.

3. Preparation of the heterogeneous catalyst Bis[1-(4-sodiumsulfonatebutyl)-3-(2,4,6-trimethylphenyl)-4,5-imidazolyl-3-ylidene] copper (I) hexafluorophosphate on Amberlyte® IRA-402 resin beads 6-IRA 402.

In a Schlenk vial 0.15 g (0.3 meq/g dried mass) of the anion resin Amberlyte® IRA-402 was placed and treated at 60°C under vacuum for 2 h. Afterwards, 47 mg of Bis[1-(4-sodiumsulfonatebutyl)-3-(2,4,6-trimethylphenyl)-4,5-imidazolyl-3-ylidene] copper (I) hexafluorophosphate **6** (0.05 mmol) and 2 mL of deoxygenated water are added to the vial and the mixture was stirred for 12 h at room temperature. Thereafter, the water phase is removed from the vial and the catalyst-impregnated beads were washed with 5 mL of deoxygenated water. The resin became brownish after the treatment.



Supplementary Picture S1. Images of the ion exchanger Amberlyte® IRA 402 in water before the reaction with the ionic catalyst **6** (**A**) and after the reaction (**B**) in water.

3.1. Procedure for the heterogeneous CuAAC reactions for the three-component Click reaction of benzyl azide and phenyl acetylene in water

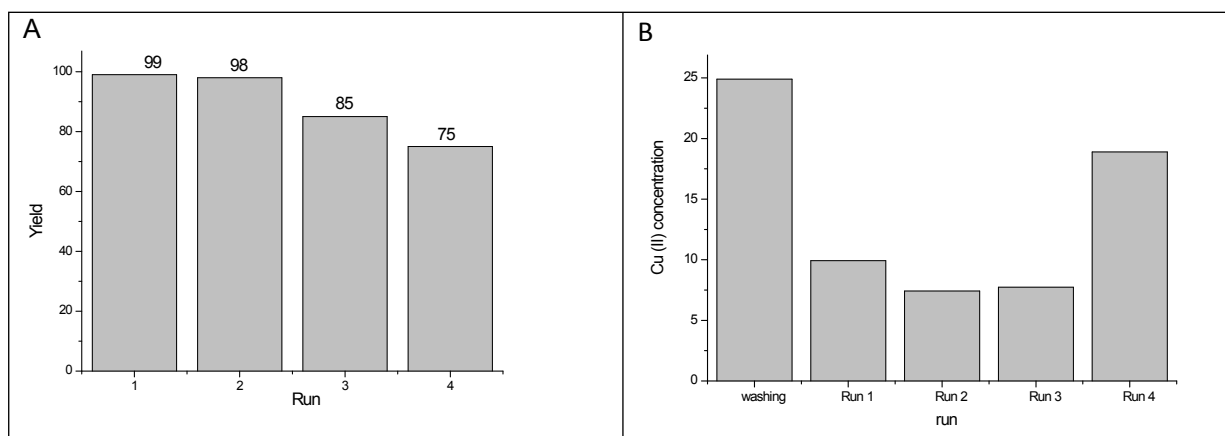
In a vial containing the heterogeneous catalysts **6-IRA 402** (0.02 eq Cu (I)), 78 mg of NaN_3 (1.2 mmol), 130 μL of phenyl acetylene (1.2 mmol) and 122 μL of benzyl bromide (1 mmol) and 1.5 mL of deoxygenated water are added. The reaction mixture was stirred for 16 h at room temperature. Thereafter, the product was extracted with dichloromethane and the organic phase was dried using MgSO_4 and finally evaporated under vacuum. The aqueous phase was removed and replaced by fresh deoxygenated water for the next reaction cycle.

3.2. Procedure for the heterogeneous CuAAC reactions for the three-component Click reaction of benzyl azide and acetylene gas in water

In a vial containing the heterogeneous catalysts **6-IRA 402** (0.02 eq Cu (I)), 78 mg of NaN_3 (1.2 mmol) and 122 μL of benzyl bromide (1 mmol) and 1.5 mL of deoxygenated water are added, the vial is purged with acetylene gas and subjected to 1 atm of this gas using a balloon. The reaction mixture was stirred for 2 h at room temperature under ultrasound. Thereafter, the product was extracted with dichloromethane and the organic phase was dried using MgSO_4 , filtered and evaporated under vacuum. The aqueous phase was removed and replaced by fresh deoxygenated water for the next reaction cycle.

3.3. Recyclability studies of the heterogeneous catalyst 6-IRA 402

The reactions for the recycling of the heterogeneous catalyst were carried out by the typical procedure described above. After the completion of the fresh reaction, the reaction was extracted with dichloromethane (3 x 20 mL) under argon atmosphere, the combined organic phases were dried using Mg_2SO_4 , filtered and evaporated at reduced pressure. The water phase containing the catalyst was removed with syringe and fresh substrates and water were added under argon atmosphere for the next catalytic cycle.



Supplementary Graph S1: A: Reusability of immobilized (NHC)₂ Cu catalyst 6-IRA-402. B: Leached Cu(II) concentration after each run using 6-IRA-402.

3.4. XRF experiments on water phase of 7-IRA 402

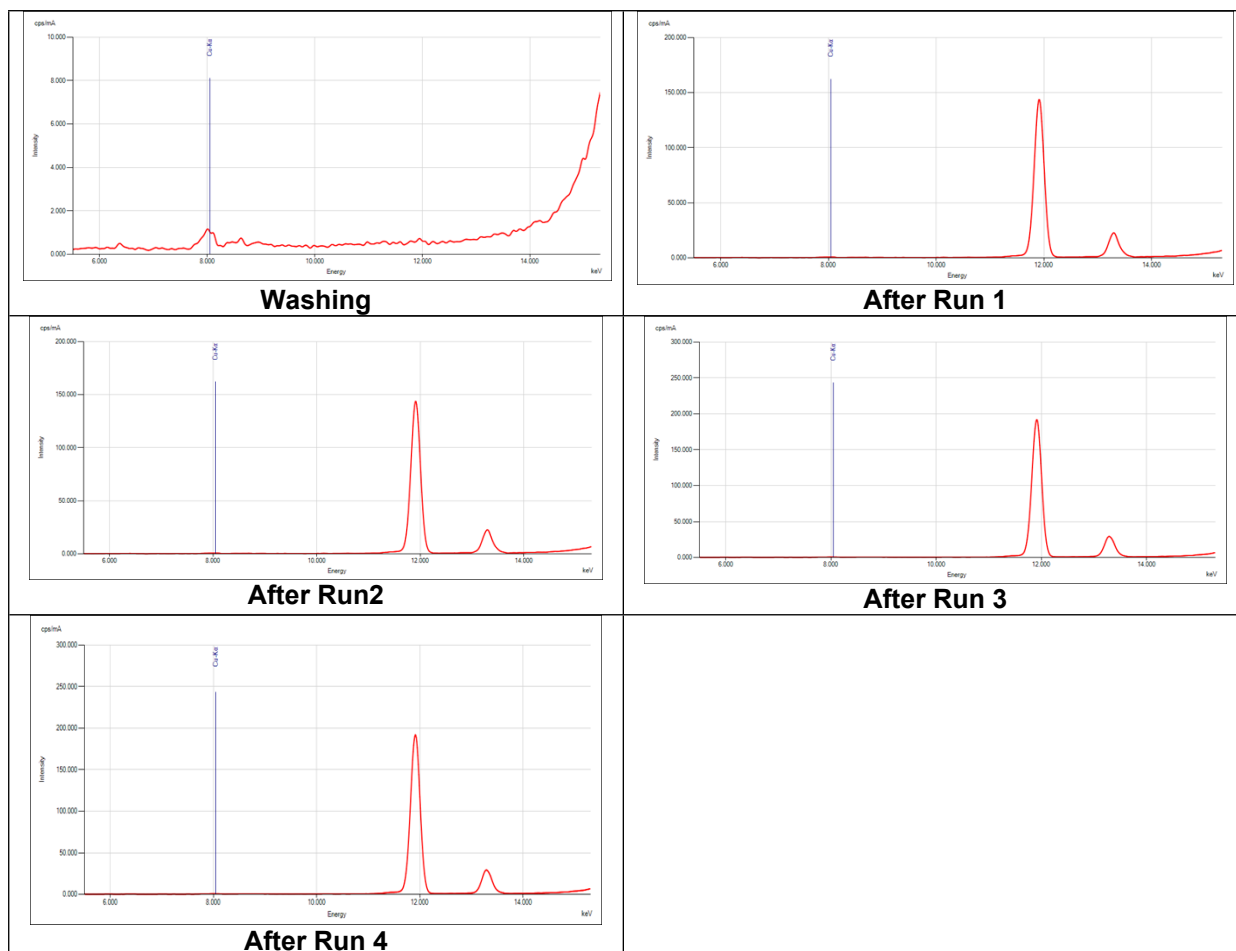


Figure S31: Obtained XRF spectra obtained of the water phase after each cycle 6-IRA-402.

4. Computational methods

The proposed catalytic cycles for complexes **6** and **8** were studied by means of Density Functional Theory (DFT)³⁰. To save computational time, the geometries of the complexes within the catalytic cycle of complex **7** were used to construct those of complex **8**; as such we have also very similar conformations which make it possible to accurately compare the saturated complex **6** with its unsaturated variant **8**. All intermediates and transition states were fully optimized at the DFT level of theory using the B3LYP hybrid functional^{31, 32} and usage of the Gaussian09 package³³. The double-zeta Pople basis set 6-31+G(d) was used for all the atoms except for Copper, for which the LANL2DZ effective core potential and basis set was applied³⁴. The frequencies were calculated at the same level of theory as the geometry optimizations and confirmed that all structures were either local minima on the potential energy surface or transition states. Afterwards the energies were refined by single point energy calculations at the B3LYP/6-311++g(3df,2p) level of theory. This type of procedure is commonly used in theoretical calculations on this type of transition metal catalysis^{35, 36, 37}. Furthermore, also the van der Waals corrections as developed by Grimme were included³⁷. More specifically, the dispersion corrections are calculated according to the third version of Grimme³⁸. Furthermore, the SMD solvation model of Marenich *et al.* was used to determine the effect of water as solvent on the catalytic cycles³⁹. The computational data was analyzed with the software module TAMKIN⁴⁰ to determine the thermodynamic data.

4.1. Description of the catalytic cycle with LCuPF₆ as intermediate

If mono-ligand complexes of the type LCuPF₆ are in equilibrium with bi-ligand complexes of type L₂CuPF₆, these can also catalyse the CuAAC reaction. A proposed mechanistic cycle is shown in Figure S32 and starts from phenylacetylene which is adsorbed on the monoligated Cu-complex (LCuPF₆ – phenylacetylene, Figure S14). After adsorption, a deprotonation step (TS-3, Figure S32) occurs using the internal sulfonate group generating a Cu(I)-acetylide complex. The availability of a sulfonate group on the NHC-ligand opens the possibility for protonation and deprotonation steps internally without the aid of additional reacting agents. Co-adsorption of benzyl-azide onto the Cu(I)-acetylide complex is followed by a subsequent coupling reaction (TS-1, Figure S32) forming a Cu-triazole complex (Figure S32). After an internal protonation step (TS-2, Figure S32), the 1-benzyl-4-phenyl-1,2,3-triazole is adsorbed onto the mono-ligated catalyst and can be exchanged with phenylacetylene, which would regenerate the Cu-complex LCuPF₆ – phenylacetylene. Dependent on the reference level for the reactants with respect to the rate determining transition state TS-1, we can compute different free energy barriers from Figure S32. The free energy difference between the reactants LH⁺CuPF₆-phenylacetylide and benzyl azide and the transition state TS-1, is 70.0 kJ/mol for complex **6**. However, if we compute the rate determining step from the L-CuPF₆—phenylacetylene complex (which lies lower on the free energy surface), we obtain a free energy barrier of 141.6 kJ/mol and 145.7 kJ/mol, for catalyst **6** and **8** respectively. With these barriers, a rate acceleration of 5.3 between the saturated versus the unsaturated complexes can be found, which seems also in agreement with the experimentally observed rate acceleration of 4 between catalyst **6** and **8** (figure 1B, main paper). As the complexes in the catalytic cycle of complex **6** were used to construct the catalytic cycle of complex **8**, they have a very similar conformation. For the theoretical catalytic cycles in the main paper, a similar rate acceleration was observed, from which we can conclude that the experimentally observed rate acceleration is typical when comparing saturated and unsaturated Cu-NHC complexes for the click reaction between benzylazide and phenylacetylene.

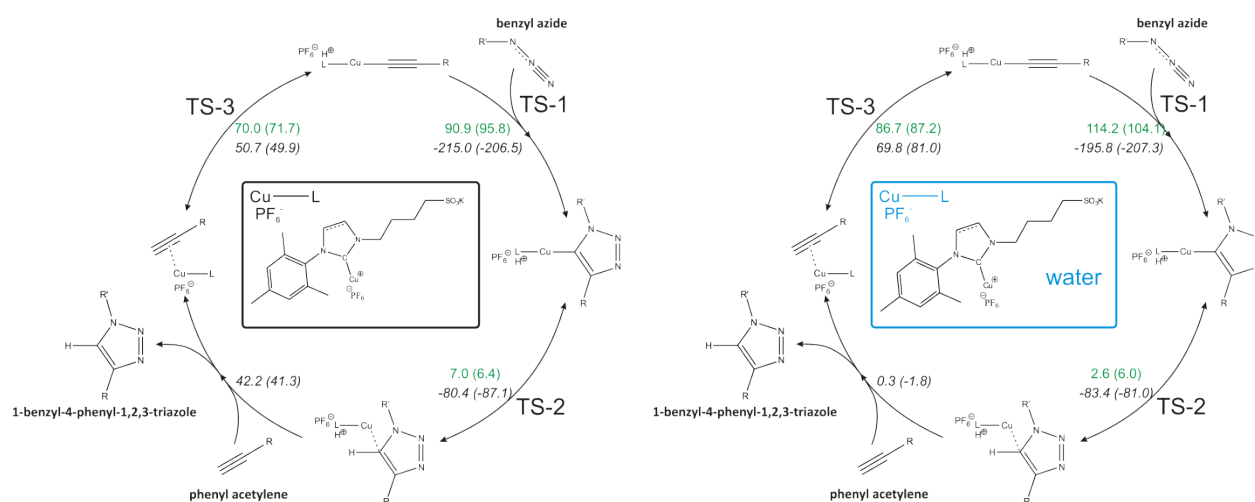


Figure S32: Catalytic cycles with mono-ligand complexes of the type LCuPF_6 as intermediate; free energy barriers (top, green) and reaction free energies (bottom, black) are given in kJ/mol at 298K for the saturated NHC complex **6** (and for unsaturated complex **8** in parentheses).

Free energy differences and their respective enthalpy and entropy contributions for all catalytic pathways in this paper are summarized in Table S8 and Table S9.

Supplementary table S8. Free energy differences (ΔG , kJ/mol), enthalpy (ΔH , kJ/mol) and entropy contributions ($-T.\Delta S$, kJ/mol) are given at 25 °C between the various states within the catalytic scheme of Figure 6 and Figure S32. The values are at the B3LYP/6-311++g(3df,2p)-D3 level of theory for the energies.

	Catalyst 6			Catalyst 8		
	ΔG	ΔH	$-T.\Delta S$	ΔG	ΔH	$-T.\Delta S$
L-Cu-acetylide cycle (main paper):						
L-Cu-acetylide + benzylazide \rightarrow TS-1	113.0	57.0	56.0	117.2	62.1	55.1
TS-1 \rightarrow L-Cu-triazole	-294.7	-308.7	14.1	-296.2	-312.2	16.0
L-Cu-triazole+ phenylacetylene \rightarrow TS-2	128.5	78.0	50.6	131.7	81.0	50.7
TS-2 \rightarrow L-Cu-acetylide + triazole	-149.4	-91.2	-58.2	-155.2	-95.7	-59.4
LH⁺Cu(PF₆⁻)-acetylide cycle:						
LH ⁺ Cu(PF ₆ ⁻)-acetylide + benzylazide \rightarrow TS-1	90.9	22.9	68.0	95.8	32.3	63.6
TS-1 \rightarrow LH ⁺ Cu(PF ₆ ⁻)-triazole	-305.9	-320.2	14.3	-302.4	-314.6	12.3
LH ⁺ Cu(PF ₆ ⁻)-triazole \rightarrow TS-2	7.0	1.0	6.0	6.4	0.0	6.4
TS-2 \rightarrow LCu(PF ₆ ⁻) - - triazole	-87.4	-67.2	-20.2	-93.6	-73.1	-20.5
LCu(PF ₆ ⁻) - - triazole + phenylacetylene \rightarrow LCu(PF ₆ ⁻) - - phenylacetylene + triazole	42.2	43.1	-0.8	41.3	40.2	1.1
LCu(PF ₆ ⁻) - - phenylacetylene \rightarrow TS-3	70.0	70.6	-0.6	71.7	71.6	0.0
TS-3 \rightarrow LH ⁺ Cu(PF ₆ ⁻)-acetylide	-19.3	-15.0	-4.3	-21.8	-21.3	-0.5
Gas phase reaction:						
benzylazide + acetylene \rightarrow TS1	132.9	79.6	53.3			
TS1 \rightarrow 1,4-triazole	-335.4	-344.5	9.1			
benzylazide + acetylene \rightarrow TS2	124.2	73.0	51.1			
TS2 \rightarrow 1,5-triazole	-326.7	-337.9	11.3			

Supplementary Table S9. Free energy differences (ΔG , kJ/mol), enthalpy (ΔH , kJ/mol) and entropy contributions ($-T.\Delta S$, kJ/mol) are given at 25 °C between the various states within the catalytic scheme of Figure 6 and Figure S32. The values are at the B3LYP/6-311++g(3df,2p)-D3 level of theory and are implicitly solvated with water.

	Catalyst 6			Catalyst 8		
	ΔG	ΔH	$-T.\Delta S$	ΔG	ΔH	$-T.\Delta S$
L-Cu-acetylide cycle (main paper):						
L-Cu-acetylide + benzylazide \rightarrow TS-1	133.0	77.0	56.0	135.2	80.0	55.1
TS-1 \rightarrow L-Cu-triazole	-317.9	-331.9	14.1	-318.3	-334.3	16.0
L-Cu-triazole + phenylacetylene \rightarrow TS-2	142.6	92.0	50.6	143.7	93.0	50.7
TS-2 \rightarrow L-Cu-acetylide + triazole	-166.8	-108.6	-58.2	-169.7	-110.3	-59.4
LH⁺Cu(PF₆⁻)-acetylide cycle:						
LH ⁺ Cu(PF ₆ ⁻)-acetylide + benzylazide \rightarrow TS-1	114.2	46.3	68.0	104.1	40.6	63.6
TS-1 \rightarrow LH ⁺ Cu(PF ₆ ⁻)-triazole	-310.1	-324.4	14.3	-311.4	-323.7	12.3
LH ⁺ Cu(PF ₆ ⁻)-triazole \rightarrow TS-2	2.6	-3.4	6.0	6.0	-0.4	6.4
TS-2 \rightarrow LCu(PF ₆ ⁻) - - triazole	-85.9	-65.8	-20.2	-87.0	-66.5	-20.5
LCu(PF ₆ ⁻) - - triazole + phenylacetylene \rightarrow LCu(PF ₆ ⁻) - - phenylacetylene + triazole	0.3	1.1	-0.8	-1.8	-2.9	1.1
LCu(PF ₆ ⁻) - - phenylacetylene \rightarrow TS-3	86.7	87.3	-0.6	87.2	87.1	0.0
TS-3 \rightarrow LH ⁺ Cu(PF ₆ ⁻)-acetylide	-16.9	-12.6	-4.3	-6.2	-5.7	-0.5
Gas phase reaction:						
benzylazide + acetylene \rightarrow TS1	143.3	90.0	53.3			
TS1 \rightarrow 1,4-triazole	-352.5	-361.6	9.1			
benzylazide + acetylene \rightarrow TS2	137.4	86.2	51.1			
TS2 \rightarrow 1,5-triazole	-346.5	-357.8	11.3			

Bibliography

1. L. R. Moore et al. *Organometallics*, **2006**, 25, 5151-5158.
2. M. A. N. Virboul. *Chem Eur. J.*, **2009**, 15, 9981-9986.
3. S. Díez-Gonzalez, S. P. Nolan. *Angew. Chem. Int. Ed.*, **2008**, 47, 8881-8884.
4. CrysAlisPro, Agilent Technologies, Version 1.171.36.28.
5. O.V. Dolomanov, L.J. Bourhis, R.J. Gildea, J.A.K. Howard, H. Puschmann *J. Appl. Cryst.*, **2009**, 42, 339-341.
6. Sheldrick G.M. A short history of *SHELX*. *Acta Cryst.*, **2008**, A64, 112-122.
7. P. Apputkuttan, W. Dehaen, V. V. Fokin, E. Van der Eycken. *Org. Lett.*, **2004**, 6, 4223-4225.
8. L. Wan, C. Cai., *Catalysis Letters* **2012**, 142(9), 1134-1140.
9. S. Díez-González, A. Correa, L. Cavallo, S. P. Nolan. *Chem. Eur. J.*, **2006**, 12, 7558-7564
10. D. Wang, Na L., Z. Mingming, S. Weilin, M. Chaowei, C. Baohua *Green Chem.*, **2010**, 12, 2120-2123.
11. S. Hashem, K. Reza, M. M. Doroodmand, *Advanced Synthesis & Catalysis*, **2009**, 351, 1+2, 207-218.
12. J. García-Alvarez, J. Díez, J. Gimeno, *Green Chem.*, **2010**, 12, 2127-2130.
13. B. R. Buckley, S. E. Dann, H. S. Heaney Emma C. *Eur. J. Org. Chem.*, **2011**, 770-776.
14. Y. Kitamura. *Heterocycles*, **2009**, 77(1), 521-532.
15. M. Liu, O. Reiser. *Organic Letters*, **2011**, 13, 5, 1102-1105.
16. J.-A. Shin, Y.-G. Lim, K.-H. Lee. *J. Org. Chem.*, **2012**, 77, 4117-4122.
17. P. Apputkuttan. W. Dehaen. V. V Fokin, E. Van der Eycken. *Org. Lett.*, **2004**, 6, 4223-4225.
18. P. Mathew, A. Neels, M. Albrecht. *J. Am. Chem. Soc.*, 2008, 130, 41, 13534-13535.
19. P. Veerakumar, M. Velayudham, K.-L. Lu., S. Rajagopal *Catalysis Science & Technology*, **2011**, 1, 8, 1512-1525.
20. B. R. B Nasir., R. S. Varma, *Green Chemistry*, **2012**, 14, 3, 625-632.
21. Sandip K., Sandeep K., Shamrao D. and Radha J. *Current Chemistry Letters*, 2012, 1 69-80.
22. O. Fleischel, N. Wu, A. and Petitjean, *Chem. Commun.*, **2010**, 46, 8454-8456.
23. S. Ladouceur, A. M. Soliman, E. Zysman-Colman, *Synthesis*, **2011**, 22, 3604-3611.
24. S. Chuprakov, N. Chernyak, A. S. Dudnik, Gevorgyan V., *Org. Lett.*, **2007**, 9, 2333.
25. A. Casimiro-Garcia et al, *Bioorganic & Medicinal Chemistry*, **2009**, 17, 20, 7113-7125.
26. Doiron J. et al, *European Journal of Medicinal Chemistry*, 2011, 46, 9, 4010-4024.
27. Gonda Z., Lorincz, K., Novak Z., *Tetrahedron Letters* **2010**, 51, 48, 6275-6277.
28. Xiaokun W., Chunxiang K., Qing Y. *Eur. J. Org. Chem.* **2012**, 2, 424-428.
29. Coelho A., Diz P., Caamano O. & Sotelo E. *Advanced Synthesis & Catalysis* **2010**, 352, 7, 1179-1152.
30. Boz, E. & Tuzun, N. S. *J. Organomet. Chem.* **2013**, 724, 167-176.
31. A Becke, *Journal of Chemical Physics*, **1993**, 98, 5648-5652.
32. C. T. Lee, W. T. Yang, R. G. Parr, *Physical Review*, **1998**, B 37, 785-789.
33. M. Meldal, C. W. Tornøe, *Chem. Rev.*, **2008**, 108, 2952-3015.
34. P. J. Hay, W. R. Wadt, *Journal of Chemical Physics*, **1985**, 82, 270-283.
35. Cantillo D., Ávalos M., *Org. Biomol. Chem.* **2011**, 9, 2952-2958.
36. B. C. Boren et al., *J. Am. Chem. Soc.*, **2008**, 130, 8923-8930.
37. S. Grimme, *J. Comput. Chem.* **2004**, 25, 1463-1473.
38. S. Grimme, J. Antony, S. Ehrlich, H. Krieg, *J. Chem. Phys.* 132, 154104-154123.
39. A. V. Marenich, C. J Cramer, D. G. Truhlar, *J. Phys Chem*, **2009**, B **113**, 6378-6396.
40. A. Ghysels, T. Verstraelen, K. Hemelsoet, M. Waroquier, Van Speybroeck, V. J. , *Inf. Model.*, **2010**, 50, 1736-1750.
41. Durden, John A., Jr.; Stansbury, Harry A.; Catlette, William H. *Journal of Chemical and Engineering Data* (1964), 9(2), 228-31.
42. Zhang, Zhongkui; Kuang, Chunxiang *Chinese Journal of Chemistry* (2013), 31(8), 1011-1014.

43. Wang, Xiao-jun; Zhang, Li; Krishnamurthy, Dhileepkumar; Senanayake, Chris H.; Wipf, Peter *Organic Letters* (2010), 12(20), 4632-4635.
44. Fletcher, James T.; Walz, Sara E.; Keeney, Matthew E. *Tetrahedron Letters* (2008), 49(49), 7030-7032.
45. Friess, Thomas; Reiff, Ulrike; Rueth, Matthias; Voss, Edgar U.S. Pat. Appl. Publ. (2006), US 20060063812 A1 20060323,
46. Jin, Tienan; Kamijo, Shin; Yamamoto, Yoshinori *Eur. J. Org. Chem.* (2004), (18), 3789-3791.
47. Olsen, Carl E. *Acta Chemica Scandinavica, Series B: Organic Chemistry and Biochemistry* (1975), B29(9), 953-62.